KINETICS OF COPPER REDUCTION BY HYDROGEN FROM AQUEOUS SOLUTIONS

by

EDMUND ALEXANDER JOACHIM HAHN

A THESIS SUBMITTED IN PARTIAL FULFILMENT OF

THE REQUIREMENTS FOR THE DEGREE OF

DOCTOR OF PHILOSOPHY

in the Department

of

METALLURGY

We accept this thesis as conforming to the
required standard

THE UNIVERSITY OF BRITISH COLUMBIA

May, 1963

In presenting this thesis in partial fulfilment of the requirements for an advanced degree at the University of British Columbia, I agree that the Library shall make it freely available for reference and study. I further agree that permission for extensive copying of this thesis for scholarly purposes may be granted by the Head of my Department or by his representatives. It is understood that copying or publication of this thesis for financial gain shall not be allowed without my written permission.

Department of **Metallurgy**

The University of British Columbia,
Vancouver 8, Canada.

Date **May 3, 1963**

ABSTRACT

The kinetics of the hydrogen reduction of aqueous cupric perchlorate and sulphate solutions were studied at 160°C and 5 to 10 atm hydrogen pressure.

In sulphate solutions the observed rates were consistent with a rate law, derived from previously proposed mechanisms, that has the form

$$-\frac{d[H_2]}{dt} = \frac{k_1[Cu^{II}]^2[H_2]}{\frac{k_{-1}}{k_2}[H^+]+[Cu^{II}]} + \frac{k_3[Cu^{II}]^2[Cu^{I}][H_2]}{\left(\frac{k_{-1}}{k_2}[H^+]+[Cu^{II}]\right)\left(\frac{k_{-3}}{k_4}[H^+]+[Cu^{II}]\right)}$$

The rate constants of the hydrogen activation steps of the reaction are represented by k_1 and k_3 which reflect the activation rates by Cu^{II} and Cu^{I} respectively and have the values $3.2 \times 10^{-3} M^{-1} sec^{-1}$ and $6.4 \times 10^{-2} M^{-1} sec^{-1}$ at 160°C.

The ratios of the back- to net forward-reaction rate constants are $\frac{k_{-1}}{k_2}$ for the Cu^{II} activation step and $\frac{k_{-3}}{k_4}$ for the Cu^{I} activation step. These have values of approximately 0.13 and 0.45 respectively at 160°C.

In perchlorate solutions the rates were also consistent with the rate law applying to sulphate solutions if a necessary correction due to perchlorate decomposition was taken into account. In this system the second term of this rate law was found to be much smaller and more difficult to resolve. For the first term the value of k_1 was found to be $6.7 \times 10^{-3} M^{-1} sec^{-1}$ at 160°C and the value of $\frac{k_{-1}}{k_2}$ was 0.51.

Exchange experiments with deuterium in place of hydrogen were also done. These gave rates consistent with previously proposed mechanisms, but in perchlorate solutions much higher exchange rates were observed than in sulphate solutions. The indicated value of k_3 is approximately the same in perchlorate as in sulphate solutions and the indicated value of $\frac{k_{-3}}{k_4}$ is much greater in perchlorate solutions.

ACKNOWLEDGEMENTS

The author wishes to express his gratitude to Dr. E. Peters for his inspiring direction of this study and the advice, help, and encouragement given throughout.

He wishes to thank the members of the faculty and staff of the Department of Metallurgy for their continued support and interest in this work.

The cooperation of Dr. J. A. Stone of Atomic Energy of Canada Limited in performing the mass spectrometric analyses is gratefully acknowledged.

The author wishes to thank the National Research Council for the award of two studentships (1960-62) and for financial aid through the N.R.C. Grant No. A-1463. The award of a Fellowship (1959-60) by the Consolidated Mining and Smelting Company Limited is gratefully acknowledged.

TABLE OF CONTENTS

	Page
INTRODUCTION	1
Hydrogen Reduction Reactions in Solution	1
Mechanism of Copper Catalyzed Hydrogen Reduction Reactions in Aqueous Solutions	4
Purpose and Scope of the Present Investigation	9
EXPERIMENTAL	10
Materials	10
Apparatus	10
Experimental Procedure and Analyses	11
RESULTS AND DISCUSSION	15
Reduction of Cupric Perchlorate	15
The Effect of Acidity on Rates	17
The Effect of Cuprous Ions on Rates	24
The Effect of Cupric Ions on Rates	27
Disproportionation Equilibria and Kinetics	30
The Integrated Rate Law	34
Reduction of Cupric Sulphate	41
The Effect of Acidity on Rates	42
The Effect of Cupric Sulphate on Rates	50
The Effect of Free Sulphate on Rates	55
Summary of Rate Constants	62
The Integrated Rate Curve	63
The Effect of Temperature on Rates	65
The Deuterium Exchange Experiments	70
The Activation of Hydrogen by Cuprous Ions	81
CONCLUSION	85
REFERENCES	87
APPENDIX A - Report on Research Work for the Period of May 1st to September 1st, 1960	91
APPENDIX B - Rate Measurements for Experiments in Perchlorate System	94
APPENDIX C - Determination of the Perchlorate Reduction Rate Constant k_{Cl}	97
APPENDIX C - Thermodynamic Data for Calculating ΔF°_{T} for the Disproportionation Reaction	100

Table of Contents Continued

Page

APPENDIX E - Integrated Rate Curves for the Perchlorate System . 101

APPENDIX F - Estimation of Hydrogen Ion Concentration in Sulphate System at 160°C 104

APPENDIX G - Rate Measurements for Experiments in Sulphate System 105

APPENDIX H - The Integrated Rate Curve for the Sulphate System . 107

APPENDIX I - Rate Curves and Rates of Exchange Experiments . . . 108

LIST OF FIGURES

Page

Figure 1. Schematic Diagram of Experimental Apparatus with Pressure Sampling System 13

Figure 2. Typical Rate Plots of $[Cu^+]$ vs Time Before and After Disproportionation 16

Figure 3. Rate Curves as a Function of Initial Perchloric Acid Concentration 18

Figure 4. Plots of $\frac{1}{2}\left(\frac{d[Cu^+]}{dt}\right)^{-1}$ vs $[H^+]$ at Different $[Cu^+]$ Levels 19

Figure 5. Plots of (Rate Function)$^{-1}$ vs $[H^+]$ at Different $[Cu^+]$ Levels 23

Figure 6. Rate Curves for Determination of Cuprous Activity 25

Figure 7. Dependence of Rate on Cuprous Concentration 26

Figure 8. Rate Curves as a Function of Initial Cupric Perchlorate Concentration 28

Figure 9. Plots of $[Cu^{++}]$/(Rate Function) vs $[Cu^{++}]^{-1}$ at Different $[Cu^+]$ Levels 29

Figure 10. Rate Plots of $[Cu^+]$, $[Cu^{++}]$ and Amount of $[Cu^{++}]$ Depleted; Together with a Calculated Curve as a Function of $[Cu^{++}]$ and $K = 26\ M^{-1}$ 33

Figure 11. Comparison of Experimental and Calculated Rate Curves . . 37

Figure 12. Comparison of Experimental and Calculated $[Cu^{++}]$ Rate Curves for Reduction in the Presence of Metallic Copper 39

Figure 13. Rate Curves as a Function of Initial Sulphuric Acid Concentration 43

Figure 14. Plots of Rate vs.$[Cu^I]$ as a Function of Acidity 44

Figure 15. Plots of I^{-1} vs $[H^+]$ for Acid Series of Experiments . . . 46

List of Figures Continued

Page

Figure 16. Plot of $\frac{I}{S}$ vs $[H^+]$ for Acid Series of Experiments 47

Figure 17. Plots of S^{-1} vs $[H^+]$ and $[H^+]^2$ for Acid Series of Experiments 49

Figure 18. Rate Curves as a Function of Initial Cupric Sulphate Concentration 51

Figure 19. Plots of Rate vs $[Cu^I]$ as a Function of Initial Cupric Concentration 53

Figure 20. Plots of S vs $[Cu^{II}]$ and $[Cu^{II}]^2$ for Cupric Series of Experiments 54

Figure 21. Plot of $\frac{[Cu^{II}]}{I}$ vs $\frac{1}{[Cu^{II}]}$ for Cupric Series of Experiments 56

Figure 22. Rate Curves as a Function of Free Sulphate Ion Concentration 58

Figure 23. Plots of Rate vs $[Cu^I]$ as a Function of Free Sulphate Concentration 59

Figure 24. Plot of I vs Free $[SO_4^{=}]$ for Sulphate Series of Experiments 60

Figure 25. Plot of S vs $[SO_4^{=}]$ for Sulphate Series of Experiments . . 61

Figure 26. Comparison of Experimental and Calculated Rate Curves . . 64

Figure 27. Rate Curves as a Function of Temperature 66

Figure 28. Plots of Rate vs $[Cu^I]$ as a Function of Temperature . . . 67

Figure 29. Plots of log k_1 and log k_3 vs T^{-1} 68

Figure 30. Rate Curves of Total Cu^I, HD, H_2 and (HD + $4H_2$) Experiment D_2-A 72

Figure 31. Rate Curves of Total Cu^I, HD, H_2 and (HD + $4H_2$) Experiment D_2-B 73

Figure 32. Rate Curves of Total Cu^+, HD, H_2 and (HD + $4H_2$) Experiment D_2-C 74

List of Figures Continued

Page

Figure 33. Rate Curves of Total Cu^{I}, HD, D_2 and (HD + $4D_2$) Experiment H_2-D 75

Figure 34. Plots of Net Forward Rate and Exchange Rate vs Cu^{I} for Each Exchange Experiment 77

Figure 35. Plots of Exchange Rate over Net Forward Rate vs Cu^{I} for Each Exchange Experiment 80

LIST OF TABLES

		Page
Table I.	Values of k_1 and $\frac{k_{-1}}{k_2}$ Obtained from Figure 5 and Earlier Studies	22
Table II.	Summary of Values of k_1 and $\frac{k_{-1}}{k_2}$ Obtained in the Perchlorate System	30
Table III.	Values of the Equilibrium Constant K for the Cu^{+}-Cu^{++}-Cu° Equilibrium at 160°C and Varying $[H^{+}]$.	31
Table IV.	Experimental Conditions for Sulphate Series and Estimated Free Sulphate, Bisulphate and Hydrogen Ion Concentrations	57
Table V.	Summary of Rate Constants for Sulphate Solutions at 160°C	62
Table VI.	Values of k_1, k_3 and Dissolved H_2 at Different Temperatures	65
Table VII.	Summary of Activation Energies and Entropies	69
Table VIII.	Experimental Conditions for Exchange Experiments . . .	71
Table IX.	Values of $\frac{k_{-1}}{k_2}$ and $\frac{k_{-3}}{k_4}$ from Exchange Experiments .	78

KINETICS OF COPPER REDUCTION BY HYDROGEN FROM AQUEOUS SOLUTIONS

INTRODUCTION

Hydrogen Reduction Reactions in Solutions

The precipitation of copper powder[1-4] from aqueous solutions of cupric salts by the action of hydrogen occurs readily at elevated temperatures and pressures, and since the discovery of this reaction considerable work has been done to establish its mechanism. It was shown from the beginning of this work that the precipitation of copper was easily distinguishable from that of nickel and cobalt[1,2,5-9], which required seeding with nucleating powder to obtain reduction, while such seeding was unnecessary for copper. The nickel and cobalt reduction mechanisms were therefore heterogeneous in nature and based on the catalytic properties of the surfaces of these metals toward hydrogen, while the copper reduction mechanism could be described as homogeneous as no metal surfaces were needed for the reaction to proceed, nor did they significantly affect the reaction rates.

These reactions are carried out in high pressure reactors at temperatures between 150 and 250°C and hydrogen partial pressures up to 400 psig. The metals are obtained in powder form and are at least as pure as electrolytically refined products of commerce.

In the case of copper a process[3] has been developed whereby the cupric species in ammonium sulphate leach solutions is reduced with hydrogen to metallic powder with a demonstrated purity of 99.51% and closely controlled screen size

down to -320 mesh. A modification of this process is employed at present[4] for the recovery of copper powder mostly from scrap brass, at a rate of about 20,000 lb per day.

Interest in the homogeneous reduction of cupric solutions has centered largely around kinetic studies of this and related reactions, particularly those where Cu^{++} catalyzes the hydrogen reduction of oxidants such as dichromate[10,11] and molecular oxygen[12]. The chief reason for interest in these reactions has been to elucidate quantitatively the mechanism of activation of hydrogen by kinetic experiments in a homogeneous system, a task that has been found to be experimentally much simpler than one of obtaining useful measurements in such heterogeneous systems as nickel and cobalt where metal surfaces serve as catalysts.

Interest in the kinetics of the copper catalyzed hydrogenation of oxygen originated from the possible application of this reaction for the recombination of the radiolytic decomposition products of water in aqueous homogeneous nuclear reactors[12].

The earliest recorded work on the hydrogen reduction of cupric salts in aqueous solution to the metallic state is that of Ipatieff and Werschowski[13], although they probably did not realize then the homogeneous nature of this reaction. This was probably suspected first by Halpern and Dakers[14,15] who studied the homogeneous precipitation of Cu_2O from cupric acetate solutions which took place according to the overall reaction

$$2\ CuAc_2 + H_2 + H_2O \longrightarrow Cu_2O + 4\ HAc \qquad .....(1)$$

The kinetics of this reaction, between 80 to 140°C and buffered between pH 3 to 5 could adequately be expressed by a second order rate law of the form

$$-\frac{d[CuAc_2]}{dt} = k[CuAc_2][H_2] \qquad .....(2)$$

where Ac = acetate and $[H_2]$ = molarity of dissolved hydrogen.

Subsequently Peters and Halpern[11] showed that substrates such as dichromate or iodate were reduced with hydrogen in the presence of cupric acetate, and thus established the homogeneous catalytic property of cupric ions in the hydrogen reduction of aqueous solutions. These workers[16] also studied the effect on dichromate reduction rates of complexing Cu^{++} with various ligands. By choosing as a standard the perchlorate system, in which Cu^{++} is believed to be complexed only as the aquo ion, they established that Cl^-, $SO_4^=$ and carboxylate ions such as acetate, propionate and butyrate enhanced the rates. This enhancement of the cupric activity by anions was ascribed to their ability to act as proton acceptors in the hydrogen activation reaction and thereby to lower the activation energy. On the other hand, a lowering of the cupric activity by such ligands as ethylenediamine and glycine was attributed to strong metal-ligand bonding.

It is noteworthy that several other metal ions besides cupric can activate hydrogen and either become reduced directly or alternately act as homogeneous catalysts for the reduction of substrates in aqueous solutions. Among these are Ag^+ [17,18], Ag^+ amine complexes[19], Hg^{++} [20,21], Hg_2^{++} [21] and certain complexes of the platinum group metals such as $PdCl_4^=$ [22], $RhCl_6^=$ [23] and chloride complexes of Ru^{III} [24,25]. Moreover, it was reported recently[26] that Cu^I in sulphate solutions catalyzed the hydrogen reduction of Cu^{II}, with Cu^I being more active than the latter. Ni^{II}, Fe^{+++}, Co^{++} and Cr^{+++}, on the other hand, were found to be inactive up to 260°C (Appendix A).

Related to these are similar reactions in non-aqueous solvents. For example, cuprous acetate dissolved in quinoline was found to catalyze the hydrogenation of quinone to hydroquinone[27], or the reduction of cupric acetate, which itself is inactive in this solvent[28]. Also, cuprous and silver acetate have been found to exhibit catalytic activity in pyridine and dodecylamine[29]

in the reduction of silver and cupric acetate, cupric acetate again being inactive. On the other hand, both cupric and cuprous heptanoates were observed to activate hydrogen in such organic media as diphenyl, octadecane and heptanoic acid in the reduction of cupric ions, with cuprous being the more active of the two[30].

It is noteworthy that only few metal ions possess the ability to activate hydrogen, whose inertness has been ascribed to its high dissociation energy (ca. 103 kcal) and the closed shell electronic configuration of the molecule. This property has been related to the relative electron affinities of the corresponding (gaseous) ions which show that the ions that activate hydrogen homogeneously have higher electron affinities and therefore lower lying vacant orbitals than ions not possessing this property[31,32]. It was further suggested that the optimum electronic configuration for catalytic activity exists when the d-shell is filled or nearly filled but when the ion has or can make available by electron promotion empty d-orbitals. This explains for example the activity of Cu^{+} ($3d^{10}$) and Ag^{+} ($4d^{10}$). The lack of catalytic activity of the isoelectronic Zn^{++} and Tl^{+++} ($3d^{10}$) and Cd^{++}($4d^{10}$) has been ascribed to their inability to promote electrons due to a larger separation of the d- and s-levels resulting from a higher nuclear charge.

Mechanism of Copper Catalyzed Hydrogen Reduction Reactions in Aqueous Solutions

The mechanism by which cupric ions activate hydrogen in reactions involving the reduction of copper or other oxidizing substrates in aqueous solutions is given by the following equations:

$$Cu^{++} + H_2 \underset{k_{-1}}{\overset{k_1}{\rightleftharpoons}} CuH^+ + H^+ \qquad .....(3)$$

$$CuH^+ + Cu^{++} \xrightarrow{k_2} 2Cu^+ + H^+ \qquad .....(4)$$

$$2Cu^+ \underset{K}{\overset{fast}{\rightleftharpoons}} Cu^\circ + Cu^{++} \qquad .....(5)$$

or

$$Cu^+ + Ox \xrightarrow{fast} Cu^{++} + Products \qquad .....(6)$$

where Ox = oxidant.

This mechanism was established by Halpern and coworkers[33] in perchlorate solutions where Cu^{++} is believed not to be complexed except as the aquo ion. It proceeds by the heterolytic splitting of the hydrogen molecule in the activation step resulting in the formation of a cupric hydride intermediate and a hydrogen ion, followed by reaction of the intermediate with another cupric ion and the production of two cuprous ions and a proton. The cuprous ions will either disproportionate when an equilibrium level has been reached or be oxidized to Cu^{++} in the presence of oxidants, e.g., dichromate. The rate law derived from this mechanism by a steady state approximation in CuH^+ is given by

$$-\frac{d[H_2]}{dt} = \frac{k_1[Cu^{++}]^2[H_2]}{\frac{k_{-1}}{k_2}[H^+] + [Cu^{++}]} \qquad .....(7)$$

with k_1 having a value of 9.5×10^{-5} $M^{-1}sec^{-1}$ and $\frac{k_{-1}}{k_2}$ a value of 0.26 at 110°C from dichromate reduction rate measurements.[33] The activation energy for the hydrogen activation step (equation 3) was found to be about 26 kcal/mole[11].

According to equation 7 reaction rates may appear to be either first or second order in $[Cu^{++}]$ depending on the relative magnitudes of the two terms in the denominator. For example if $\frac{k_{-1}}{k_2}[H^+] < [Cu^{++}]$, the rate expression will reduce to

$$-\frac{d[H_2]}{dt} = k_1[Cu^{++}][H_2] \qquad .....(8)$$

A rate law of this form was in fact observed by Peters and Halpern[11] between 80 and 140°C at 0.1 M [$Cu(ClO_4)_2$] and 0.004 to 0.1 M [$HClO_4$]. It is the same as that obtained by Halpern and Dakers for cupric acetate solution at pH 3 to 5, as shown above.

Macgregor and Halpern[34] subsequently studied the copper precipitation itself at temperatures between 150 and 175°C in both perchlorate and sulphate solutions. Although they did not analyse the complete rate curves they were able to check out the above mechanism (equations 3, 4, and 5) in the perchlorate system from initial rate measurements, and obtained the following constants for the rate law (equation 7) at 160°C: $k_1 = 7.5 \times 10^{-3} M^{-1} sec^{-1}$, $\frac{k_{-1}}{k_2} = 1.3$. This value of k_1 is consistent with $k_1 = 4.5 \times 10^{-3} M^{-1} sec^{-1}$, obtained by extrapolation of the Arrhenius plot in the dichromate work[11]. It was therefore apparent that initial copper reduction rates and the homogeneously catalyzed reduction of dichromate yielded the same values under the same conditions and thus the same mechanism appeared applicable to both systems. The larger value of $\frac{k_{-1}}{k_2}$ (1.3) at 160°C than that at 110°C (0.26)[33] suggested that this ratio might be increasing with temperature.

However, McDuffie and coworkers[12] were not able to find any acid dependence at 250°C in their kinetic studies of the Cu^{++}-catalyzed hydrogen-oxygen recombination reaction although this would be expected if the above mechanism were extrapolated to that temperature with oxygen replacing dichromate as the oxidant. Their solutions were 0.001 M in [Cu^{++}] and from 0.005 to 0.050 M in [$HClO_4$]. Under these conditions an acid dependence should have been observable* unless $\frac{k_{-1}}{k_2}$ was much smaller at 250°C than the 0.26 value at 110°C. Hence these results suggested a decrease in $\frac{k_{-1}}{k_2}$ with increasing temperature which was not consistent with the observations of the copper reduction reaction[34].

---

* An acid effect is observable when $\frac{k_{-1}}{k_2}$ [H^+] is of the order of [Cu^{++}] or greater.

To resolve this anomaly Hahn and Peters[35] studied the dichromate reaction again, this time in the 160 and 200°C range. Because of the strong temperature effect, which doubled the reaction rates for every 10°C increase in temperature the cupric perchlorate concentration was lowered from 0.10 M (used earlier in the range of 80 to 140°C[11]), to 0.02 M and the initial dichromate concentration raised substantially in order to obtain reaction times long enough for good rate measurements.

The results of this study showed that a dichromate dependence appeared under these conditions that indicated a direct attack by the oxidant on CuH^+, the reactive intermediate. The former mechanism (equations 3, 4, 6) still applied but with the addition of a supplementary reaction to account for the dichromate dependence, i.e.,

$$CuH^+ + Cr^{VI} \xrightarrow{k_3} Cu^{++} + \text{Products} \qquad .....(4a)$$

The rate law resulting by inclusion of equation 4a into the mechanism is

$$-\frac{d[H_2]}{dt} = \frac{k_1[Cu^{++}][H_2]\left\{\frac{k_2}{k_{-1}}[Cu^{++}] + \frac{k_3}{k_{-1}}[Cr^{VI}]\right\}}{[H^+] + \frac{k_2}{k_{-1}}[Cu^{++}] + \frac{k_3}{k_{-1}}[Cr^{VI}]} \qquad .....(9)$$

The values obtained at 160°C for k_1, $\frac{k_2}{k_{-1}}$ and $\frac{k_3}{k_{-1}}$ were 5.4 X $10^{-3}M^{-1}sec^{-1}$, 2.7 and 42 respectively. It was found also that both $\frac{k_2}{k_{-1}}$ and $\frac{k_3}{k_{-1}}$ were quite insensitive to temperature, being 2.6 and 49 respectively at 200°C.

It is apparent from equation 9 that the acid dependence would fall off if $\frac{k_3}{k_{-1}}[Cr^{VI}] > [H^+]$, and by cancellation the rate law would take the form of equation 8. If oxygen reacts with CuH^+ directly, like Cr^{VI}, the anomaly in the rate law observed by McDuffie et al.[12] could be explained by replacing $\frac{k_3}{k_{-1}}[Cr^{VI}]$ with $\frac{k_4}{k_{-1}}[O_2]$[35] in equation 9, assuming that the rate constant ratios are temperature insensitive up to 250°C.

---

* More than one species of Cr^{VI} is present in solution at these temperatures and acidities (see reference 36).

The inverse of $\frac{k_2}{k_{-1}}$ is 0.37 at 160°C which is comparable to the value of $\frac{k_{-1}}{k_2}$ = 0.26 at 110°C[33]. However, the value of 1.3 from the copper precipitation work is considerably higher and represents an additional anomaly.

The results of the dichromate work now appear to contain conclusive evidence for the validity of the mechanism including equation 4a and of the rate law given in expression 9 for all copper catalyzed reactions in which an oxidant exists that is capable of preventing the appearance of the cuprous state. In the precipitation of metallic copper, however, considerable amounts of cuprous ions make their appearance at least transiently and a knowledge of their role in the kinetics is essential for the complete understanding of the reaction mechanism. In this regard it is of interest that Dunning and Potter[26] reported a catalytic activity of cuprous in the hydrogen reduction of cupric sulphate solutions which accounted for a considerable portion of the observed rates. In perchlorate and sulphate solutions no cuprous activity was reported by Macgregor and Halpern[34]. Their copper reduction curves were analyzed by measuring initial rates only, and under these conditions Cu^+ levels never became significant.

Another point that needed explanation was the marked slowing down of the reduction rates observed by Macgregor and Halpern, which was much greater than predicted by the rate law (equation 7). Although the rate slows down as a result of decreasing $[Cu^{++}]$ and increasing $[H^+]$ it should not decrease to nearly zero after only about 60% of all Cu^{++} has been reduced (see for example Figure 11); particularly since thermodynamic estimates by Macgregor[37] indicated that the reaction at this point was far from equilibrium.

Hence, for the complete understanding of this system, particularly the role of Cu^+ in the kinetics, further work appeared necessary.

Purpose and Scope of the Present Investigation

In view of the foregoing discussion it is evident that several points still remained to be clarified for a complete understanding of the mechanism and rate law of the hydrogen reduction of cupric ions in aqueous solutions. Accordingly the present investigation was undertaken with the following objectives.

1. To explain the large value of $\frac{k_{-1}}{k_2}$ obtained by Macgregor and Halpern, in the copper reduction work.

2. To investigate the cuprous effect in both perchlorate and sulphate solutions.

3. To explain the marked slowing down of rates in the later stages of copper reduction from perchlorate solutions as observed by Macgregor and Halpern.

4. To establish whether metallic copper appearing after the disproportionation of Cu^+ had any effect on the reaction kinetics.

The copper reduction mechanism predicts that part of the hydrogen consumed will be regenerated from aqueous protons in the back reaction, equation 3. In order to verify this prediction a number of isotope exchange experiments were performed by replacing hydrogen with deuterium in either the gas or aqueous phase and measuring the rate of appearance of HD in each case.

Since cuprous ions disproportionate rapidly on cooling this reaction was utilized by Macgregor and Halpern[34] to measure rates of copper reduction. In the present work, however, it was decided to determine the $[Cu^+]$ levels at experimental temperatures in order to obtain rate curves that would show the effect of cuprous on the reduction rates. Hence, part of the experimental problem in this study was to develop a method of determining high temperature cuprous concentrations.

EXPERIMENTAL

Materials

All materials used were of Baker and Adamson Reagent Grade quality. Stock solutions of 2 M cupric perchlorate and about 1.3 M cupric sulphate were prepared by dissolving excess cupric oxide powder in a hot aqueous solution of the appropriate acid, filtering after dissolution was complete and diluting sufficiently to prevent crystallization of the copper salts at room temperature. Distilled water was used throughout.

Hydrogen, Nitrogen and Helium of commercial grade were supplied by Canadian Liquid Air Company in cylinders and used without further purification.

For the exchange experiments 100 liters (NTP) of D_2 was obtained at 500 psig in a 2.8 liter cylinder and also 1200 grams of D_2O in 100 gram ampoules. Both were supplied by the Liquid Carbonics Division of the General Dynamics Corporation. Both had a purity of better than 99.5 mole %; the chief impurity in D_2 being approximately 0.34 mole % HD.

Apparatus

All experiments were performed in either one of two autoclaves capable of working pressures up to 1000 psig at 300°C. One of these, of one-gallon capacity, was manufactured by Autoclave Engineers Inc., the other a 2-liter vessel, by the Parr Instrument Company. Both were of stainless steel, but, because of the corrosive solutions used in this work, they were lined with titanium. These liners were fitted closely into the vessel[*] and provided with

---

[*] Shrinkfitted into the Parr vessel.

a welded flange at the top which served as the gasket seat. In this way possible entrance of the experimental solutions or steam into the annular space between the liner and vessel was prevented. All other parts in contact with the solution, such as sampling-tube and -valve, stirrer, and thermowell were also of titanium. The lower end of the sampling tube was provided with a fritted glass filter which was attached with a teflon adapter, in order to prevent metallic copper particles from entering the sampling system. The stainless steel autoclave covers were protected from the splashing solution with teflon shields. The stirrer shafts were belt driven at speeds between 700 and 1000 rpm.

The solutions were heated with external ring type gas burners and the gas flow accurately controlled with a Brooksmite twin flow gas meter. Temperature control was maintained to within ± 0.3°C with either a Leeds and Northrup Micromax controller-recorder or a Thermistemp temperature controller made by the Yellowsprings Instrument Company.

Pressure was regulated with standard high pressure regulators and measured with a Bourdon type pressure gauge to within ± 3 psig. The gauge calibration was checked periodically against steam pressure at various temperatures.

Experimental Procedure and Analyses

The experimental procedure comprised the following steps:

1. flushing of the gas space above the solution to purge the residual air with nitrogen or helium,

2. heating of the solution to the desired temperature under the inert atmosphere at a pressure close to the total hydrogen and steam pressure during reduction,

3. flushing of the inert gas at temperature,

4. addition of hydrogen and,

5. periodic sampling of the solution to follow the rate of appearance of cuprous ions.

The Cu^{+} concentration was determined by oxidizing the sample solution with a measured volume of dichromate solution. The excess dichromate was analyzed with a Beckman Model DU spectrophotometer at 350 mu using silica cells, and the amount of Cu^{+} calculated by difference. No interference from absorption by both Cu^{++} or Cr^{+++} took place at this wavelength.

Sampling posed a special problem in this study because cuprous ions disproportionate rapidly on cooling and thus cause low results in the dichromate method of analysis. Hence a method was devised for removing solution samples from the autoclave and oxidizing them with dichromate before disproportionation from cooling could occur. This sampling arrangement is shown schematically in Figure 1. The sample solution flows via 0.062" O.D. X 0.032" I.D. titanium tubing into a 100 ml volumetric flask located in a vessel which is pressurized sufficiently to prevent flashing of the solution. A measured volume of dichromate solution is introduced from a pressure "burette" via a titanium "Tee" and reacts with the sample solution on its way to the flask. The pressure in the "burette" is adjusted initially to that in the autoclave and during sampling it drops to that in the sampling vessel. Sampling time was 7 to 15 seconds depending on the autoclave pressure, and the resulting sample volumes 35 to 50 ml. These volumes were determined by difference after cooling the solution to room temperature and filling the flask with distilled water from a burette.

As a further precaution the sampling valve body, the "Tee" and the interconnecting titanium tube were wrapped with an Electrothermal heating tape

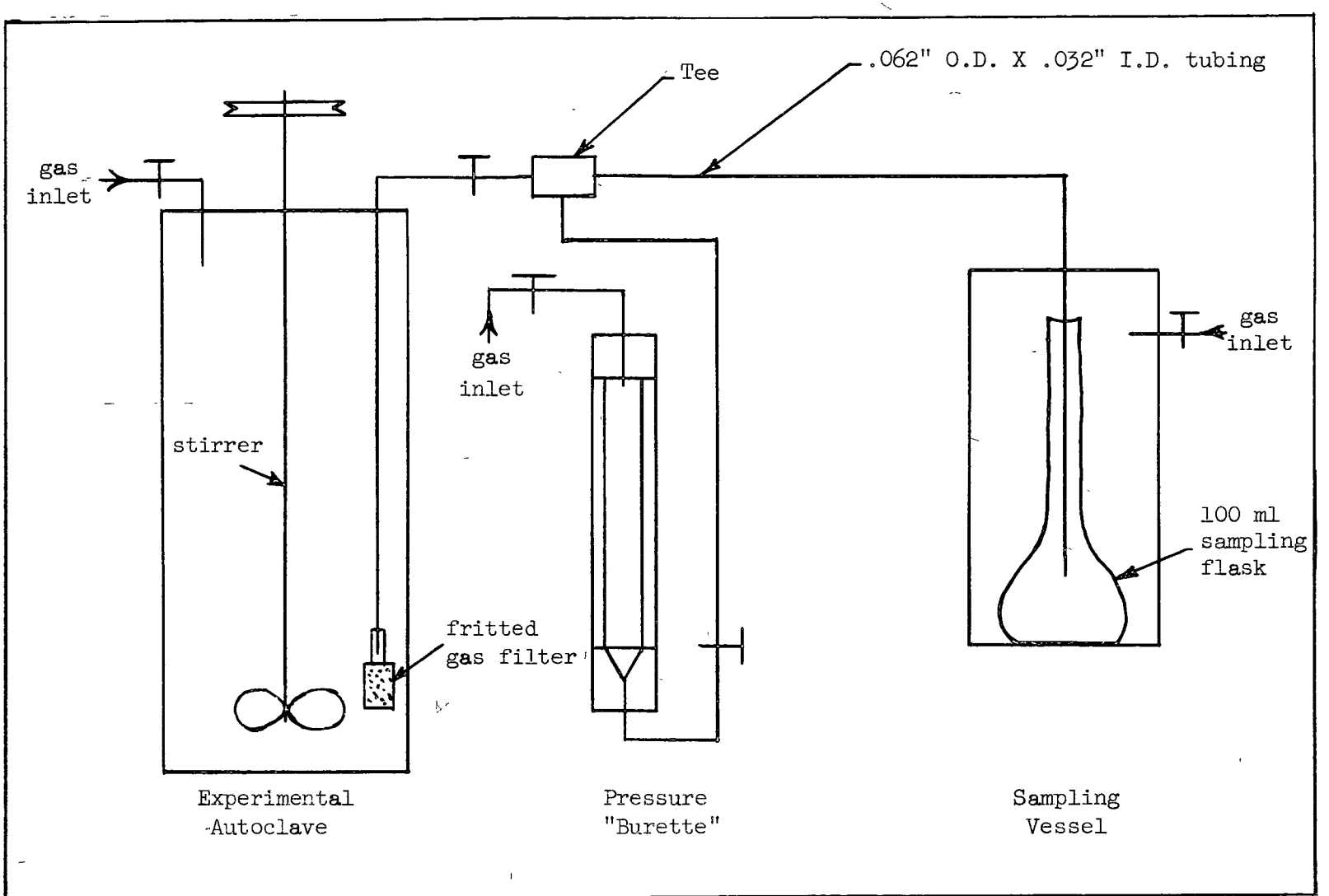

Figure 1. Schematic Diagram of Experimental Apparatus with Pressure Sampling System

and heated to a temperature close to the experimental. It was also found necessary to prepare the dichromate solutions with oxygen free water and keep them under a nitrogen atmosphere at all times, because small amounts of dissolved oxygen reacted with Cu^+ and lowered the dichromate consumption. Nitrogen was also used in the pressure sampling vessel.

The dichromate method of analysis was checked by precipitating Cu^+ with NH_4CNS, NaBr and KI or by letting Cu^+ disproportionate in the sample flask on cooling to room temperature. Analyses were then made by dissolution with nitric acid and electrolysis. The results agreed well with those obtained by the dichromate method, except in the disproportionation procedure which yielded generally lower Cu^+ values. This may have been due to incomplete disproportionation or to accidental oxygen contamination.

Total cupric (i.e. cupric and oxidized cuprous) was determined either electrolytically or by titration with EDTA solution[38] using Murexide as indicator. $[H^+]$ was determined by titration with sodium tetraborate[39], $[SO_4^=]$ as barium sulphate, and $[Cl^-]$ appearing in perchlorate solutions, by the Volhardt method[39].

In the exchange experiments gas samples were taken, at the same time as liquid samples, into evacuated sample bottles of about 1.5 ml capacity. The gas mixtures were analyzed with a mass spectrometer for D_2, HD and H_2 content by the Research Chemistry Branch, Chemistry and Metallurgy Division, Atomic Energy of Canada Limited, Chalk River, Ontario.

RESULTS AND DISCUSSION

Reduction of Cupric Perchlorate

The kinetic experiments were conducted under various initial conditions ranging from 0.01 to 0.10 M $[Cu(ClO_4)_2]$ and 0.01 to 0.10 M $[HClO_4]$ with a hydrogen partial pressure of 10 atm. Reduction rates were measured at stirring speeds varying between 700 and 1000 rpm. No differences were observed at these extremes, from which it was concluded that the rates were not controlled by a mass transport mechanism. Moreover it was found that no reduction took place in the absence of hydrogen. The experimental temperatures ranged from 160 to 220°C; however most experiments were performed at 160°C.

Typical rate curves are shown in Figure 2 as plots of $[Cu^+]$ vs time. It is evident that the initial rates and the maximum $[Cu^+]$ levels are a function of the starting Cu^{++} concentrations. The maxima of the upper two curves occur at the onset of Cu^+ disproportionation which takes place according to the following stoichiometry

$$2\ Cu^+ \underset{}{\overset{K}{\rightleftharpoons}} Cu^\circ + Cu^{++} \qquad .....(5)$$

where the disproportionation constant is given by

$$K = \frac{[Cu^{++}]}{[Cu^+]^2} \qquad .....(10)$$

After the start of disproportionation the $[Cu^+]$ level starts to fall since it remains in equilibrium with the declining Cu^{++} content of the solution. It is also evident in Figure 2 that below an initial $[Cu^{++}]$ of 0.03 M no disproportionation occurs at the experimental temperature. This may result from the rate becoming sufficiently slow so that $[Cu^+]$ cannot build up to the disproportionation level within the duration of the experiment.

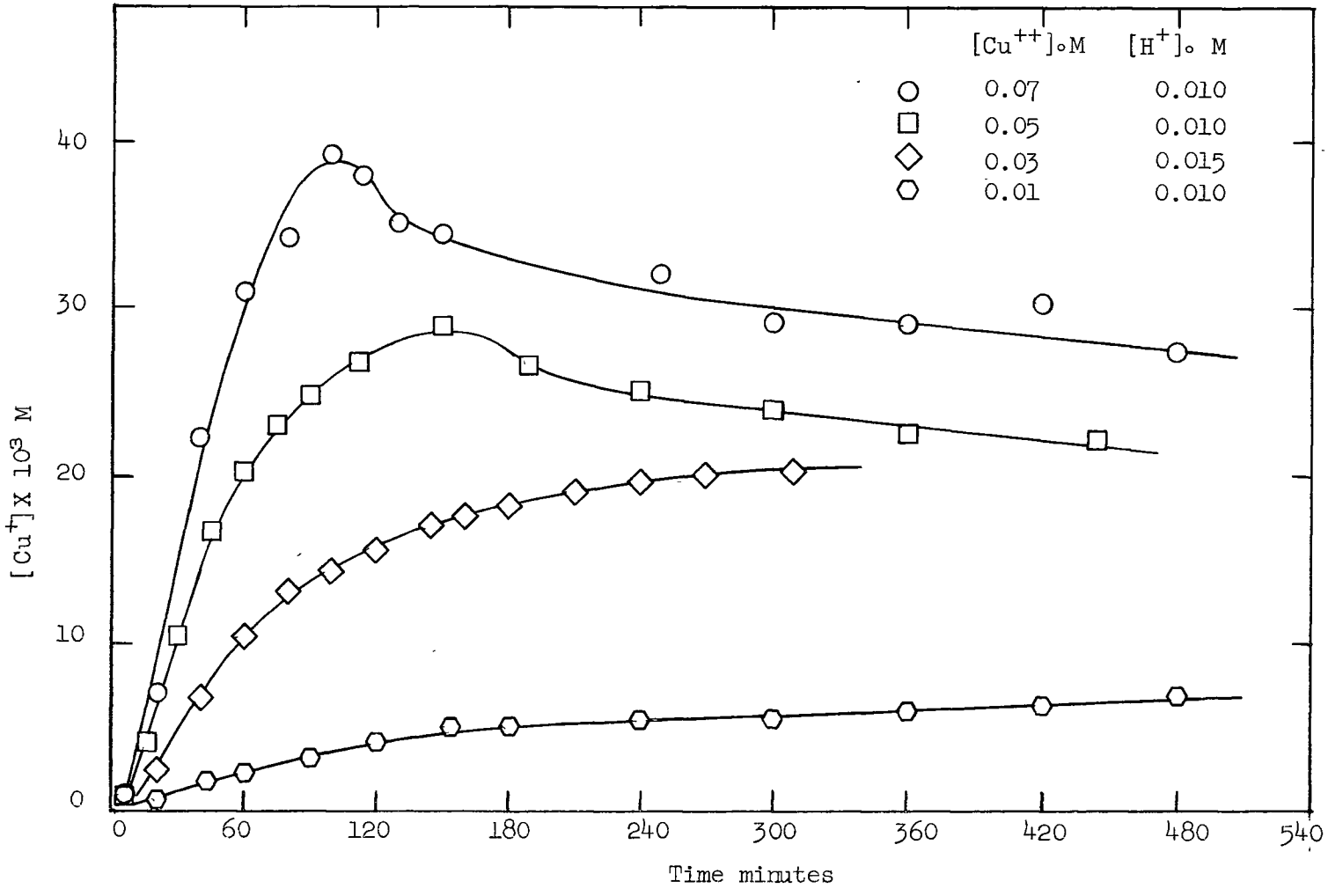

Figure 2. Typical Rate Plots of $[Cu^+]$ vs. Time Before and After Disproportionation; 10 atm H_2, 160°C.

Analytical results on samples after a significant amount of reaction had taken place revealed a copper to acid stoichiometry consistent with the overall equations

$$H_2 + 2\,Cu^{++} \longrightarrow 2\,Cu^{+} + 2\,H^{+} \qquad .....(11)$$

and

$$H_2 + Cu^{++} \longrightarrow Cu^{\circ} + 2\,H^{+} \qquad .....(12)$$

Equation 11 only applies to conditions before disproportionation at the experimental temperature, while both equations apply to conditions after disproportionation has begun. Under the former conditions the reaction rate $-\frac{d[H_2]}{dt}$ is simply equal to $+\frac{1}{2}\frac{d[Cu^{+}]}{dt}$ while after disproportionation begins the hydrogen consumption rate is $-\frac{d[Cu^{++}]}{dt} - \frac{1}{2}\frac{d[Cu^{+}]}{dt}$ [*]. Some experiments were performed with Cu^{+} initially equilibrated with Cu^{++} and metallic copper to study the reduction kinetics under conditions at which the disproportionation reaction occured from the start of a run.

The Effect of Acidity on Rates

A number of experiments were performed to investigate the effect of acidity on the copper reduction rates, with initial $[HClO_4]$ varying between 0.015 and 0.1 M and $[Cu^{++}]_o$ being 0.03 M. The rate curves of this series are shown in Figure 3. Rates were measured along these curves at five different $[Cu^{+}]$ levels and are shown plotted in Figure 4 as inverse rate, i.e., $\left(\frac{1}{2}\frac{d[Cu^{+}]}{dt}\right)^{-1}$, against $[H^{+}]$. These plots are non-linear especially for the higher $[Cu^{+}]$ levels and suggest a square dependence of $rate^{-1}$ on $[H^{+}]$. A rearrangement of equation 7 requires that such a plot of inverse rate vs $[H^{+}]$ should be linear with an intercept[**] given by

---

[*] Rate measurements for each experiment are listed in Appendix B.

[**] The intercepts of the curves in Figure 4 were calculated theoretically with equation 13 using $k_1 = 5.4 \times 10^{-3} M^{-1} sec^{-1}$ [35] because they were difficult to estimate as a result of the non-linearity of the plots.

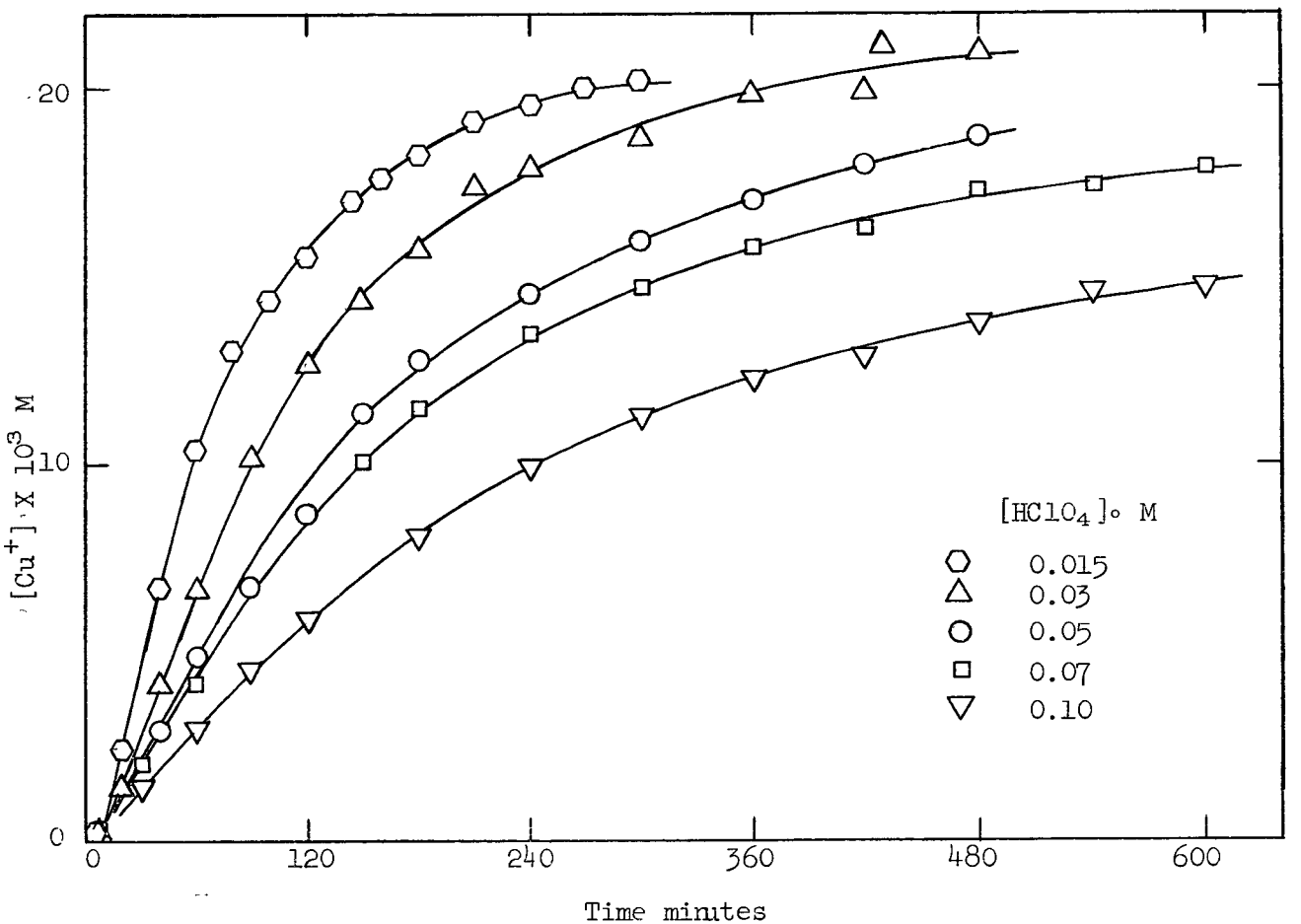

Figure 3. Rate Curves as a Function of Initial Perchloric Acid Concentration; 0.03 M$[Cu(ClO_4)]_o$, 10 atm H_2, 160°C.

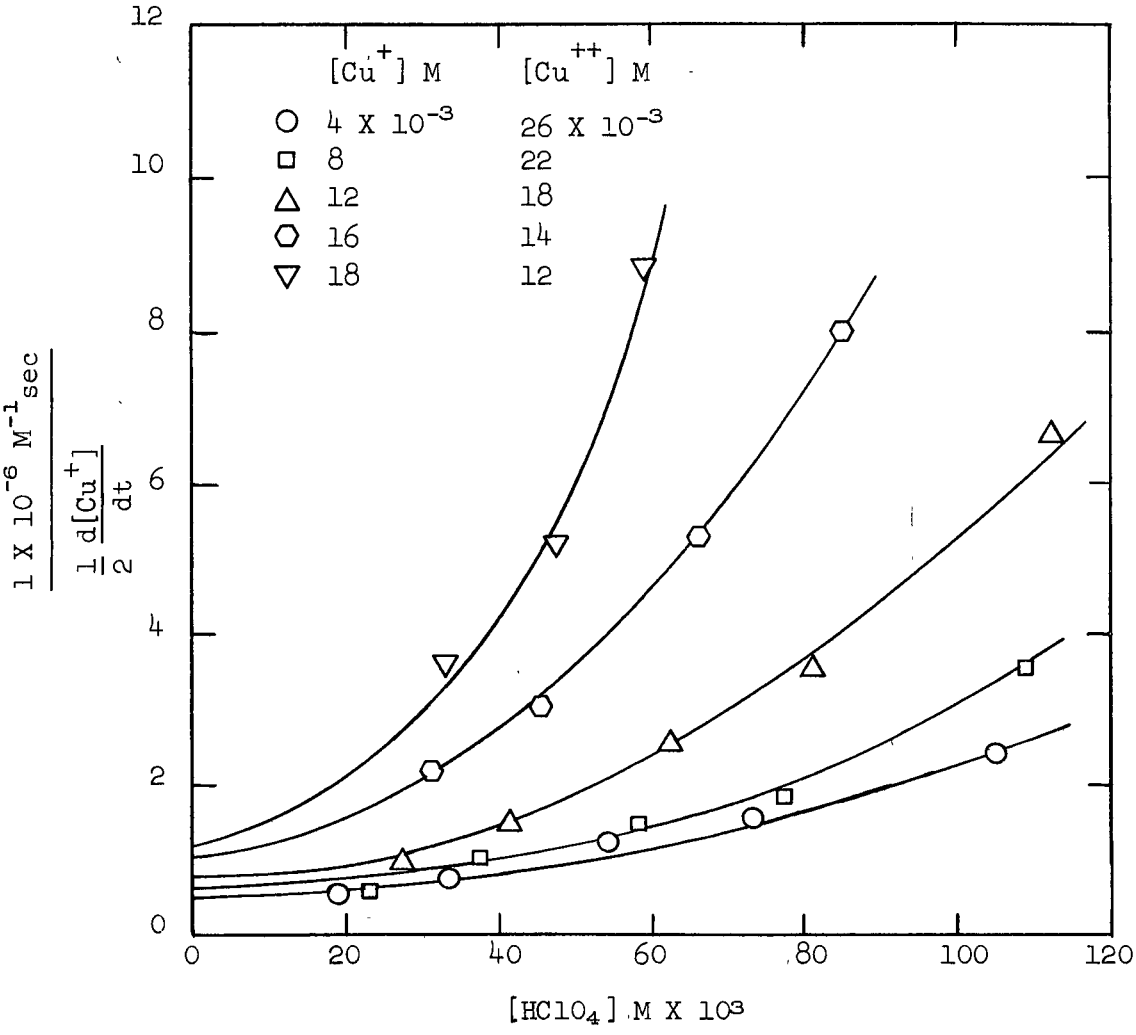

Figure 4. Plots of $\left(\frac{1}{2}\frac{d[Cu^+]}{dt}\right)^{-1}$ vs. $[H^+]$ at Different $[Cu^+]$ Levels; 0.03 M$[Cu^{++}]_o$, 10 atm H_2, 160°C.

$$I = \frac{1}{k_1[Cu^{++}][H_2]} \qquad .....(13)$$

and a slope corresponding to

$$S = \frac{\frac{k_{-1}}{k_2}}{k_1[Cu^{++}]^2[H_2]} \qquad .....(14)$$

This relationship assumes that there are no interfering side reactions that consume hydrogen by the copper activation route but do not reduce either cupric or cuprous stoichiometrically.

During the experiments, however, chloride ions made their appearance due to decomposition of perchlorate.

Since the stoichiometry of this reaction is probably

$$8\ Cu^{+} + 8\ H^{+} + ClO_4^{-} \longrightarrow 8\ Cu^{++} + Cl^{-} + 4\ H_2O \qquad .....(15)$$

the appearance of chloride ions corresponds to additional hydrogen consumption and becomes a serious interfering side reaction [*]. An experiment performed under the usual conditions but without cupric perchlorate added to the solution failed to produce measurable amounts of Cl^- indicating that the presence of Cu^+ is probably responsible for perchlorate decomposition. Thus, it became necessary to take into account the rate of perchlorate reduction in order to obtain a meaningful kinetic analysis of the experimental results. This was achieved by assuming a simple rate expression for the appearance of Cl^- of the form

$$\frac{d[Cl^-]}{dt} = k_{Cl}\,[Cu^{+}][H^{+}][ClO_4^{-}] \qquad .....(16)$$

---

[*] Perchlorate decomposition was found to be more serious at 180 to 220°C.

and incorporating it in the rate equation for the reduction of copper, i.e.,

$$\frac{1}{2}\frac{d[Cu^+]}{dt} = \frac{k_1[Cu^{++}]^2[H_2]}{\frac{k_{-1}}{k_2}[H^+]+[Cu^{++}]} - 4^{\ast} k_{Cl}[Cu^+][H^+][ClO_4^-] \quad .....(17)$$

The value of k_{Cl} was estimated by a graphical integration of equation 16 to the time at which $[Cl^-]$ was measured, and calculated with the following expression

$$k_{Cl} = \frac{[Cl^-]_t}{[ClO_4^-]\int_o^t ([Cu^+]^2 + [Cu^+][H^+]_o)\, dt} \quad .....(18)$$

where $[Cu^+]$ was measured directly from the rate curves. The details of the integration are shown in Appendix C. The value of k_{Cl} determined from eight different experiments was found to be $k_{Cl} = 2.07 \times 10^{-4} \pm 7\%\ M^{-2}sec^{-1}$. Although no attempt was made to establish if the rate law for Cl^- appearance was rigorously correct as given by equation 16, it appeared to be adequate for explaining the deviations from linearity of the plots in Figure 4.

The corrected rate law, equation 17, can be rearranged to the form

$$\frac{1}{\frac{1}{2}\frac{d[Cu^+]}{dt} + 4\, k_{Cl}[Cu^+][H^+][ClO_4^-]} = \frac{\frac{k_{-1}}{k_2}[H^+]}{k_1[Cu^{++}]^2[H_2]} + \frac{1}{k_1[Cu^{++}][H_2]} \quad .....(19)$$

Since $\frac{1}{2}\frac{d[Cu^+]}{dt} + 4\, k_{Cl}[Cu^+][H^+][ClO_4^-] = -\frac{d[H_2]}{dt}$ the function

$\frac{1}{\frac{1}{2}\frac{d[Cu^+]}{dt} + 4\, k_{Cl}[Cu^+][H^+][ClO_4^-]}$ can be plotted against $[H^+]$ and should yield a straight line with intercept and slope of the same form as given by equations

---

* The factor 4 results from the stoichiometry of the reaction

$$-\frac{1}{2}\frac{d[Cu^+]}{dt} \equiv -\frac{d[H_2]}{dt} \equiv 4\frac{d[Cl^-]}{dt}$$

13 and 14, i.e. $\frac{1}{k_1[Cu^{++}][H_2]}$ and $\frac{k_{-1}}{k_2} \times \frac{1}{k_1[Cu^{++}]^2[H_2]}$. Plots of this form are shown in Figure 5. Intercepts and slopes were determined for each plot from the best straight line drawn through the points and values of k_1 and $\frac{k_{-1}}{k_2}$ calculated*. They are listed in Table I together with the values of the earlier dichromate[35] and copper[34] reduction studies.

TABLE I.

Values of k_1 and $\frac{k_{-1}}{k_2}$ Obtained from Figure 5 and Earlier Studies

Curve No.	k_1 $M^{-1}sec^{-1}$	$\frac{k_{-1}}{k_2}$	Ref.
1	20.4×10^{-3}	3.0	
2	19.3×10^{-3}	2.3	
3	9.6×10^{-3}	0.85	
4	6.4×10^{-3}	0.54	
5	4.0×10^{-3}	0.28	
-	$(5.4 \pm 15\%) \times 10^{-3}$	$0.37 \pm 30\%$	35
-	7.5×10^{-3}	1.3	34

Average values of k_1 and $\frac{k_{-1}}{k_2}$ were calculated from the values of curves 3, 4 and 5 only, and are $k_1 = 6.7 \times 10^{-3} M^{-1}sec^{-1}$ and $\frac{k_{-1}}{k_2} = 0.56$. The values obtained from curves 1 and 2 are inconsistent with the other values shown in this table. The discrepancy in k_1 (hence $\frac{k_{-1}}{k_2}$) is probably due to the small values of the intercepts for these two curves in Figure 5. Also the magnitudes of these intercepts are very sensitive to the choice of the best straight line. Larger intercepts and smaller slopes giving more consistent values of these constants would be obtained if the initial rates of the low acid experiments were slower. They may be too fast due to a contribution from a hydrolyzed cupric species of higher activity such as $Cu(OH)^+$. This would give rise to activation of hydrogen

---

* Assuming the hydrogen solubility to be equal to that of pure water, i.e. $= 11.8 \times 10^{-4}$ M atm^{-1} at 160°C. See reference 40.

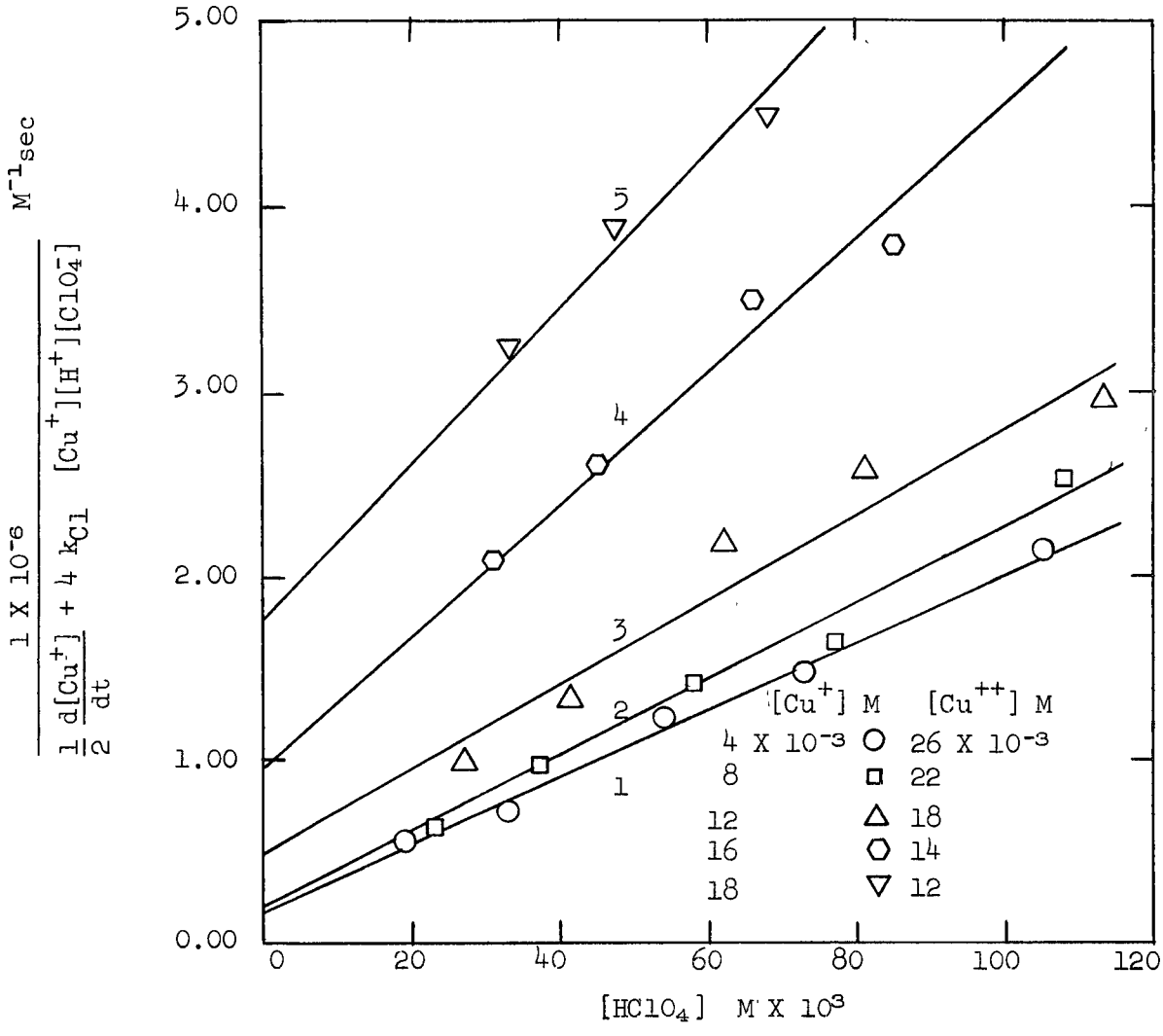

Figure 5. Plots of (Rate Function)$^{-1}$ vs. $[H^+]$ at Different $[Cu^+]$ Levels; 0.03 M $[Cu^{++}]_o$, 10 atm H_2, 160°C.

according to

$$Cu(OH)^{+} + H_2 \underset{k-}{\overset{k+}{\rightleftharpoons}} CuH^{+} + H_2O \qquad .....(20)$$

This explanation is supported by the observation (see page 38) that for low acid experiments the experimental rate curves exhibited considerably faster initial rates than those obtained from calculated rate curves. As Cu^{++} is reduced and $[H^{+}]$ increases this effect will disappear as evidenced by the lower values of k_1 and $\frac{k_{-1}}{k_2}$ obtained from curves 3, 4 and 5.

The Effect of Cuprous Ions on Rates

Several experiments were performed to determine if the substantial amounts of Cu^{+} produced during reduction had any effect on the rates in the perchlorate system, since Dunning and Potter[26] had observed a strong catalytic activity of cuprous ions in sulphate solutions. The initial Cu^{++} and H^{+} concentrations were so chosen that in a series of three experiments the $[Cu^{++}]$ and $[H^{+}]$ levels would remain constant across the series although the $[Cu^{+}]$ concentrations differed from one experiment to the next. The rate curves of this series are shown in Figure 6 and plots of rate* vs $[Cu^{+}]$ for three levels of $[Cu^{++}]$ and $[H^{+}]$ are depicted in Figure 7. The intercepts of these curves at zero $[Cu^{+}]$ were calculated with equation 7 using k_1 and $\frac{k_{-1}}{k_2}$ from the dichromate work[35]. It is evident that the rates increase measurably with $[Cu^{+}]$ (20 to 30% at the highest cuprous values). This contribution to the rates by cuprous ions probably explains the somewhat larger values of k_1 obtained by Macgregor and Halpern and in the present work as compared to the value from the dichromate work (see Table I.).

---

* Corrected for the perchlorate decomposition effect.

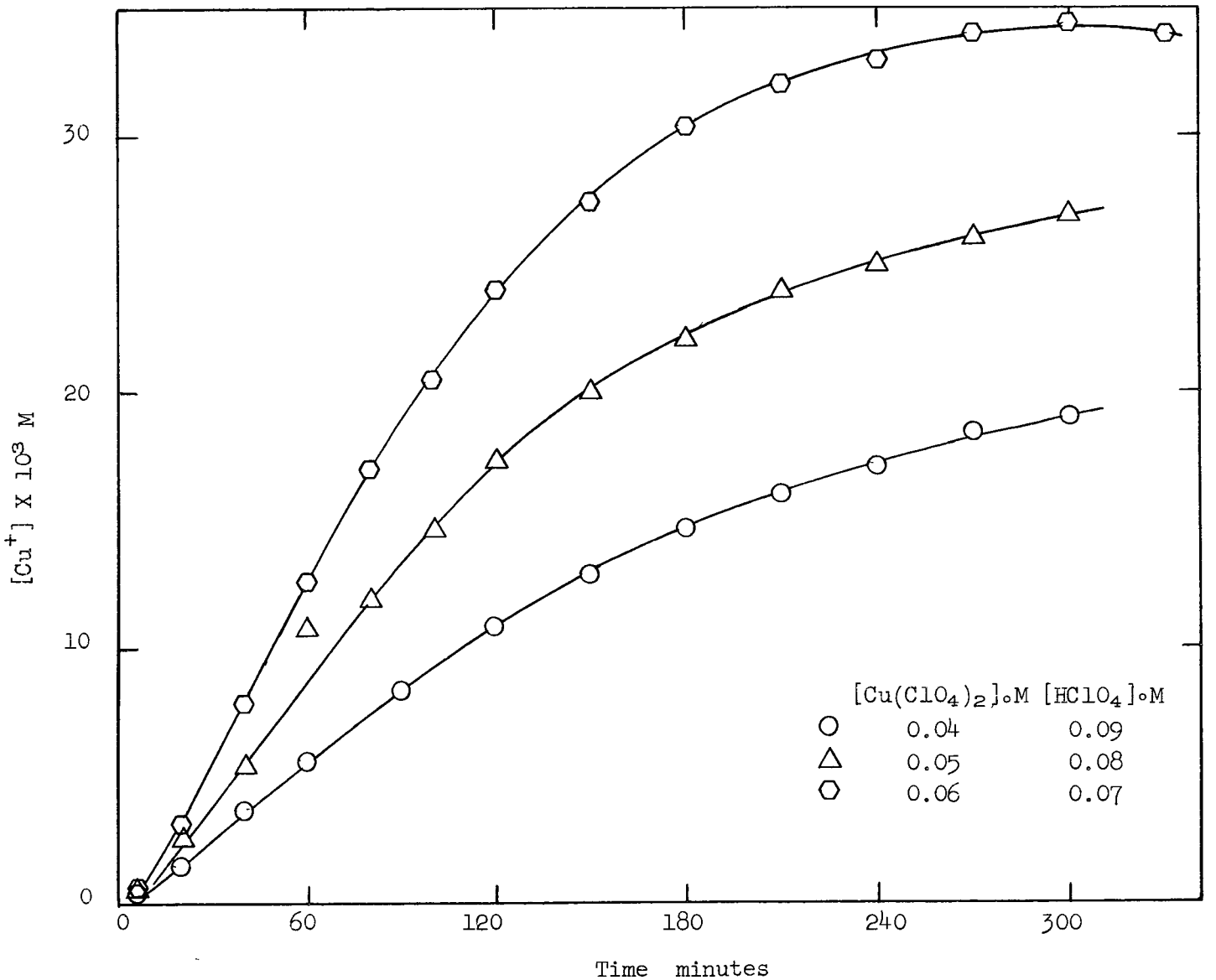

Figure 6. Rate Curves for Determination of Cuprous Activity; 10 atm H_2, 160°C.

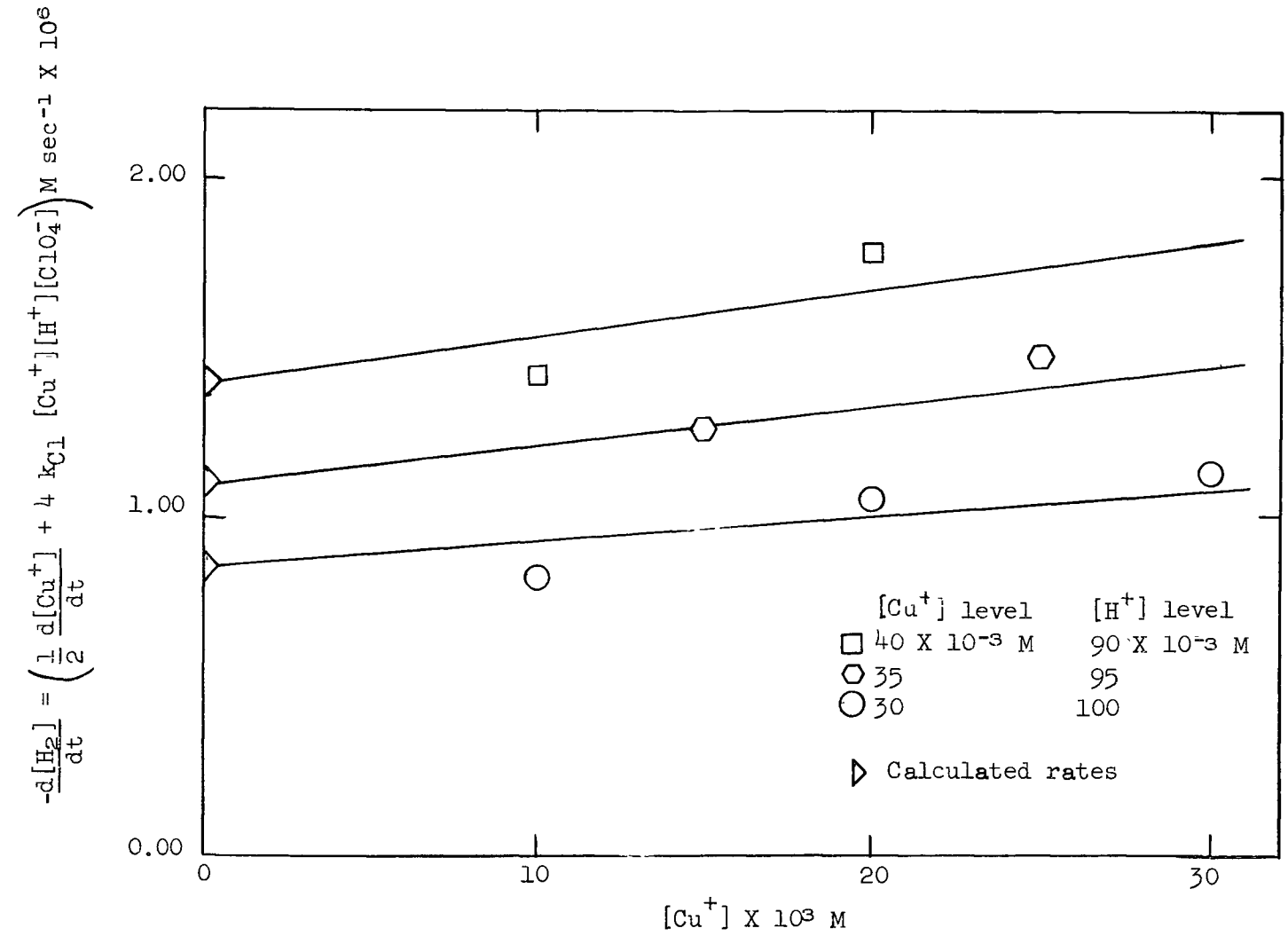

Figure 7. Dependence of Rate on Cuprous Concentration; 10 atm H_2, 160°C.

Although the curves in Figure 7 were drawn linear, the exact nature of the cuprous effect is difficult to assess, firstly because it is relatively small and secondly because of the uncertainty introduced by the perchlorate reduction effect. Moreover, the cuprous effect is hardly noticeable if the correction for perchlorate reduction is disregarded in the rate measurements.

The Effect of Cupric Ions on Rates

The inverted form of the rate law, equation 19, which contains a perchlorate decomposition correction but neglects contributions to the rate by Cu^+ may be rearranged to the form

$$\frac{[Cu^{++}]}{\frac{1}{2}\frac{d[Cu^+]}{dt} + 4\,k_{Cl}\,[Cu^+][H^+][ClO_4^-]} = \frac{\frac{k_{-1}}{k_2}[H^+]}{k_1\,[Cu^{++}][H_2]} + \frac{1}{k_1\,[H_2]} \quad \ldots\ldots(21)$$

and linear plots of the left hand side of this equation against $\frac{1}{[Cu^{++}]}$ yield intercepts of $\frac{1}{k_1[H_2]}$ and slopes of $\frac{\frac{k_{-1}}{k_2}[H^+]}{k_1\,[H_2]}$.

A series of experiments of varying initial cupric concentration was made to check out this equation. The rate curves of this series are depicted in Figure 8, and in Figure 9 a number of linear plots of the left hand side of equation 21 against $\frac{1}{[Cu^{++}]}$ are shown. The average value of k_1 obtained from the intercepts is $6.7 \times 10^{-3} M^{-1} sec^{-1}$ and $\frac{k_{-1}}{k_2}$ estimated from the slopes is 0.51. These values are in good agreement with those obtained in the acid series; k_1 again is somewhat larger than that from the dichromate work which may be due to neglecting the Cu^+ effect on rates in this case.

The values of k_1 and $\frac{k_{-1}}{k_2}$ obtained in both the acid and copper series of the present work are compared in Table II with those of the earlier studies. Those obtained from the dichromate work[35] are to be considered the most reliable because of the absence of interfering side reactions, i.e., the perchlorate decomposition and the cuprous effects, encountered in the copper reduction work.

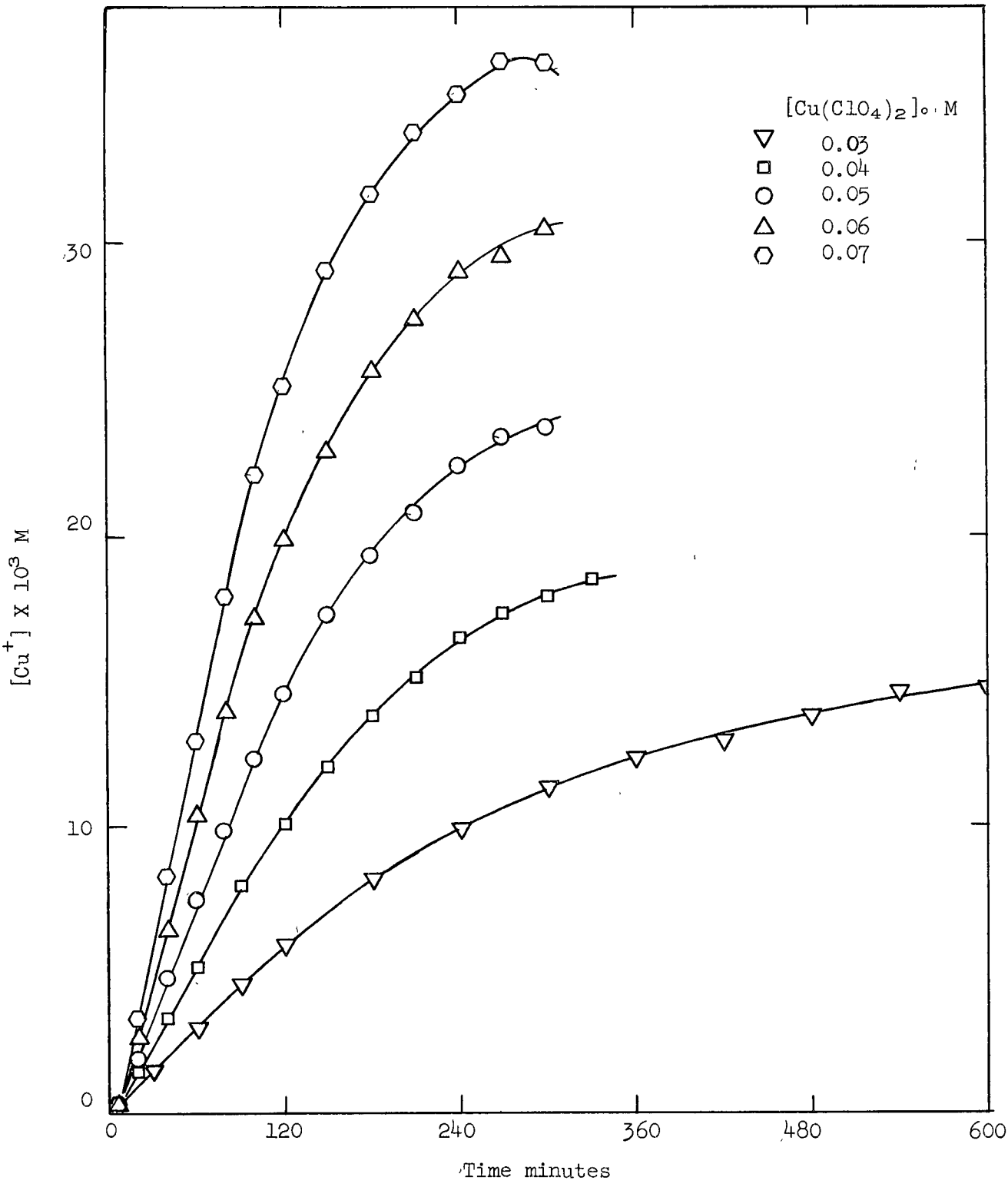

Figure 8. Rate Curves as a Function of Initial Cupric Perchlorate Concentration; 0.10 M[$HClO_4$]$_o$, 10 atm. H_2, 160°C.

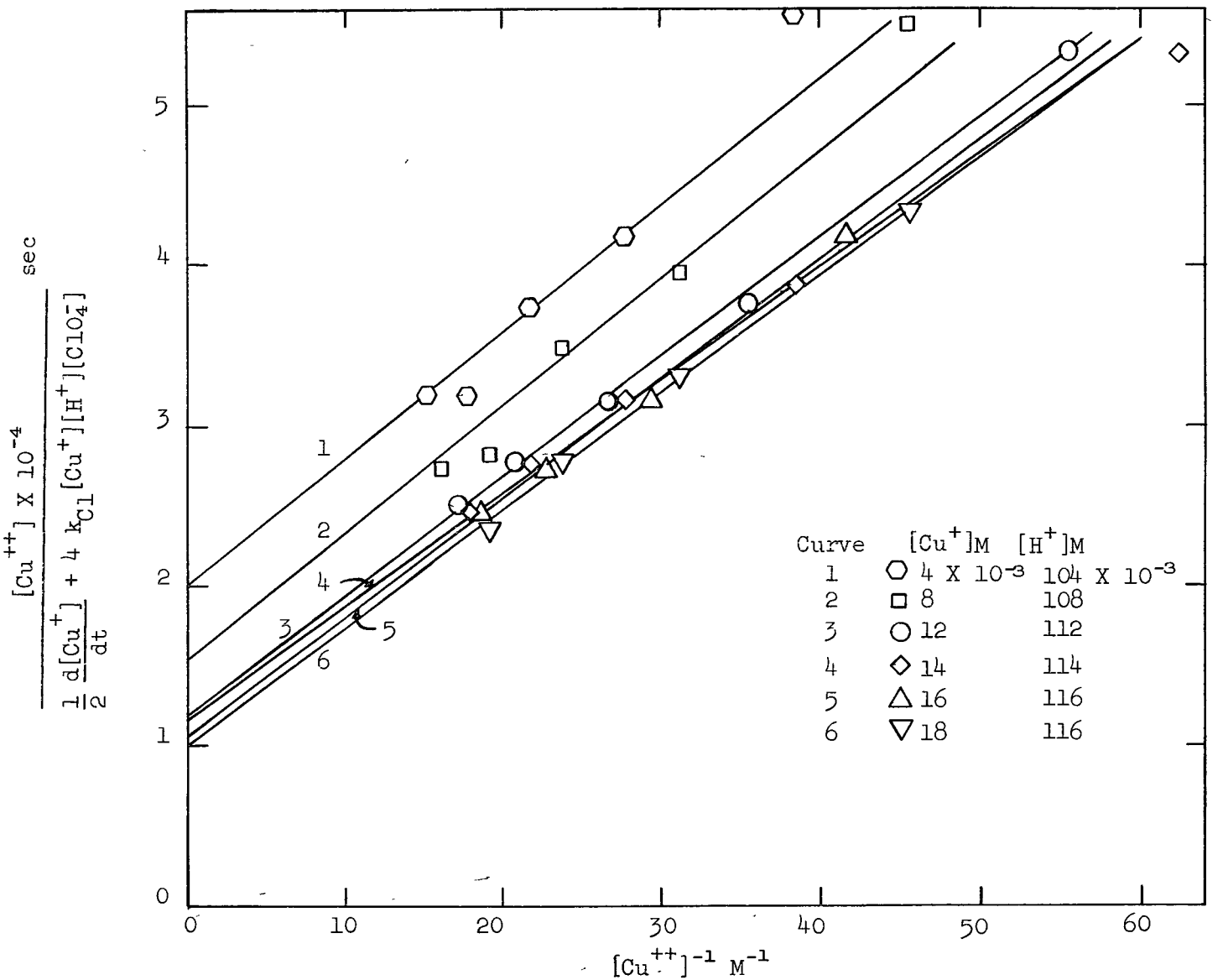

Figure 9. Plots of $[Cu^{++}]$/(Rate Function) vs $[Cu^{++}]^{-1}$ at Different $[Cu^+]$ Levels. 0.10 M$[HClO_4]$, 10 atm H_2, 160°C.

TABLE II.

Summary of Values of k_1 and $\frac{k_{-1}}{k_2}$ Obtained in the Perchlorate System

Temperature °C.	k_1 $M^{-1}sec^{-1}$	$\frac{k_{-1}}{k_2}$	Ref. or Figure
160	4.8×10^{-3} ✱	-	41
160	7.5×10^{-3}	1.3	34
160	$5.4 \times 10^{-3} \pm 15\%$	$0.37 \pm 30\%$	35
160	$6.7 \times 10^{-3} \pm 45\%$	$0.56 \pm 50\%$	Figure 5
160	$6.7 \times 10^{-3} \pm 20\%$	$0.51 \pm 20\%$	Figure 9

✱ By extrapolation from Arrhenius Plot

According to equation 21 the plots made from rate measurements at different $[Cu^+]$ levels should all have a common intercept, instead of the spread shown in Figure 9. This observed spread is attributable to neglecting the Cu^+ effect on rates. If contributions to the rate due to cuprous are deducted from the rate measurements these curves would be shifted upward and the largest correction would apply to those curves having the highest Cu^+ levels, i.e., the bottom curves. Thus they would be brought together as required by equation 21. Corrected curves of this kind are not presented because the form of the cuprous dependent contribution has not been resolved in perchlorate solutions. Also according to equation 21 the slopes of the plots in Figure 9 should shift slightly upward as the acidity increases during the course of a run. However, this shift is hardly observable firstly because the initial acidity is high (0.1 M) and does not increase significantly in the region where rate measurements were taken, and secondly because of the uncertainties introduced by both the perchlorate and cuprous effects.

Disproportionation Equilibria and Kinetics

It is evident from equation 5 that the disproportionation reaction is responsible for the appearance of metallic copper. This emphasizes the need for determining the extent to which the disproportionation reaction affects the copper reduction kinetics. Separate experiments were therefore conducted

at 160°C to determine the disproportionation constant under equilibrium conditions. A cupric perchlorate solution was equilibrated with about 2100 cm^2 of copper foil cut into small squares. An inert atmosphere of helium was used over the solutions. Samples were withdrawn in the usual way and several additions of perchloric acid were made during the experiment. The disproportionation equation, i.e.,

$$2\,Cu^{+} \overset{K}{\rightleftharpoons} Cu^{\circ} + Cu^{++} \qquad .....(5)$$

indicates that the reaction is pH independent but if a significant amount of cupric is hydrolyzed to $Cu(OH)^{+}$ an apparent pH dependence of the resulting constant due to the associated equilibrium

$$2\,Cu^{+} + H_2O \rightleftharpoons Cu(OH)^{+} + Cu^{\circ} + H^{+} \qquad .....(22)$$

will appear. The results of this experiment are given in Table III and indicate that above 0.03 M $[H^{+}]$ less than 15% of the cupric is hydrolyzed.

TABLE III.

Values of the Equilibrium Constant K for the Cu^{+}-Cu^{++}-Cu° Equilibrium at 160°C and Varying $[H^{+}]$

$HClO_4$ M	$K = \frac{[Cu^{++}]}{[Cu^{+}]^2}$ M^{-1}
0.007	44.3 ± 3.1
0.035	26.1 ± 2.0
0.083	25.5 ± 2.0

The resulting disproportionation constants at 160°C. for equation 5 is

$$K = \frac{[Cu^{++}]}{[Cu^{+}]^2} = 26 \pm 2\ M^{-1} \qquad .....(11)$$

if the activity coefficient ratio is assumed to be unity. Heinerth[42] found this to be a valid assumption between 20 and 60°C for copper sulphate solutions of varying ionic strength. In addition complexing of Cu^{+} with small amounts of Cl^{-}

ions, appearing from decomposition of perchlorate, was ignored as its effect was found to be within the given limits of accuracy of K, even, if it was assumed that all Cl^- was complexed as CuCl.

When K is used to calculate the equilibrium $[Cu^+]$ levels corresponding to the determined $[Cu^{++}]$ levels in a kinetic experiment, good agreement with the measured cuprous levels is obtained as shown in Figure 10. There appears a small amount of supersaturation at the maximum in the experimental curve, indicating that nucleation of metallic copper may be somewhat slow in this region. However, the amount of supersaturation shown could also be within experimental limits of precision, since very small nuclei of metallic copper could pass through the sample filter and be determined as cuprous through oxidation by dichromate.

Rates of nucleation for the disproportionation reaction have been measured by Courtney[43] at room temperature. The method used involved the observation of the time of appearance of a Tyndall effect in a solution of cuprous ammonium sulphate that was rapidly acidified to destroy the stable cuprous ammine complex ions. A tenth power dependence on cuprous concentration for the reciprocal of this time was interpreted as evidence that the critical nucleus contained 5 copper atoms. The same nucleation mechanism probably applies in the case of hydrogen reduction, but does not become rate determining, except perhaps transiently at the onset of copper precipitation.

The value of K = 26 M^{-1} at 160°C for the disproportionation reaction is significantly lower than that calculated for this reaction (equation 5) with the relation

$$\Delta F^\circ_T = \Delta F^\circ_{298°K} - \Delta S^\circ_{298°K} (T - 298) \quad .....(23)$$

by extrapolation of room temperature thermodynamic data (Appendix D) to 160°C. This extrapolation is based on the approximation that $\Delta H_T - \Delta H_{298} = T(\Delta S_T - \Delta S_{298})$.

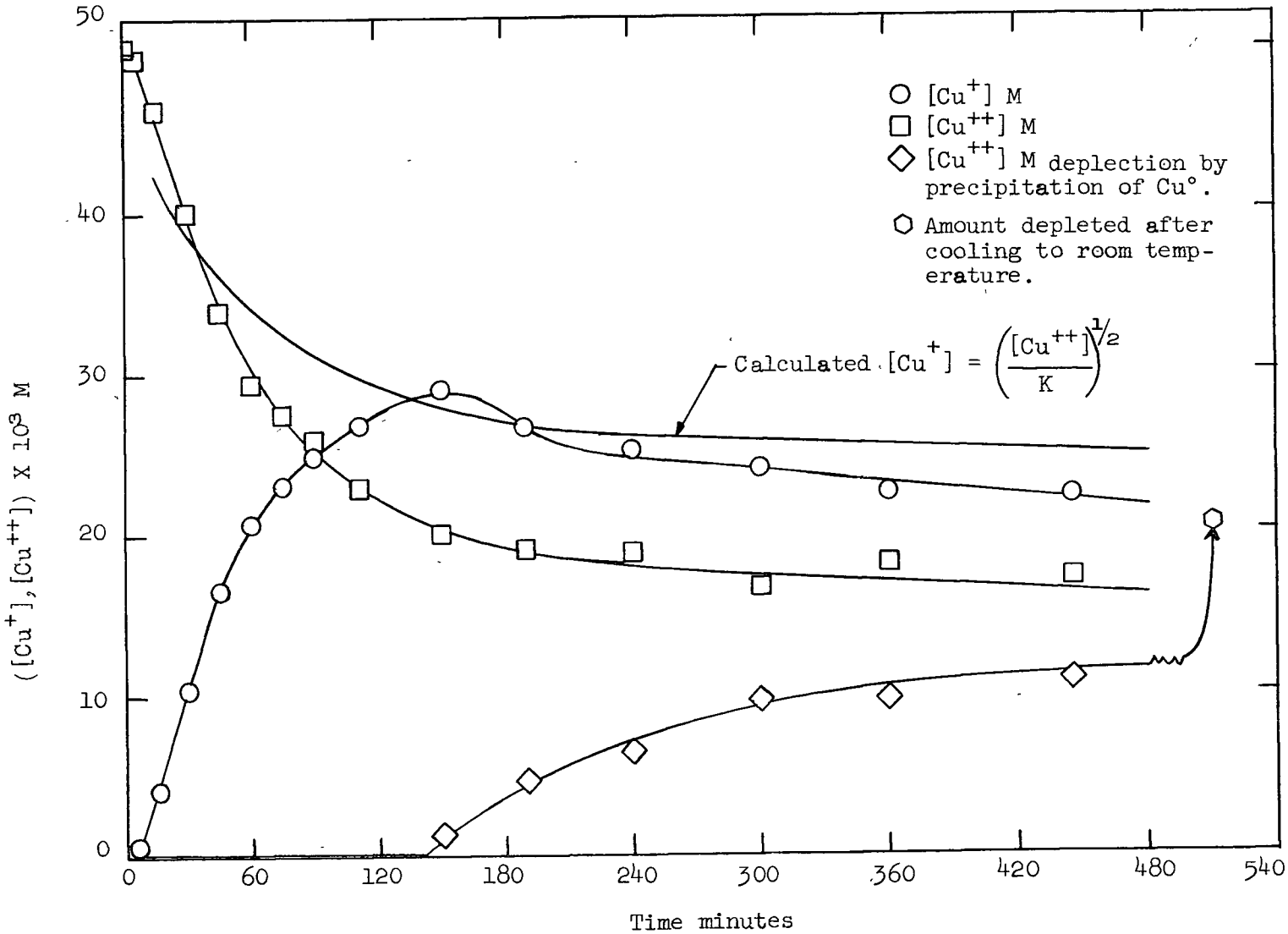

Figure 10. Rate Plots of $[Cu^{+}]$, $[Cu^{++}]$ and Amount of $[Cu^{++}]$ Depleted; Together with a Calculated $[Cu^{+}]$ Curve as a Function of $[Cu^{++}]$ and K = 26 M^{-1}; 0.01 M$[HClO_4]$, 10 atm H_2, 160°C.

The value of the equilibrium constant K is 89 M^{-1} when calculated with equation 23. This larger than experimental value is attributable to the foregoing approximation which, however, does not appear to be entirely valid. Very little has been done either experimentally or theoretically to show accurately the variation of thermodynamic properties from room temperature to high temperature (above 100°C.) in ionic aqueous solutions. In this regard the method of Criss[44] offers some promise for calculating the high temperature values of the entropies of ions with the aid of empirical equations. From these the correct values of the difference between $\Delta H_T - \Delta H_{298}$ and $T(\Delta S_T - \Delta S_{298})$ can theoretically be determined.

The Integrated Rate Law

Confirmation of the practical validity of a proposed rate law can be obtained by integrating the rate equation, using the derived constants to calculate a theoretical rate curve, and comparing it with one obtained experimentally under the same conditions.

The rate law given in equation 7 can be integrated mathematically both before and after disproportionation of cuprous ions. To perform this integration the differential form, i.e.,

$$-\frac{d[H_2]}{dt} = \frac{k_1[Cu^{++}]^2[H_2]}{\frac{k_{-1}}{k_2}[H^+] + [Cu^{++}]} \qquad .....(7)$$

must be defined in terms of a single dependent variable which may be either $[Cu^+]$ or $[Cu^{++}]$ depending on the experimental rate curve with which the theoretical curve is to be compared. Thus for $[Cu^+]$ as the dependent variable the relationship before disproportionation is

$$-\frac{d[H_2]}{dt} = \frac{1}{2}\frac{d[Cu^+]}{dt} \qquad .....(24)$$

which represents the stoichiometry of equation 11.

Also before disproportionation the following relations apply: $[Cu^{++}] = [Cu^{++}]_o - [Cu^+]$ and $[H^+] = [H^+]_o + [Cu^+]$, the subscript referring to initial concentrations. The rate law rewritten with $[Cu^+]$ as the dependent variable is then

$$\frac{d[Cu^+]}{dt} = \frac{2\,k_1\,([Cu^{++}]_o - [Cu^+])^2\,[H_2]}{\frac{k_{-1}}{k_2}\,([H^+]_o + [Cu^+]) + [Cu^{++}]_o - [Cu^+]} \qquad .....(25)$$

Integration of equation 25 yields an expression for t as a function of $[Cu^+]$ as follows

$$t = \frac{k_{-1}}{2k_1k_2[H_2]} \left(\frac{[H^+]_o + [Cu^{++}]_o}{[Cu^{++}]_o + [Cu^+]} - \frac{[H^+]_o}{[Cu^{++}]_o} - 1 \right) + \left(\frac{\frac{k_{-1}}{k_2} - 1}{2k_1[H_2]} \right) \times 2.3 \log \left(\frac{[Cu^{++}]_o - [Cu^+]}{[Cu^{++}]_o} \right) \qquad .....(26)$$

For the case after disproportionation it is convenient to use $[Cu^{++}]$ as the dependent variable. Then one writes

$$-\frac{d[H_2]}{dt} = -\frac{d[Cu^{++}]}{dt} - \frac{1}{2}\,\frac{d[Cu^+]}{dt} \qquad .....(27)$$

and since

$$[Cu^+] = \left(\frac{[Cu^{++}]}{K} \right)^{\frac{1}{2}} \qquad .....(28)$$

equation 27 can be written

$$-\frac{d[H_2]}{dt} = -\left(1 + \frac{1}{4\,K^{1/2}\,[Cu^{++}]^{1/2}} \right) \times \frac{d[Cu^{++}]}{dt} \qquad .....(29)$$

At the same time

$$[H^+] = [H^+]_o + 2[Cu^{++}]_o - 2[Cu^{++}] - \left(\frac{[Cu^{++}]}{K} \right)^{1/2} \qquad .....(30)$$

By substituting equations 29 and 30 into equation 7 the rate law valid after disproportionation is obtained, e.g.,

$$-\frac{d[Cu^{++}]}{dt} = \left\{ \frac{k_1[Cu^{++}]^2[H_2]}{\frac{k_{-1}}{k_2}\left[[H^+]_o + 2[Cu^{++}]_o - 2[Cu^{++}] - \left(\frac{[Cu^{++}]}{K}\right)^{1/2}\right] + [Cu^{++}]} \right\} \quad X$$

$$\left\{ \frac{1}{1 + \frac{1}{4K^{1/2}[Cu^{++}]^{1/2}}} \right\} \qquad \text{.....(31)}$$

The integrated form associated with equation 31 is

$$t = \left(\frac{1}{x} - \frac{1}{x_o}\right) \frac{k_{-1}\left(Q - \frac{1}{4K}\right)}{k_1 k_2 [H_2]} + \frac{\left(1 - \frac{2k_{-1}}{k_2}\right)}{k_1[H_2]} 2.3 \log\left(\frac{x_o}{x}\right) + \left(\frac{1}{x^{1/2}} - \frac{1}{x_o^{1/2}}\right) X$$

$$\frac{\left(\frac{1}{2} - \frac{3k_{-1}}{k_2}\right)}{k_1 K^{1/2}[H_2]} + \left(\frac{1}{x^{3/2}} - \frac{1}{x_o^{3/2}}\right) \frac{k_{-1} Q}{6k_1 k_2 K^{1/2}[H_2]} \qquad \text{.....(32)}$$

where $x = [Cu^{++}]$

$x_o = [Cu^{++}]_o$

$Q = [H^+]_o + 2[Cu^{++}]_o$

Equations 26 and 32 may then be used to calculate theoretical rate curves for given experimental conditions both in the absence and presence of metallic copper, and these curves can be compared with those obtained experimentally under the same conditions. A comparison of this kind is depicted in Figure 11 where curve A was calculated with equation 26 (Appendix E). It is seen that the agreement is quite good initially except for a slight lag in the experimental curve at the start of the run due to undetermined transient effects; however, in the later stages of the run the experimental rates decrease much faster than those predicted theoretically. This discrepancy between experimental and theoretical rates undoubtedly results from the perchlorate decomposition effect which was not included in the integrated rate law.

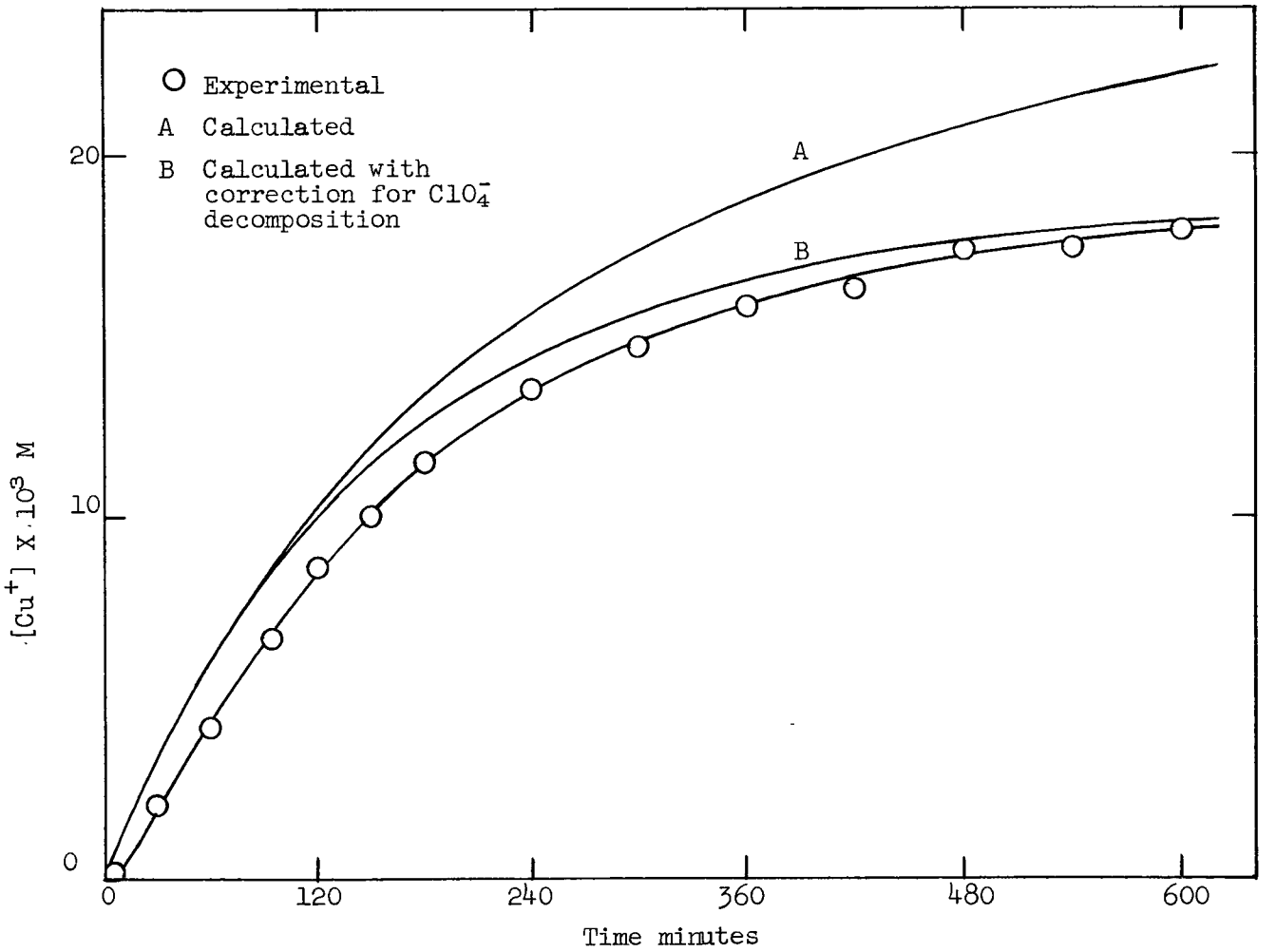

Figure 11. Comparison of Experimental and Calculated Rate Curves; 0.03 M$[Cu(ClO_4)_2]$∘, 0.07 M$[HClO_4]$∘, 10 atm H_2, 160°C.

To check the validity of the perchlorate effect as given by equation 16 the corrected rate law (equation 17) was also integrated*. The resulting curve B shown in Figure 11 is in good agreement with the experimental rate curve and illustrates the magnitude of the perchlorate decomposition effect.

Rate curves were also calculated for low acid experiments (0.01 M $[HClO_4]_o$). It was found that the initial rates of the experimental curves were faster than calculated. This discrepancy probably results from partial hydrolysis of cupric ions to $Cu(OH)^+$ which would give rise to activation of hydrogen that is faster than that by Cu^{++}.

One reduction experiment was performed with metallic copper (foil cut in small pieces) present at the beginning of the run to determine whether the rate law applying before disproportionation continues to be valid when copper begins to precipitate. The experimental solution, which was 0.137 M in $[Cu(ClO_4)_2]$ and 0.103 M in $[HClO_4]$ initially, was heated under an atmosphere of helium and held at 160°C for 70 minutes to allow full equilibration between Cu^{++}, Cu^+ and metallic copper before adding hydrogen. The experimental rate curves for $[Cu^{++}]$, $[Cu^+]$ and $[Cu^{++}]+[Cu^+]$ are depicted in Figure 12, with the values of $[Cu^{++}]$ obtained by difference from the measured $[Cu^+]$ and $[Cu^{++}]+[Cu^+]$ levels. The rate curve for $[Cu^{++}]$ is compared with curve A, calculated by graphical integration of a rate law that includes equation 31 and the perchlorate decomposition correction. This correction is significant for this experiment because of the large amounts of Cu^+ present initially. The rate law has the form

---

* Equation 17 was integrated graphically (Appendix E).

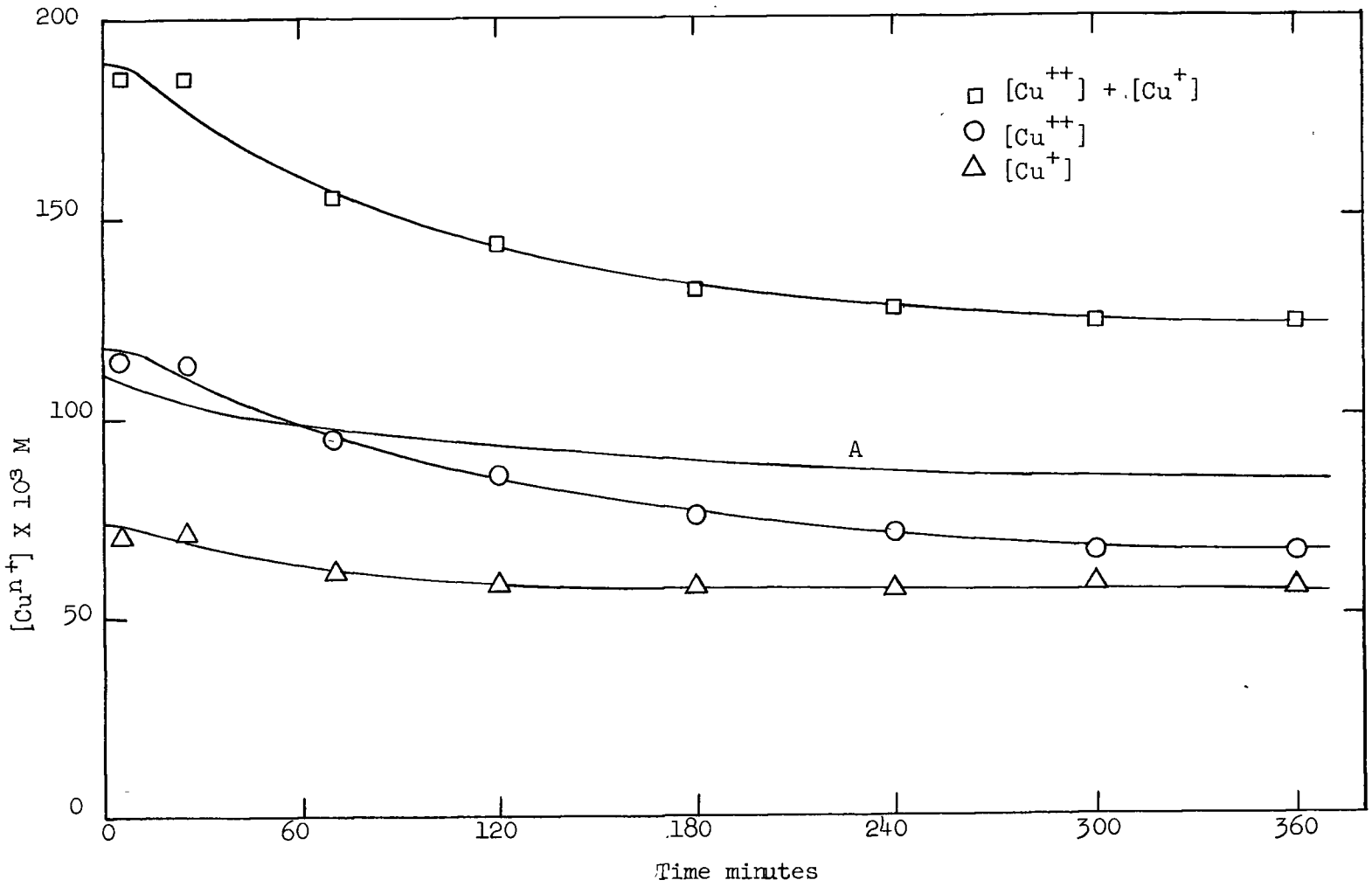

Figure 12. Comparison of Experimental and Calculated $[Cu^{++}]$ Rate Curves for Reduction in the Presence of Metallic Copper; 0.137 M $[Cu(ClO_4)_2]_o$, 0.103 M$[HClO_4]_o$, 10 atm H_2, 160°C.

$$-\frac{d[Cu^{++}]}{dt} = \left\{ \frac{k_1[Cu^{++}]^2[H_2]}{\frac{k_{-1}}{k_2}[H^+]+[Cu^{++}]} - 4\,k'_{Cl}\left(\frac{[Cu^{++}]}{K}\right)^{1/2}[H^+][ClO_4^-] \right\} \quad X$$

$$\left\{ \frac{1}{1+\frac{1}{4K^{1/2}[Cu^{++}]^{1/2}}} \right\} \qquad .....(33)$$

where $[H^+]$ is given by equation 30.

The experimental curve is steeper, at least initially, than the calculated curve A. This is not too surprising in view of the fact that the catalytic effect of cuprous ions was not taken into account when calculating curve A. Both curves show that the rate of copper reduction eventually decreases to zero. This decrease, as evident from equation 33, results from the perchlorate decomposition effect which increases markedly with the buildup of the hydrogen ion concentration. When this effect becomes equal to the forward rate, no net reduction of copper will occur until the perchlorate concentration is depleted sufficiently to slow down its rate of decomposition.

These observations also explain the results of Macgregor and Halpern[34]. Their copper reduction rates in the perchlorate system slowed to virtually zero at considerably higher $[Cu^{++}]$ levels than expected from thermodynamic estimates[37] that indicated the reduction reaction at these levels was far from equilibrium.

Reduction of Cupric Sulphate

Reduction experiments with cupric sulphate revealed a considerable increase in rates with rising Cu^{I} concentration despite decreasing $[Cu^{II}]$ (Figure 13) which is evidence that a reaction mechanism involving the cuprous species is involved.

The kinetics of cupric sulphate reduction had been studied earlier by Dunning and Potter[26] who had also observed this effect and had proposed the following mechanism for this reaction,

$$Cu^{II} + H_2 \underset{k_{-1}}{\overset{k_1}{\rightleftharpoons}} CuH^+ + H^+ \qquad .....(34)$$

$$CuH^+ + Cu^{II} \xrightarrow{k_2} 2Cu^{I} + H^+ \qquad .....(35)$$

$$Cu^{I} + H_2 \underset{k_{-3}}{\overset{k_3}{\rightleftharpoons}} CuH + H^+ \qquad .....(36)$$

$$CuH + Cu^{II} \xrightarrow{k_4} CuH^+ + Cu^{I} \qquad .....(37)$$

$$2\,Cu^{I} \underset{K}{\overset{fast}{\rightleftharpoons}} Cu^{\circ} + Cu^{II} \qquad .....(5)$$

A two term rate law derived from this mechanism by a steady state approximation in CuH^+ and CuH has the form

$$-\frac{d[H_2]}{dt} = \frac{k_1[Cu^{II}]^2[H_2]}{\frac{k_{-1}}{k_2}[H^+]+[Cu^{II}]} + \frac{k_3[Cu^{II}]^2[Cu^{I}][H_2]}{\left(\frac{k_{-1}}{k_2}[H^+]+[Cu^{II}]\right)\left(\frac{k_{-3}}{k_4}[H^+]+[Cu^{II}]\right)} = R_{Cu^{II}} + R_{Cu^{I}} \qquad .....(38)$$

where $R_{Cu^{II}}$ and $R_{Cu^{I}}$ are respectively the rate of direct reduction of cupric and the cuprous dependent part of the total rate.

Several series of experiments performed in the present study, revealed that the above mechanism and rate law appear to describe adequately the hydrogen reduction kinetics of the aqueous copper sulphate system. Dunning and Potter verified the first term of this rate law, however, their cuprous dependent term was linear in both $[Cu^{I}]$ and $[H^{+}]$ in the denominator.

The experimental series in this work included studies of the effects on rate of acidity, initial cupric concentration, free sulphate concentration and temperature. Throughout these series the total sulphate concentration was kept constant at 1 M by addition of a sufficient amount of a "neutral"* salt such as $MgSO_4$, to keep the initial formal ionic strength relatively constant for all series.

The Effect of Acidity on Rates

A series of experiments to investigate the acidity on rates, was performed under the following initial conditions: $[CuSO_4]_o$ 0.15 M, $[H_2SO_4]_o$ 0.5 to 0.85 M, sufficient $MgSO_4$ to make the solution 1 M in total sulphate, hydrogen partial pressure 5 atm and temperature 160°C. Rate curves for this series are shown in Figure 13. Rates** were measured along these curves at several $[Cu^{I}]$ levels and plotted against $[Cu^{I}]$ as seen in Figure 14. The linearity of these plots indicates that the cupric reduction rate is first order in $[Cu^{I}]$. The intercepts, I, of these curves obtained by extrapolating to zero cuprous correspond to rates independent of $[Cu^{I}]$, i.e., the direct activation of hydrogen by cupric according to equation 34. These rates should follow the first term of the rate equation 38 and as in the perchlorate case one

---

* Catalytically inactive toward hydrogen.

** Appendix G.

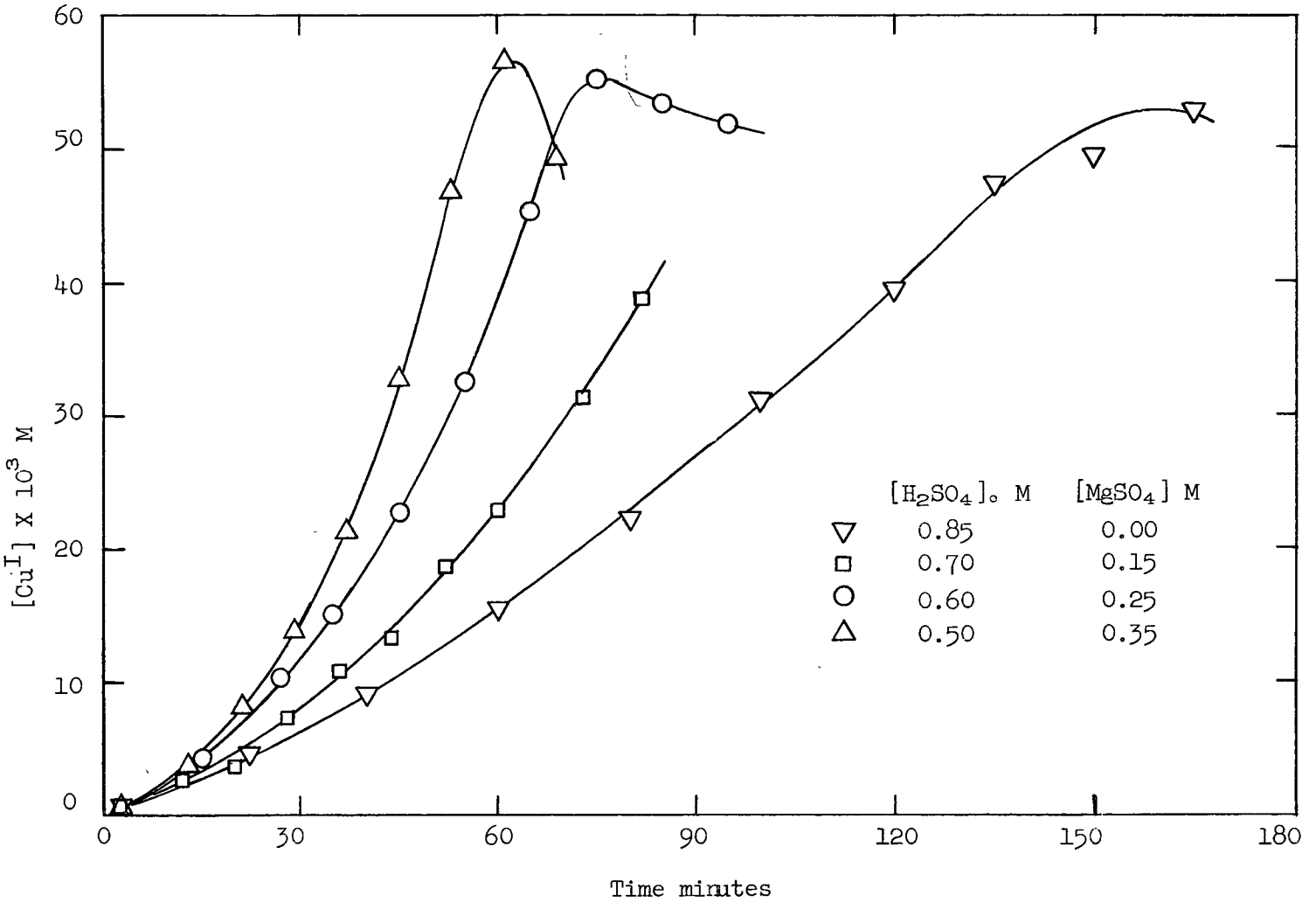

Figure 13. Rate Curves as a Function of Initial Sulphuric Acid Concentration; 0.15 M[CuSO$_4$]$_o$, 5 atm H_2, 160°C.

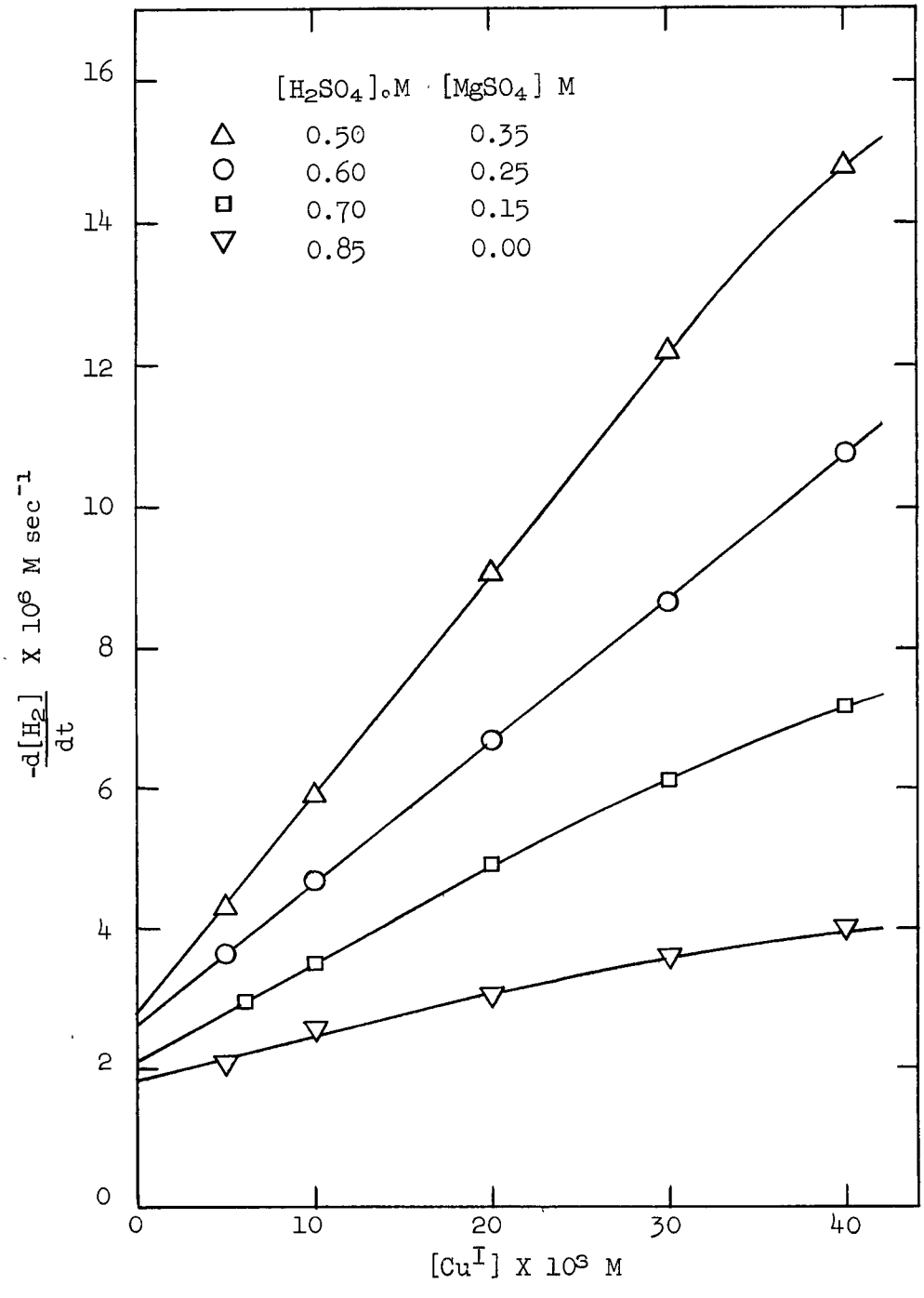

Figure 14. Plots of Rate vs $[Cu^{I}]$ as a Function of Acidity; 0.15 M$[CuSO_4]$◦, 5 atm H_2, 160°C.

may write

$$\frac{1}{R_{Cu^{II}}} = \frac{1}{I} = \frac{\frac{k_{-1}}{k_2}[H^+]}{k_1[Cu^{II}]^2[H_2]} + \frac{1}{k_1[Cu^{II}][H_2]} \qquad .....(39)$$

which is a linear equation of I^{-1} in $[H^+]$. A plot of this form is depicted in Figure 15, and average values of k_1 and $\frac{k_{-1}}{k_2}$ calculated from the expressions for intercept and slope in equation 39 are respectively $k_1 = 3.2 \times 10^{-3} M^{-1}sec^{-1}$ and $\frac{k_{-1}}{k_2} = 0.13$. The spread shown in Figure 15 for the values of the hydrogen ion concentration results from the assumption that K_b, the bisulphate dissociation constant, which is not known at 160°C, has a value between 10^{-3} and $10^{-2}M$, and that complexing of $SO_4^=$ by cupric ions can be neglected (Appendix F).

The cuprous dependent part of the rate, $R_{Cu}I$, can be evaluated from the initial slopes of the rate vs $[Cu^I]$ plots in Figure 13. According to the expression for $R_{Cu}I$ in equation 38 these slopes are given by

$$S = \frac{R_{Cu^I}}{[Cu^I]} = \frac{k_3[Cu^{II}]^2[H_2]}{\left(\frac{k_{-1}}{k_2}[H^+]+[Cu^{II}]\right)\left(\frac{k_{-3}}{k_4}[H^+]+[Cu^{II}]\right)} \qquad .....(40)$$

If the expression for $R_{Cu}{}^{II}$ in equation 38 is divided by S one obtains

$$\frac{R_{Cu^{II}}}{S} = \frac{I}{S} = \frac{k_1}{k_3}\cdot\left(\frac{k_{-3}}{k_4}[H^+]+[Cu^{II}]\right) \qquad .....(41)$$

which is a linear expression of $\frac{I}{S}$ in $[H^+]$ with an intercept $I = \frac{k_1}{k_3}[Cu^+]$ and a slope $S = \frac{k_1}{k_3}.\frac{k_{-3}}{k_4}$. The plot of $\frac{I}{S}$ vs $[H^+]$ is depicted in Figure 16. Using the average value of k_1 ($3.2 \times 10^{-3} M^{-1}sec^{-1}$), obtained from Figure 15, the following average values of k_3 and $\frac{k_{-3}}{k_4}$ were calculated from the intercept and slope in Figure 16: $k_3 = 6.4 \times 10^{-2} M^{-1}sec^{-1}$ and $\frac{k_{-3}}{k_4} = 0.45$. k_3 is therefore considerably larger than k_1. This accounts for the fact that the Cu^{II} reduction rates are enhanced markedly with increasing Cu^I concentration.

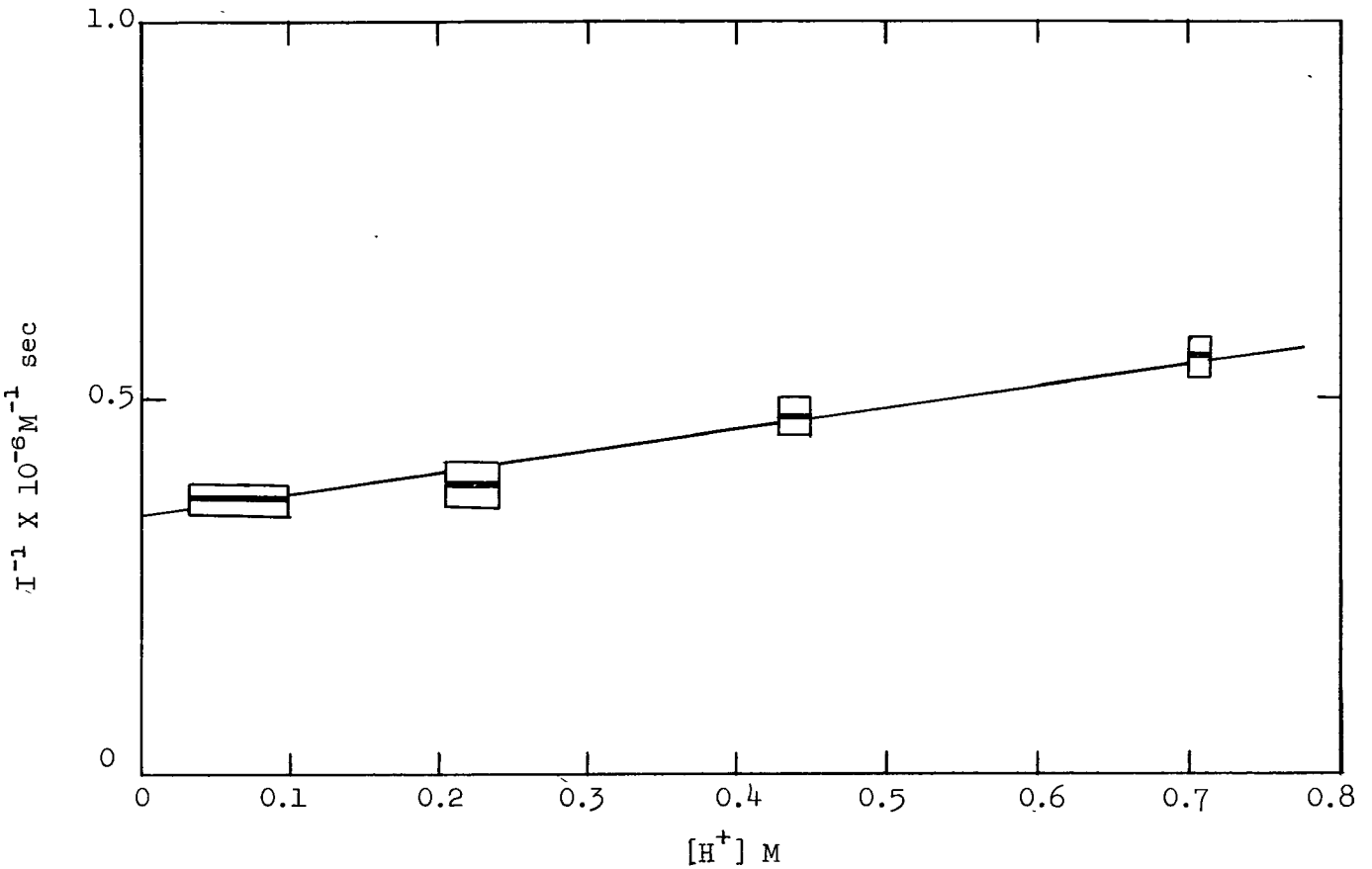

Figure 15. Plot of I^{-1} vs $[H^+]$ for Acid Series of Experiments; 0.15 M$[CuSO_4]_o$; 5 atm H_2, 160°C.

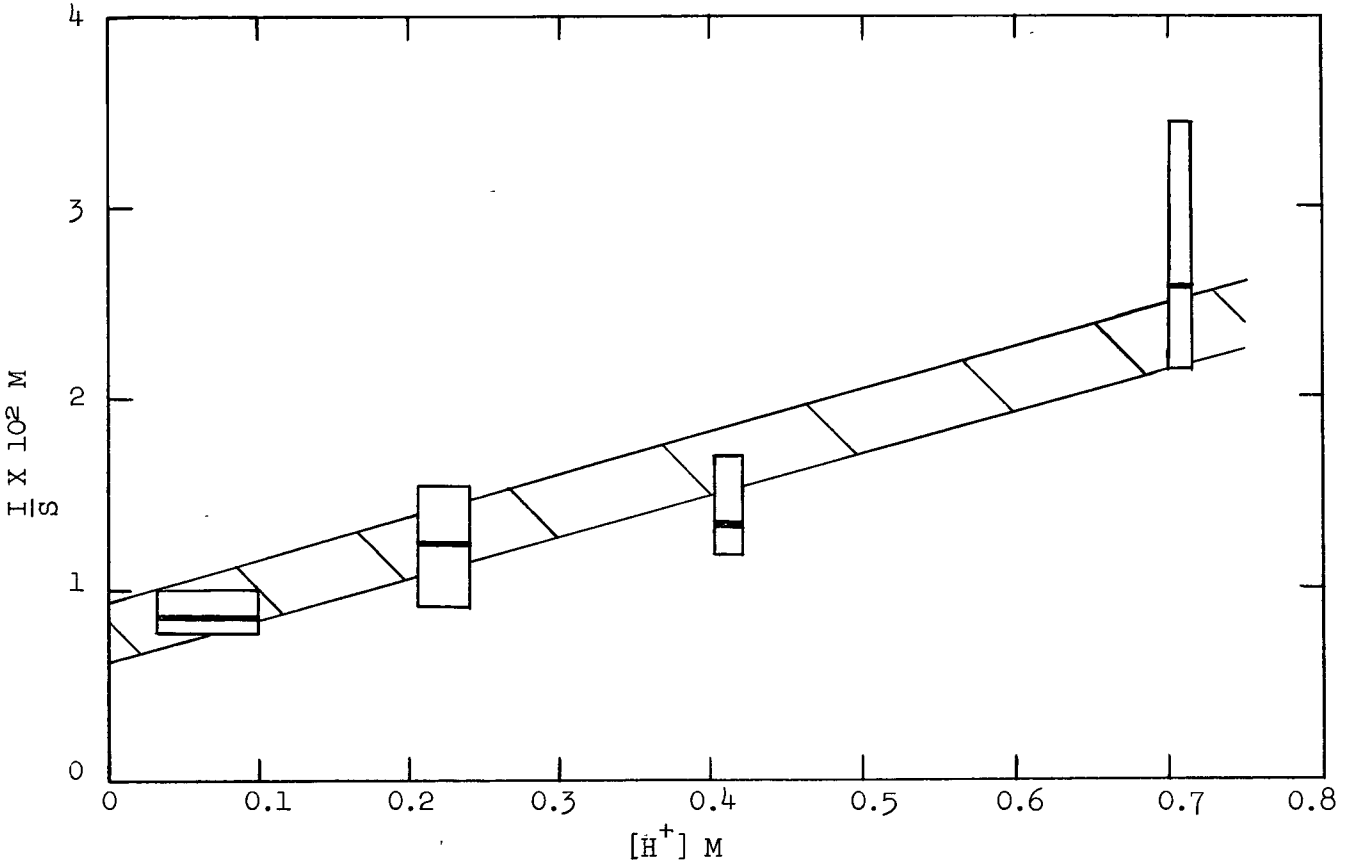

Figure 16. Plot of $\frac{I}{S}$ vs. $[H^+]$ for Acid Series of Experiments; 0.15 M$[CuSO_4]$, 5 atm H_2, 160°C.

This is of interest in view of the relatively low cuprous activity in perchlorate solutions and suggests that complexing with sulphate (or possibly bisulphate) is responsible for the considerable enhancement of catalytic activity of cuprous ions.

Because of the fairly large uncertainties in the $\frac{I}{S}$ values shown in Figure 16. the second term in equation 38, i.e., $R_{Cu}I$, was compared with that of a simpler mechanism for the cuprous catalyzed reduction path. This mechanism simply omits the back reaction given in equation 36, in other words, k_{-3} is assumed to be negligibly small. The corresponding complete rate law also obtained by the steady state approximation in CuH^+ and CuH is

$$-\frac{d[H_2]}{dt} = \frac{k_1[Cu^{II}]^2[H_2]}{\frac{k_{-1}}{k_2}[H^+]+[Cu^{II}]} + \frac{k_3[Cu^{II}][Cu^{I}][H_2]}{\frac{k_{-1}}{k_2}[H^+]+[Cu^{II}]} \qquad .....(42)$$

A comparison of equations 38 and 42 shows that the first terms of these rate laws are identical, and the second part in equation 42 is obtained by cancellation, because $\frac{k_{-3}}{k_4}[H^+]$ is absent in the denominator of equation 38.

Taking the cuprous dependent term in equation 42 separately, one obtains by inverting and multiplying both sides with $[Cu^I]$

$$\frac{[Cu^I]}{R_{Cu^I}} = \frac{1}{S} = \frac{\frac{k_{-1}}{k_2}[H^+]}{k_3[Cu^{II}][H_2]} + \frac{1}{k_3[H_2]} \qquad .....(43)$$

which indicates that a plot of $\frac{1}{S}$ vs. $[H^+]$ should be linear. A plot was made with the previously obtained values of S for the acid series and is depicted in Figure 17. It is reasonably linear initially but curves upward at higher $[H^+]$ values suggesting a greater than first power dependence of $\frac{1}{S}$ on $[H^+]$. The value of k_3 estimated from the intercept of the linear approximation at low $[H^+]$ is 6.2×10^{-2} $M^{-1}sec^{-1}$ which agrees well with that obtained from the intercept in Figure 16.

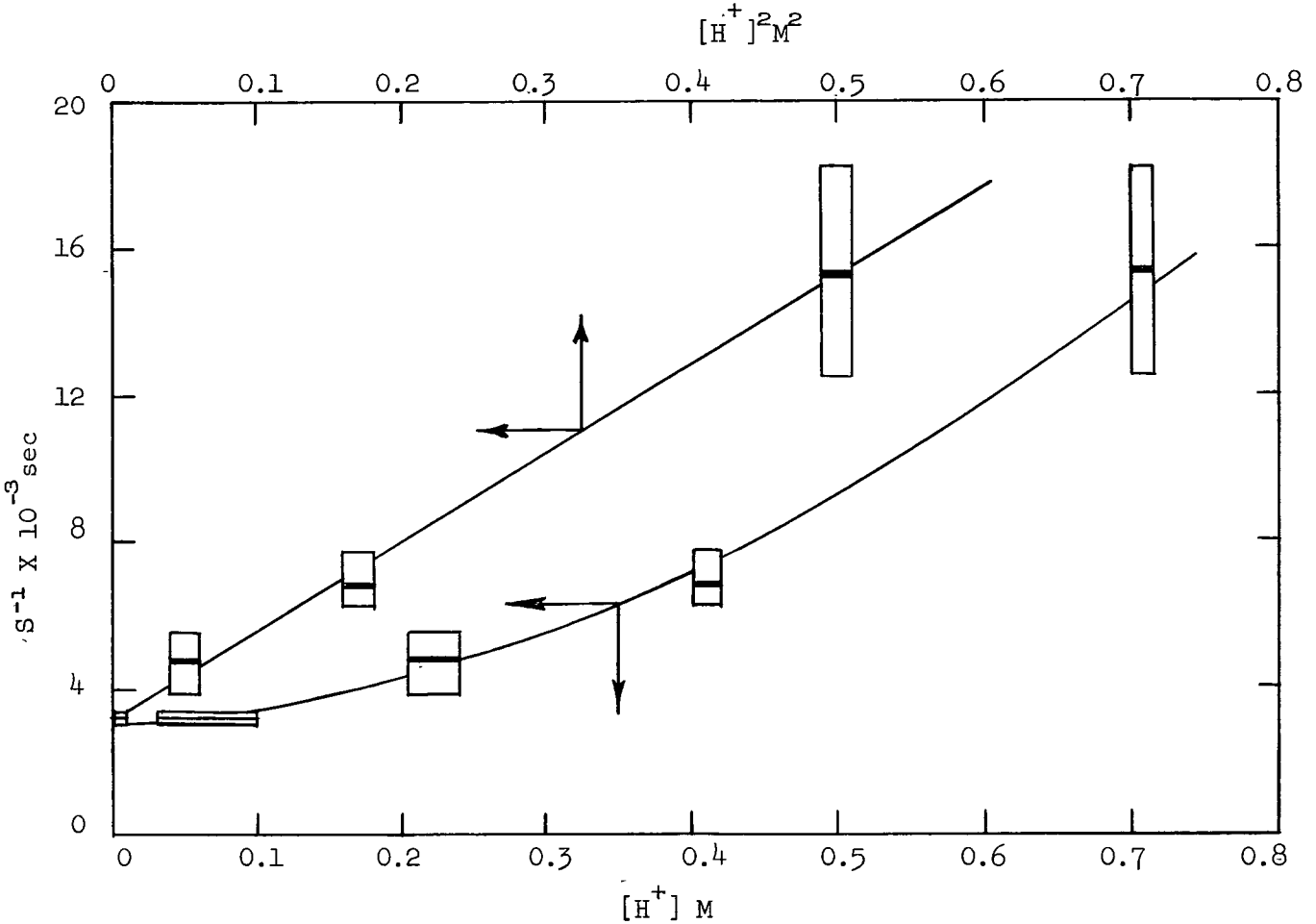

Figure 17. Plots of S^{-1} vs $[H^+]$ and $[H^+]^2$ for Acid Series of Experiments; 0.15 M$[CuSO_4]$., 5 atm H_2, 160°C.

Thus the simplified rate law (equation 42) may be considered a good approximation at low $[H^+]$.

However the deviation from linearity with increasing acidity of the plot in Figure 17 is greater than expected from probable errors in the measurements and suggests that this rate law is in error. Therefore a plot of $\frac{1}{S}$ vs $[H^+]^2$ was also made as shown in Figure 17. This plot appears to be linear and supports the validity of the second term of the rate law as given in equation 38 since it contains a term in $[H^+]^2$ in the denominator. The $[H^+]^2$ dependence of $\frac{1}{S}$ is demonstrated in equation 44, e.g.,

$$\frac{[Cu^I]}{R_{Cu^I}} = \frac{1}{S} = \frac{\frac{k_{-1}}{k_2}\frac{k_{-3}}{k_4}[H^+]^2}{k_3[Cu^{II}]^2[H_2]} + \frac{\left(\frac{k_{-1}}{k_2} + \frac{k_{-3}}{k_4}\right)[H^+]}{k_3[Cu^{II}][H_2]} + \frac{1}{k_3[H_2]} \qquad .....(44)$$

which is derived from the second term in equation 38.

As expected the intercept of the $\frac{1}{S}$ vs $[H^+]^2$ plot at $[H^+] = 0$ is close to that of the $\frac{1}{S}$ vs $[H^+]$ plot and will therefore yield the same value of k_3. Although equation 44 contains both a linear and square term in $[H^+]$ it can be seen from the $\frac{1}{S}$ vs $[H^+]^2$ plot that the latter term is sufficiently important in this equation to permit the plot to appear linear in confirmation of the rate law given by equation 38.

The Effect of Cupric Sulphate on Rates

A series of rate curves illustrating the effect on rates of varying the initial $CuSO_4$ concentration is shown in Figure 18. The experimental conditions were as follows: 0.05 to 0.25 M $[CuSO_4]_o$, 0.7 M $[H_2SO_4]_o$, sufficient $[MgSO_4]$ to make the solution 1 M in total sulphate, H_2 partial pressure 5 atm and 160°C.

The acidity was kept as high as practical so that free sulphate in solution for complexing of cupric and cuprous ions was minimized.

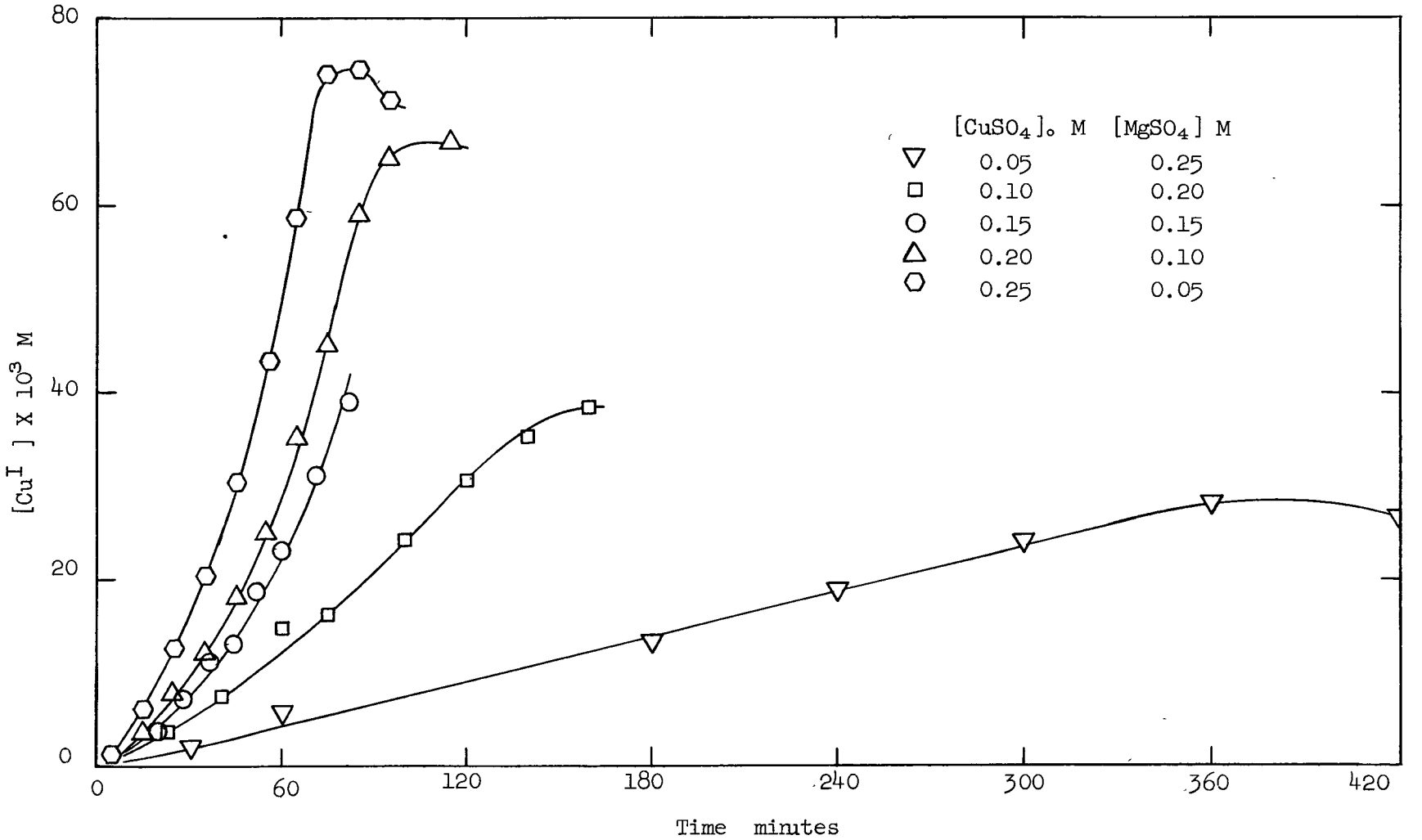

Figure 18. Rate Curves as a Function of Initial Cupric Sulphate Concentration; 0.70 M[H_2SO_4]$_o$, 5 atm H_2, 160°C.

Rates were measured, as in the acid series, at several $[Cu^I]$ levels along the reduction curves and are depicted in Figure 19 as plots of rate vs. $[Cu^I]$. These plots are linear initially but tend to decrease in slope at the higher $[Cu^I]$ levels particularly for the experiments with high initial $[CuSO_4]$. The slopes decrease because the reaction is also $[Cu^{II}]$ dependent and the cupric levels are declining in that region.

For analysis of the plots in Figure 19, the $[Cu^I]$ dependent part of the rate, i.e., the slopes S will be considered first. It is evident that in the initial portions of these curves the slopes increase from a low value for the experiment with low initial cupric sulphate (0.05 M) to an approximately constant value for the runs with high initial $[CuSO_4]$ (0.20 to 0.25 M). The significance of this observation is illustrated in Figure 20 where the initial slopes of Figure 19, i.e., $S = \frac{R_{Cu^I}}{[Cu^I]}$, have been plotted against both $[Cu^{II}]$ and $[Cu^{II}]^2$. The S vs. $[Cu^{II}]$ curve indicates that at low initial cupric concentrations the dependence of S is second order in $[Cu^{II}]$; as $[Cu^{II}]$ is increased this dependence shifts to first and finally to nearly zero order at the highest initial cupric sulphate levels. The shape of this curve is consistent with the expression for the slope, S, (equation 40) which may be explained as follows. At low initial $[Cu^{II}]$ both $\frac{k_{-1}}{k_2}[H^+]$ and $\frac{k_{-3}}{k_4}[H^+]$ will be the dominant terms in the denominator of 40 and this equation will approach the form

$$S = \frac{k_3[Cu^{II}]^2[H_2]}{\frac{k_{-1}}{k_2}\frac{k_{-3}}{k_4}[H^+]^2} \qquad .....(45)$$

resulting in a second order dependence of S on $[Cu^{II}]$. As the initial $[Cu^{II}]$ is increased the dependence of S on $[Cu^{II}]$ will shift to first and finally to zero order at the highest $[Cu^{II}]$ levels. In this limiting case when $[Cu^{II}] > \frac{k_{-3}}{k_4}[H^+]$ and $> \frac{k_{-1}}{k_2}[H^+]$ equation 40 will reduce to

$$S = k_3[H_2] \qquad .....(46)$$

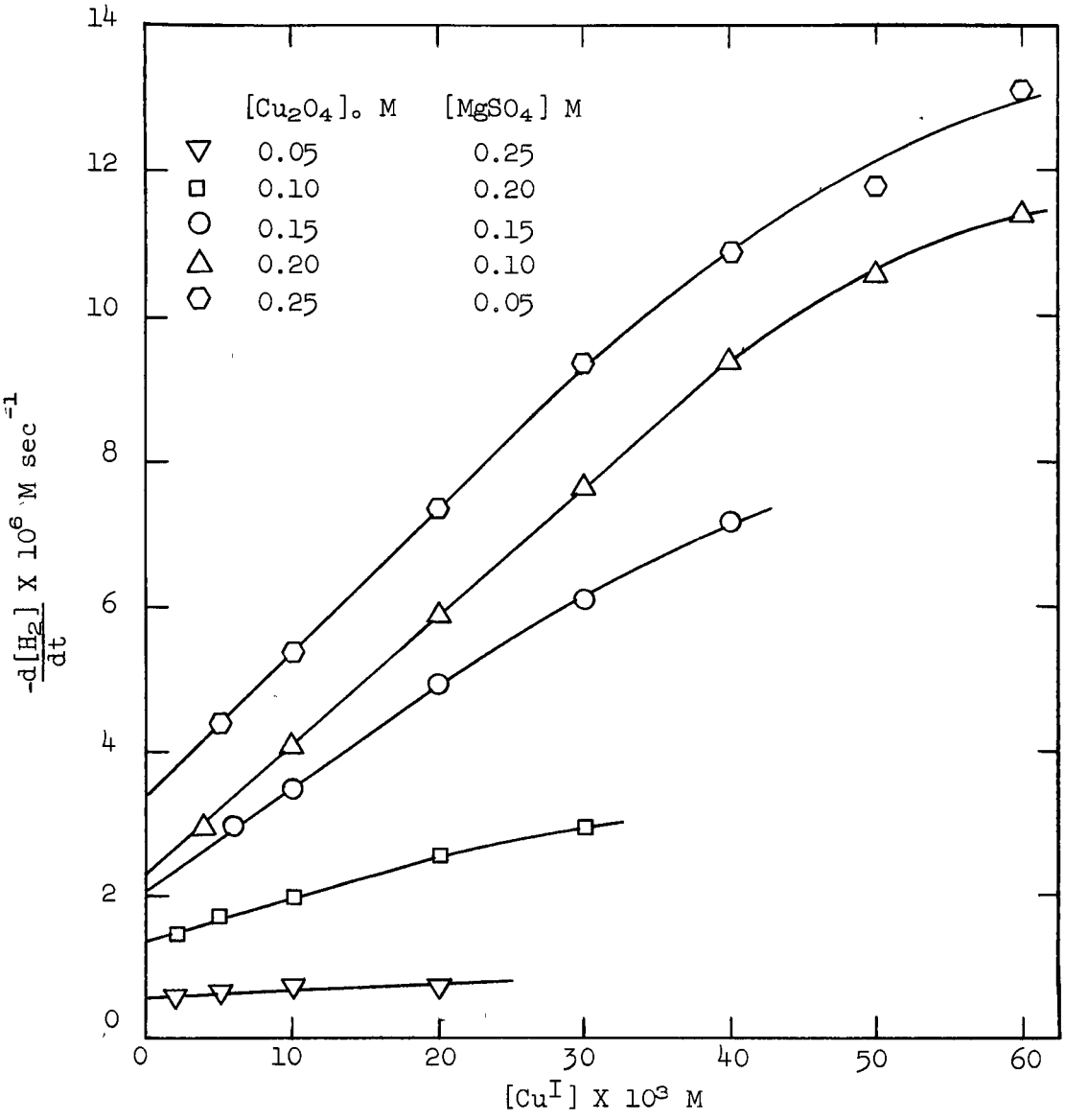

Figure 19. Plots of Rate vs. $[Cu^I]$ as a Function of Initial Cupric Concentration; 0.70 M $[H_2SO_4]_o$, 5 atm. H_2, 160°C.

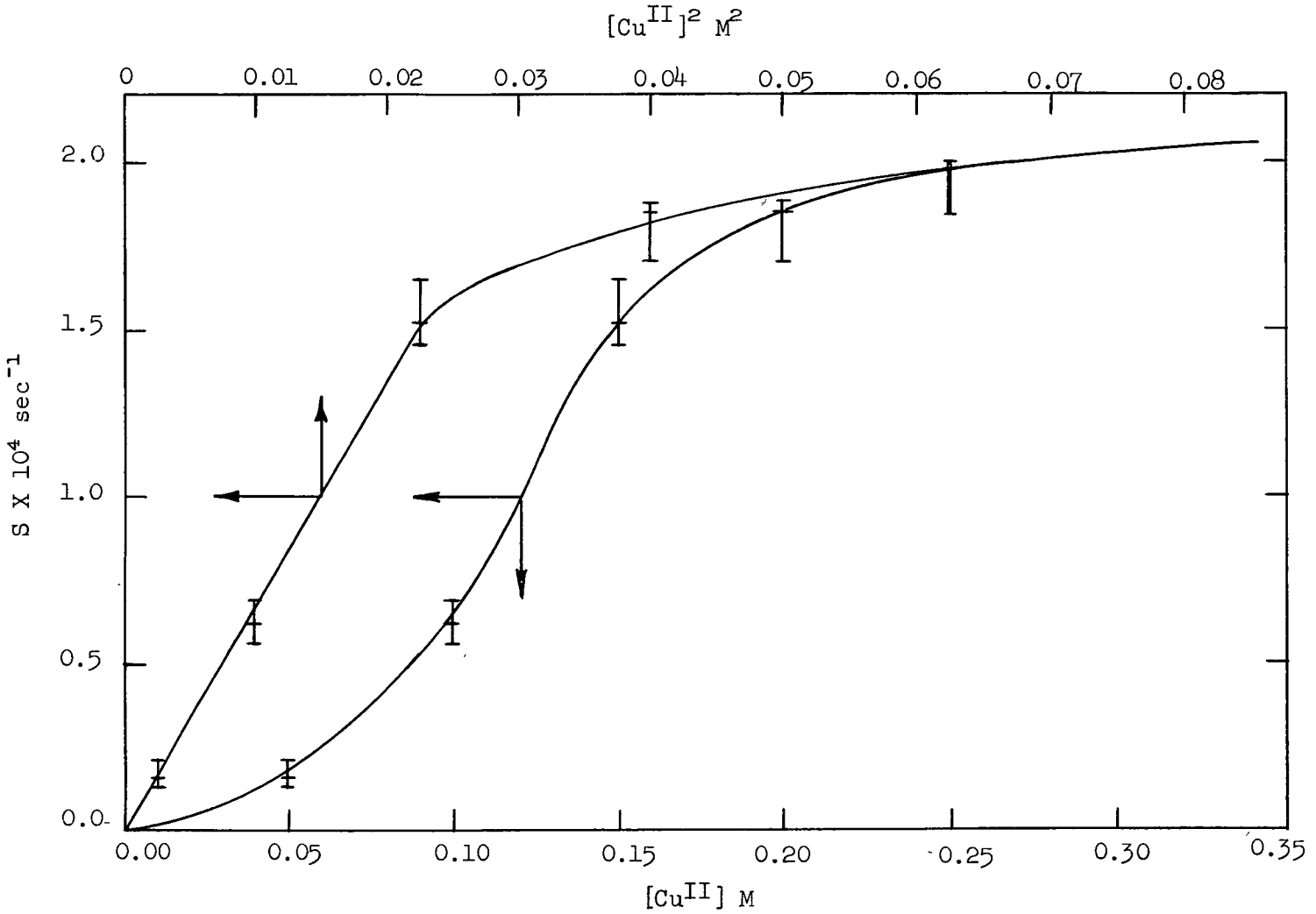

Figure 20. Plots of S vs $[Cu^{II}]$ and $[Cu^{II}]^2$ for Cupric Series of Experiments; 0.70 M$[H_2SO_4]$, 5 atm H_2, 160°C.

and further increases in the initial cupric sulphate concentration should have no effect on S as seen in Figure 19. The arguments are supported by the shape of the second curve in Figure 20, i.e., the S vs $[Cu^{II}]^2$ plot, which, as would be predicted, is linear initially and curves toward zero slope at high $[Cu^{II}]^2$ values. k_3 can be estimated with equation 46 from the asymptote that the plots in Figure 20 approach at high $[Cu^{II}]$ levels and has a value of approximately $3.5 \times 10^{-2} M^{-1} sec^{-1}$. The value obtained from the earlier acid series is 6.4×10^{-2} $M^{-1} sec^{-1}$.

The intercepts, I, of the rate vs $[Cu^{I}]$ plots in Figure 19 were used to determine values of k_1 and $\frac{k_{-1}}{k_2}$ for $R_{Cu^{II}}$, the first term in the rate equation 38. Inverting the expression for $R_{Cu^{II}}$ and multiplying both sides with $[Cu^{II}]$ yields

$$\frac{[Cu^{II}]}{R_{Cu^{II}}} = \frac{[Cu^{II}]}{I} = \frac{\frac{k_{-1}}{k_2}\,[H^+]}{k_1[Cu^{II}][H_2]} + \frac{1}{k_1[H_2]} \qquad .....(47)$$

and from a linear plot of $\frac{[Cu^{II}]}{I}$ vs. $\frac{1}{[Cu^{II}]}$ values of k_1 and $\frac{k_{-1}}{k_2}$ may be extimated from the slope and intercept respectively. This plot is shown in Figure 21. The large uncertainties in the $\frac{[Cu^{II}]}{I}$ values make it difficult to draw a satisfactory straight line. Values of k_1 and $\frac{k_{-1}}{k_2}$ obtained from the intercept and slope of the best straight line that can be drawn are respectively $2.6 \times 10^{-3} M^{-1} sec^{-1}$ and 0.05.

The Effect of Free Sulphate on Rates

A number of experiments were performed to investigate the effect of free sulphate ions on the rates of copper reduction. All experiments were carried out at 160°C and a hydrogen partial pressure of 5 atm. Further experimental details are listed in Table IV together with the estimated free sulphate, bisulphate and hydrogen ion concentrations.

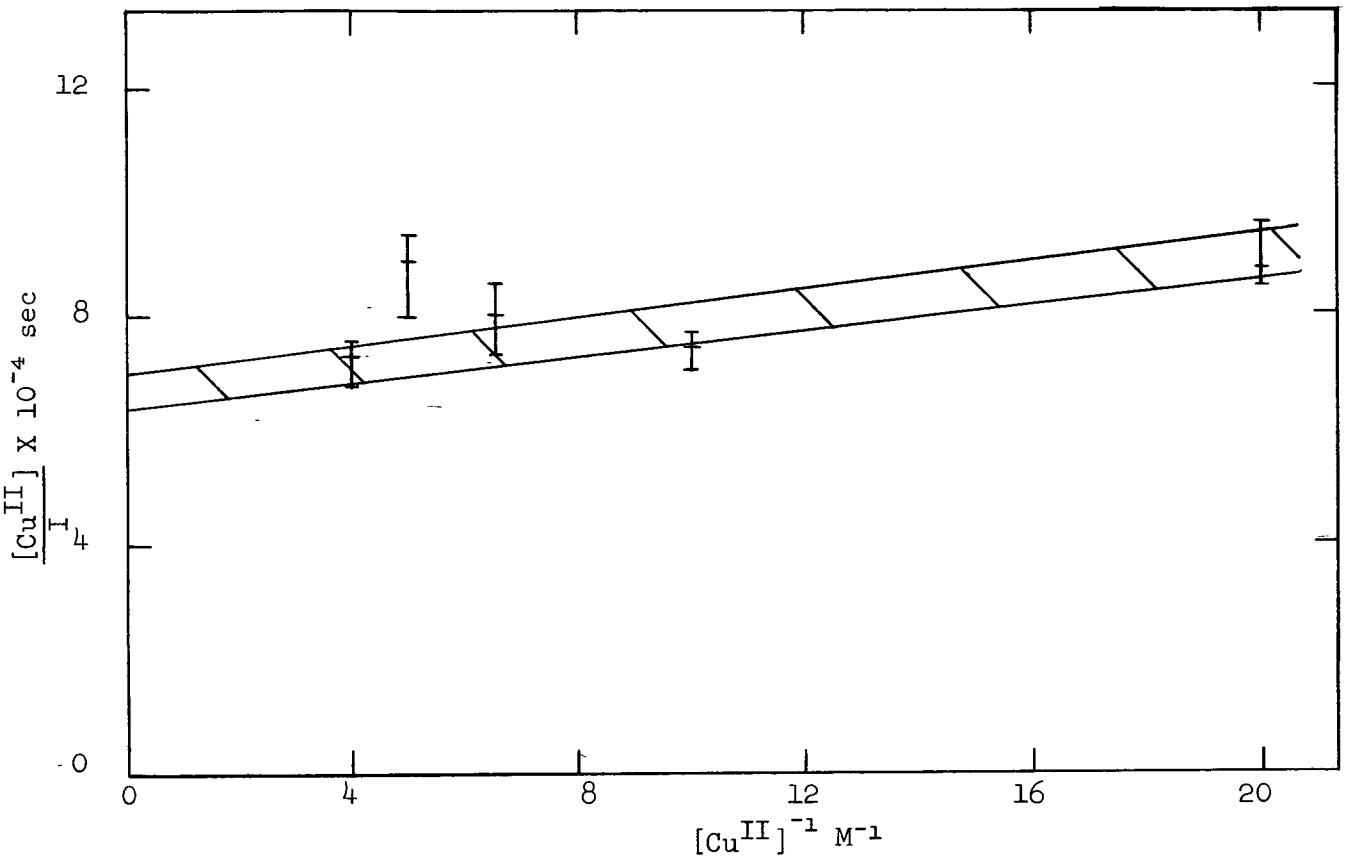

Figure 21. Plot of $\frac{[Cu^{II}]}{I}$ vs. $\frac{1}{[Cu^{II}]}$ for Cupric Series of Experiments; 0.70 M$[H_2SO_4]$, 5 atm H_2, 160°C.

TABLE IV.

Experimental Conditions for Sulphate Series and Estimated Free Sulphate, Bisulphate and Hydrogen Ion Concentrations

Experiment	$[CuSO_4]$	$[H_2SO_4]_o$	$[MgSO_4]$	$[SO_4^=]_{free}$ ✱	$[HSO_4^-]$ ✱	$[H^+]$ ✱
H_2SO_4 - 2	0.15M	0.50M	0.35M	0.03 - 0.1	0.97 - 0.9	0.03 - 0.1
$SO_4^=$ - 1	0.15	0.40	0.45	0.2 - 0.23	0.8 - 0.77	0.004 - 0.03
$SO_4^=$ - 2	0.15	0.30	0.55	0.4 - 0.42	0.6 - 0.58	0.002 - 0.02
$SO_4^=$ - 3	0.15	0.20	0.65	0.6 - 0.61	0.4 - 0.39	0.0007 - 0.01
$SO_4^=$ - 4	0.15	0.10	0.75	0.8	0.2	0.003

✱ Free sulphate, bisulphate and hydrogen ion concentration estimated by neglecting complexing with Cu^{II} and assuming the bisulphate dissociation constant $K_b \simeq 10^{-3} - 10^{-2}\ M^{-1}$ (Appendix F).

The experimental rate curves✱ obtained in this series are depicted in Figure 22 and the plots of rate vs. $[Cu^I]$ are shown in Figure 23. These figures show that the rates increase initially with increasing free sulphate concentration but then level off. This is also illustrated in Figures 24 and 25, where the values of the intercepts, I, and slopes, S, of Figure 23 are plotted against $[SO_4^=]$ and it is apparent that the levelling off occurs at about 0.4 M free sulphate concentration. This enhancing effect is relatively small and quite possibly within the limits of an effect that can be explained in terms of hydrogen ion concentration changes within the series. It has therefore not been possible to determine the complexing effect of sulphate on the rate constants k_1 and k_3 respresenting the hydrogen activation steps. Peters and Halpern[16, 41], who studied the effect of complexing on dichromate reduction rates were able to show an enhancing effect on k_1 of about a factor of 7 in a series of measurements of increasing sulphate concentration.

✱ The break in the rate curve of experiment $SO_4^=$ - 4 may be attributed to hydrolysis of cuprous ions due to the low acidity in that run.

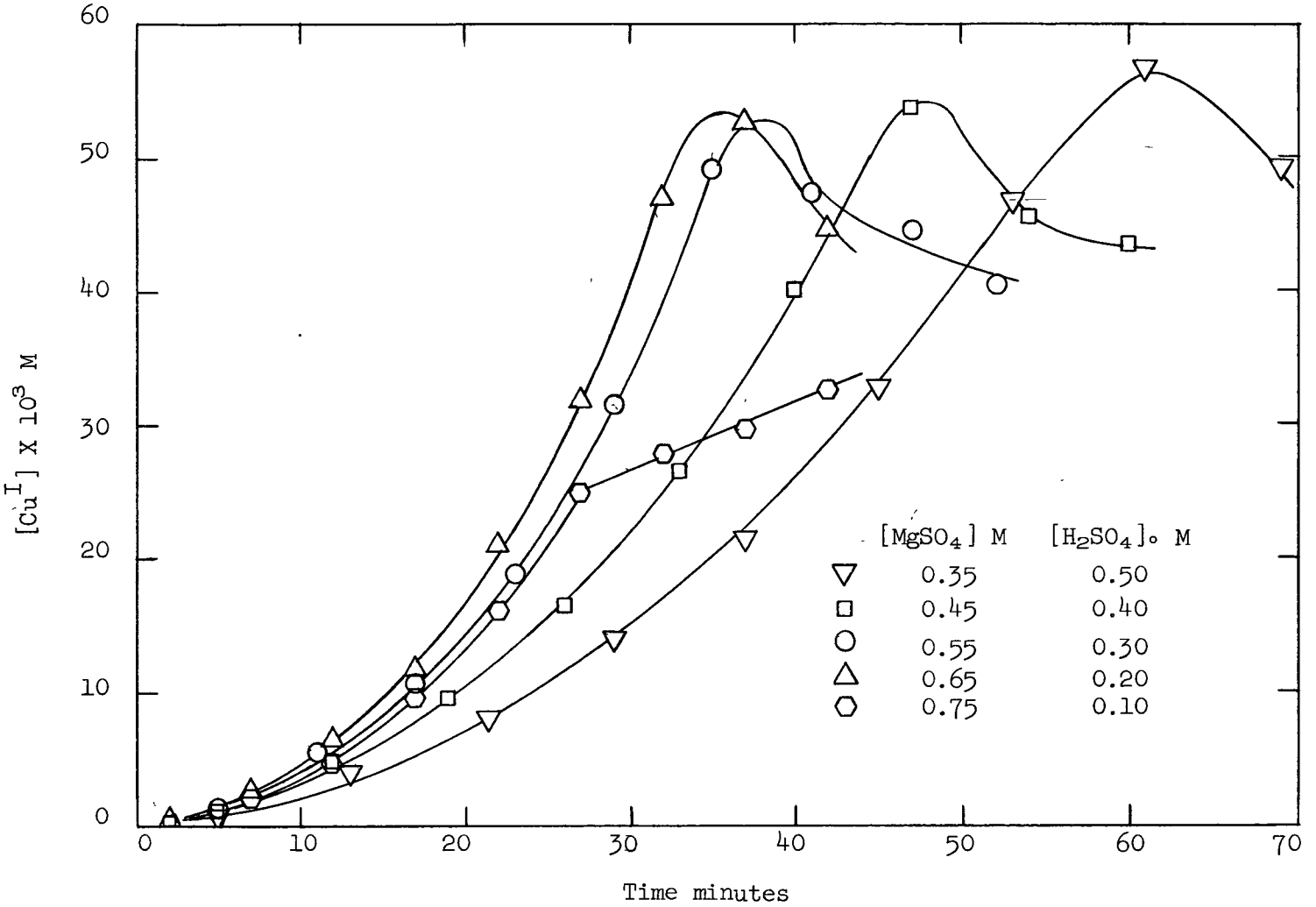

Figure 22. Rate Curves as a Function of Free Sulphate Ion Concentration; 0.15 M[$CuSO_4$]$_o$, 5 atm H_2, 160°C.

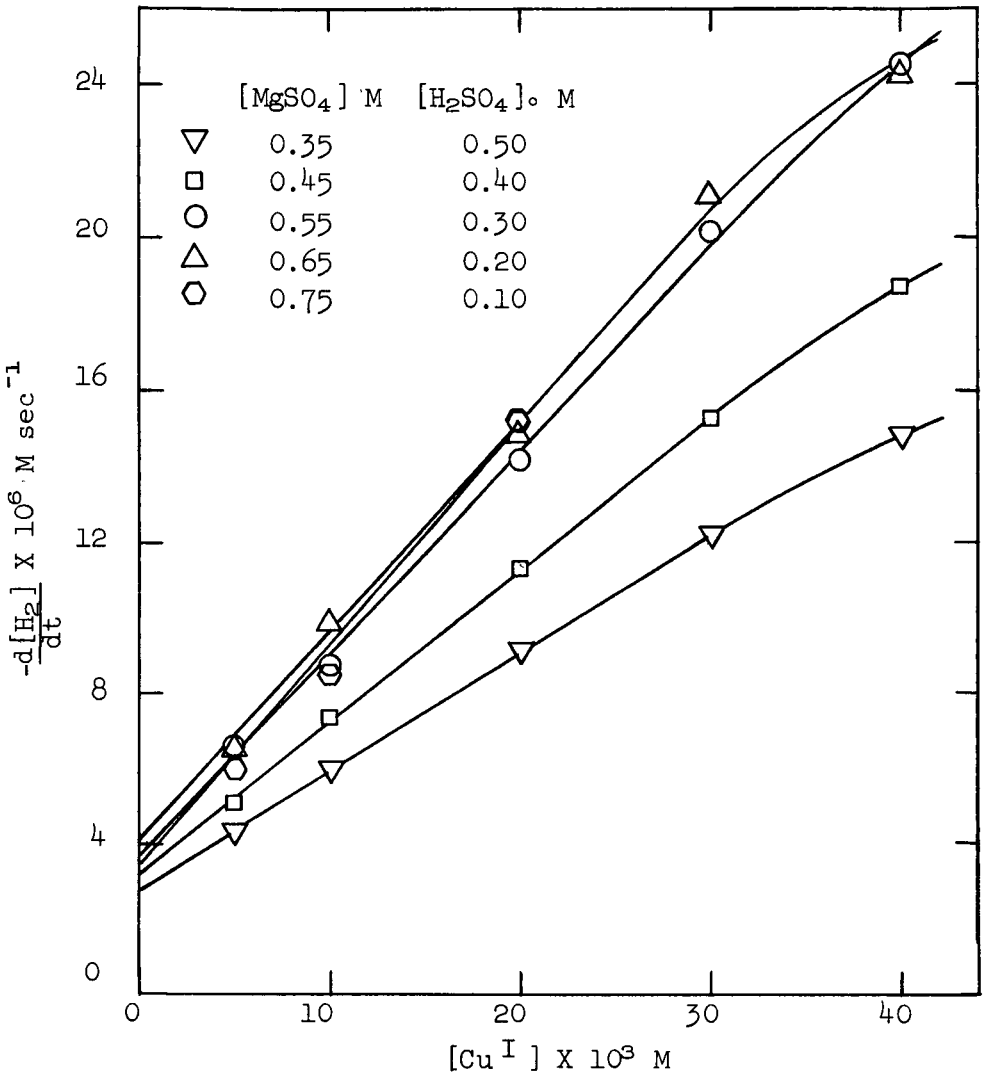

Figure 23. Plots of Rate vs. $[Cu^{I}]$ as a Function of Free Sulphate Concentration. 0.15 M $[CuSO_4]_o$, 5 atm H_2, 160°C.

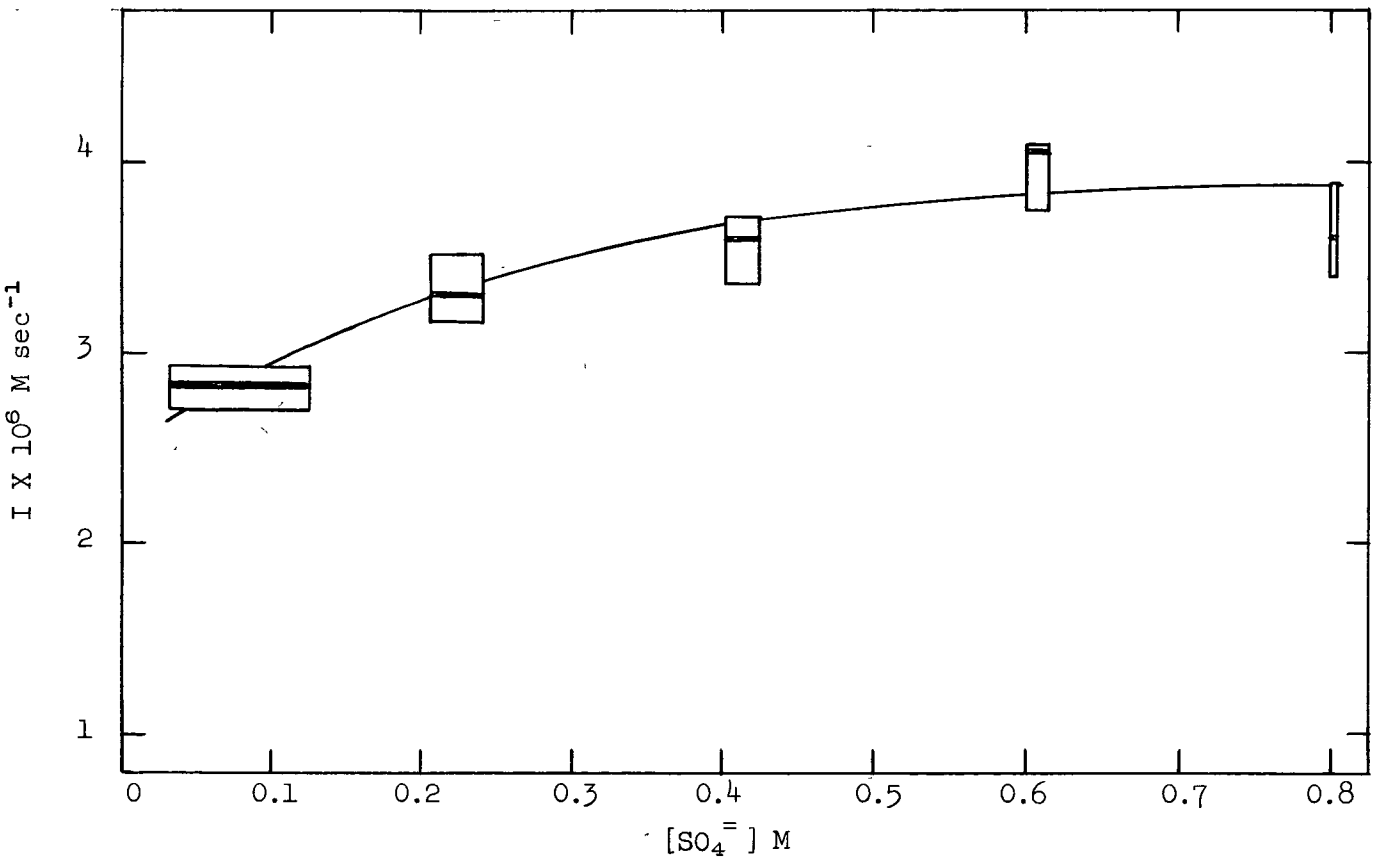

Figure 24. Plot of I vs. Free $[SO_4^{=}]$ for Sulphate Series of Experiments; 0.15 M$[CuSO_4]_o$, 5 atm H_2, 160°C.

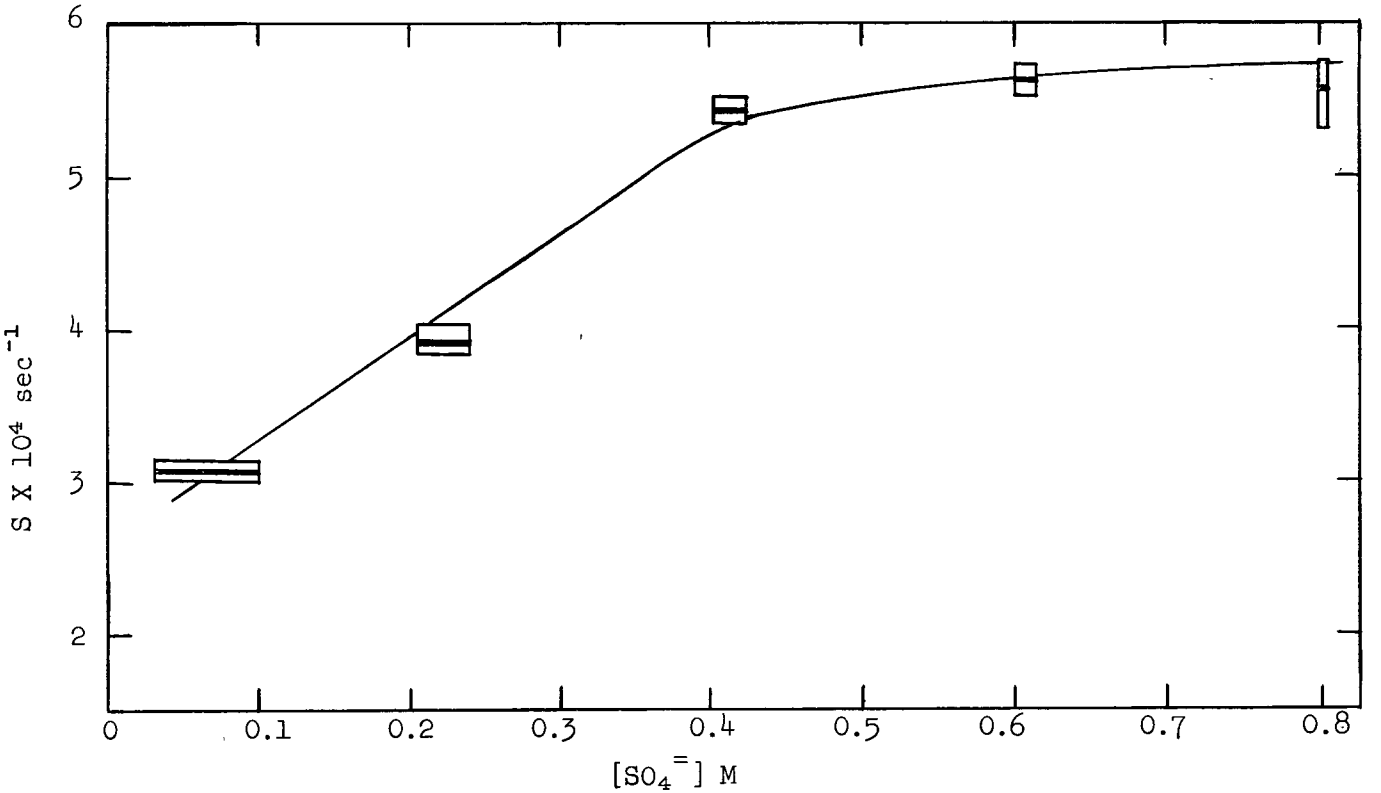

Figure 25. Plot of S vs. $[SO_4^{=}]$ for Sulphate Series of Experiments; 0.15 M$[CuSO_4]_o$, 5 atm H_2, 160°C.

At high sulphate concentrations and low acidities the rate equation 38 reduces to

$$-\frac{d[H_2]}{dt} = k_1[Cu^{II}][H_2] + k_3[Cu^{I}][H_2] \qquad .....(48)$$

and the values for k_1 and k_3 obtained from the limiting (high $[SO_4^{=}]$) asymptotes of the curves in Figures 24 and 25 are $k_1 = 4.5 \times 10^{-3} M^{-1}sec^{-1}$ and $k_3 = 9.6 \times 10^{-2} M^{-1}sec^{-1}$.

Summary of Rate Constants

The values of the rate constants obtained in the acid, copper and sulphate series of experiments have been summarized for comparison in Table V.

TABLE V.

Summary of Rate Constants for Sulphate Solutions at 160°C.

$k_1 M^{-1}sec^{-1}$	$\frac{k_{-1}}{k_2}$	$k_3 M^{-1}sec^{-1}$	$\frac{k_{-3}}{k_4}$	Series	Estimated from Figure
$3.2\times10^{-3}\pm10\%$	$0.13\pm30\%$	-	-	Acid	15
-	-	$6.4\times10^{-2}\pm25\%$	$0.45\pm40\%$	Acid	16
-	-	6.2×10^{-2}	-	Acid	17
-	-	3.5×10^{-2}	-	Cupric	20
$2.6\times10^{-3}\pm10\%$	$0.05\pm30\%$	-	-	Cupric	21
4.5×10^{-3}	-	-	-	Sulphate	24
-	-	9.6×10^{-2}	-	Sulphate	25

The magnitudes of these constants are of the same order for all three series. Variations in their values can be attributed to the errors inherent in the method of analysis of the sulphate system. These errors are all subjective

except those of $[Cu^{I}]$ determination. They result from the following:

1. fitting of rate curves to the experimental points,
2. estimation of slopes along the non-linear rate curves,
3. estimation of intercepts and slopes from the rate vs $[Cu^{I}]$ plots, and
4. fitting of curves to plots derived from the latter measurements.

The values of k_1 obtained here are somewhat low compared to that from the dichromate reduction work[35] in perchlorate solutions ($k_1 = 5.4 \times 10^{-3} M^{-1} sec^{-1}$), and this is probably only due to the use of hydrogen solubilities in water in the calculations. Sulphate solutions are known to have lower hydrogen solubilities at room temperature[45], which probably also applies at elevated temperatures. For example, an observed 30% decrease in the dichromate reduction rate at 100°C. by addition of 0.75 M $[MgSO_4]$ or $[Na_2SO_4]$ to cupric acetate solutions has been attributed to the lowering of H_2 solubility due to these salts[41]. Also, recent measurements[46] have shown that the solubility of CO in aqueous solutions decreases markedly with increasing ammonium sulphate concentration (40% in 1 M $[(NH_4)_2SO_4]$ at 160°C).

The Integrated Rate Curve

The validity of the rate law for copper reduction in the sulphate system, as given in equation 38, i.e.,

$$-\frac{d[H_2]}{dt} = \frac{k_1[Cu^{II}]^2[H_2]}{\frac{k_{-1}}{k_2}[H^+]+[Cu^{II}]} + \frac{k_3[Cu^{II}]^2[Cu^{I}][H_2]}{\left(\frac{k_{-1}}{k_2}[H^+]+[Cu^{II}]\right)\left(\frac{k_{-3}}{k_4}[H^+]+[Cu^{II}]\right)} = R_{Cu^{II}} + R_{Cu^{I}} \quad .....(38)$$

was checked by numerical integration of this expression for the experimental conditions of one run. One experiment from the acid series was chosen for this comparison and the constants (Table V) obtained from this series were used in the calculations (Appendix H). Figure 26 depicts the resulting integrated rate curve together with that obtained experimentally.

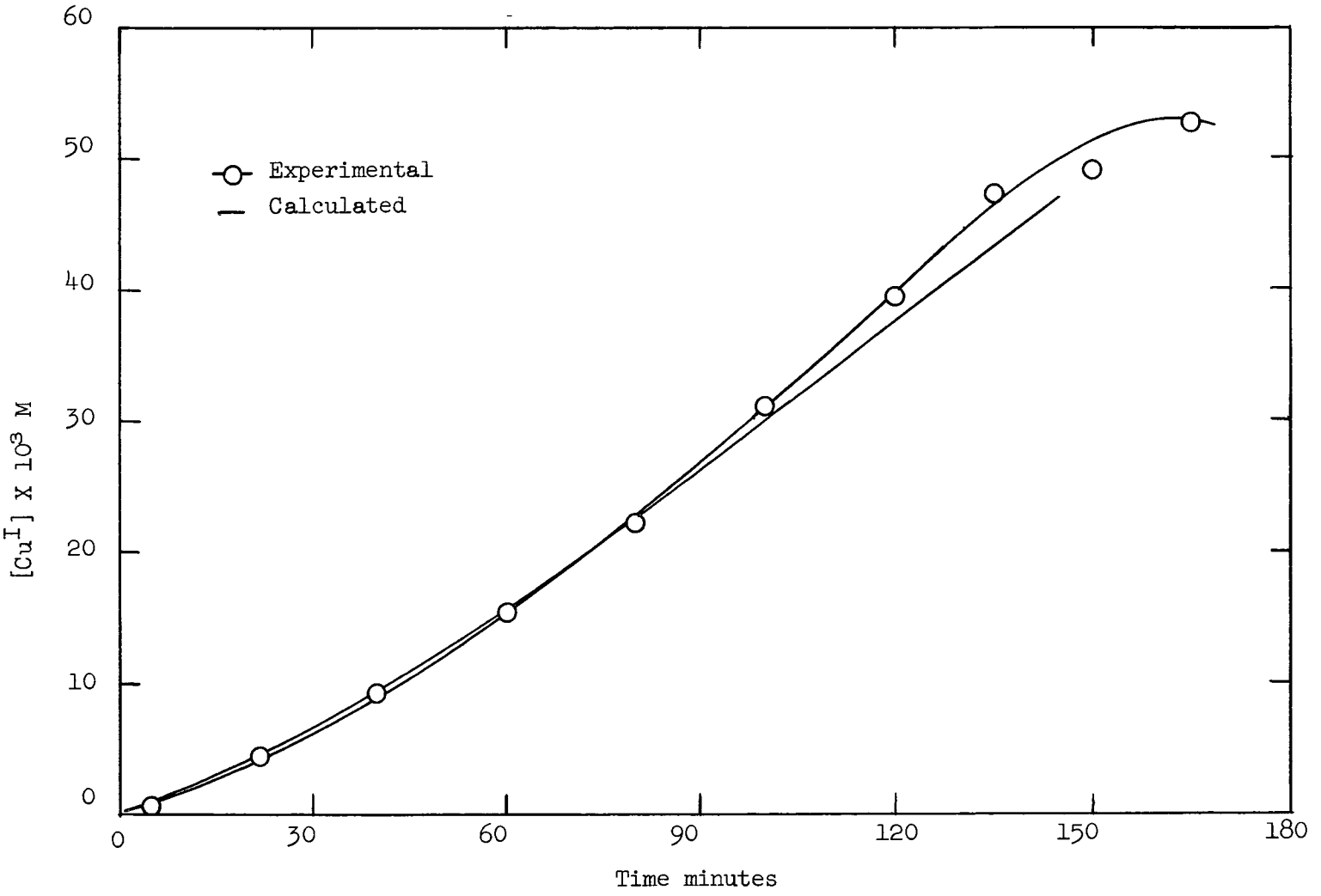

Figure 26. Comparison of Experimental and Calculated Rate Curves; 0.15 M[$CuSO_4$]$_o$, 0.85 M[H_2SO_4]$_o$, 5 atm H_2, 160°C.

The Effect of Temperature on Rates

The effect of temperature on the copper reduction rates was studied to obtain an estimate for the activation energies for both the $[Cu^{II}]$ and $[Cu^{I}]$ reaction paths. Rate curves for this series are depicted in Figure 27. They were obtained under the following experimental conditions: 0.15 M initial $[CuSO_4]$, 0.70 M initial $[H_2SO_4]$, 0.15 M $[MgSO_4]$, 5 atm hydrogen partial pressure and 120, 140, 160 and 180°C temperature. The rate vs $[Cu^{I}]$ plots of this series are shown in Figure 28.

As only one experiment was made at each of the four temperatures, except at 160°C, it was not possible to measure k_1 and k_3 directly, but they could be estimated from measured intercepts, I, and initial slopes, S, in Figure 28 through their relationships as defined by equation 38. The assumption was made that both of the rate constant ratios $\frac{k_{-1}}{k_2}$ and $\frac{k_{-3}}{k_4}$ do not change with temperature*. The values chosen for these two ratios were $\frac{k_{-1}}{k_2} = 0.13$ and $\frac{k_{-3}}{k_4} = 0.45$ (Table V). The values of k_1 and k_3 calculated for each temperature are listed in Table VI.

TABLE VI.

Values of k_1, k_3 and Dissolved H_2 at Different Temperatures

Temperature	$k_1 M^{-1} sec^{-1}$ **	$k_3 M^{-1} sec^{-1}$ **	$[H_2]$ M ***
120 °C	1.9×10^{-4}	1.3×10^{-2}	4.50×10^{-3}
140	1.1×10^{-3}	2.4×10^{-2}	5.13×10^{-3}
160	3.2×10^{-3}	6.4×10^{-2}	5.90×10^{-3}
180	7.8×10^{-3}	16.2×10^{-2}	6.80×10^{-3}

** Estimated range for k_1 ± 10%, for k_3 ± 25% for each temperature as in Table V for 160°C.

*** H_2 solubility at 5 atm H_2 pressure for pure water[40].

These rate constants are shown plotted in Figure 29 as log k_1 and k_3 respectively

* $\frac{k_{-1}}{k_2}$ was in fact observed to be nearly constant with temperature in earlier work in the perchlorate system[35].

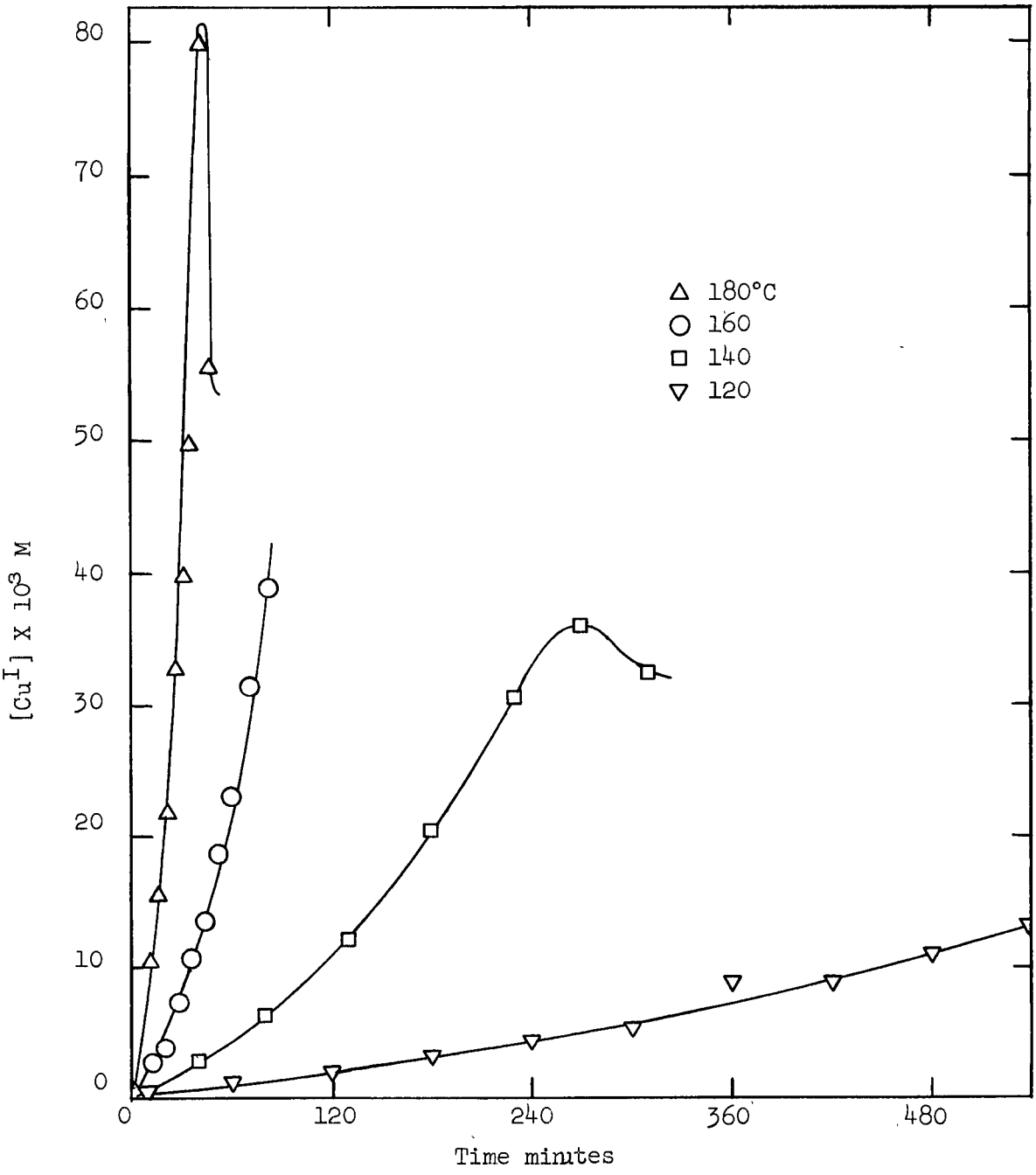

Figure 27. Rate Curves as a Function of Temperature; 0.15 M[$CuSO_4$]$_o$, 0.70 M[H_2SO_4]$_o$, 0.15 M [$MgSO_4$], 5 atm H_2.

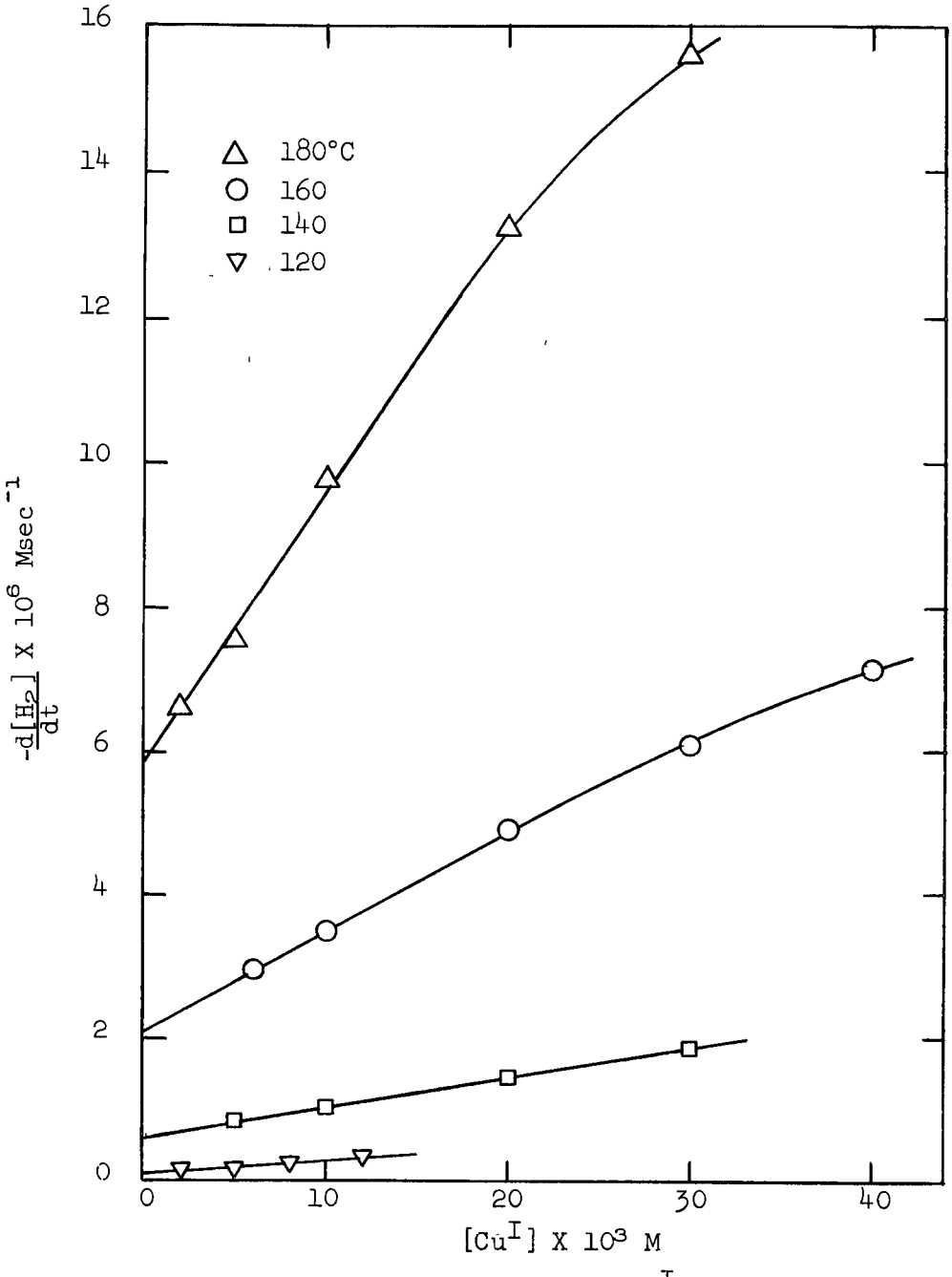

Figure 28. Plots of Rate vs. [Cu^I] as a Function of Temperature; 0.15 M[$CuSO_4$]$_o$, 0.70 M[H_2SO_4]$_o$, 0.15 M[$MgSO_4$], 5 atm H_2.

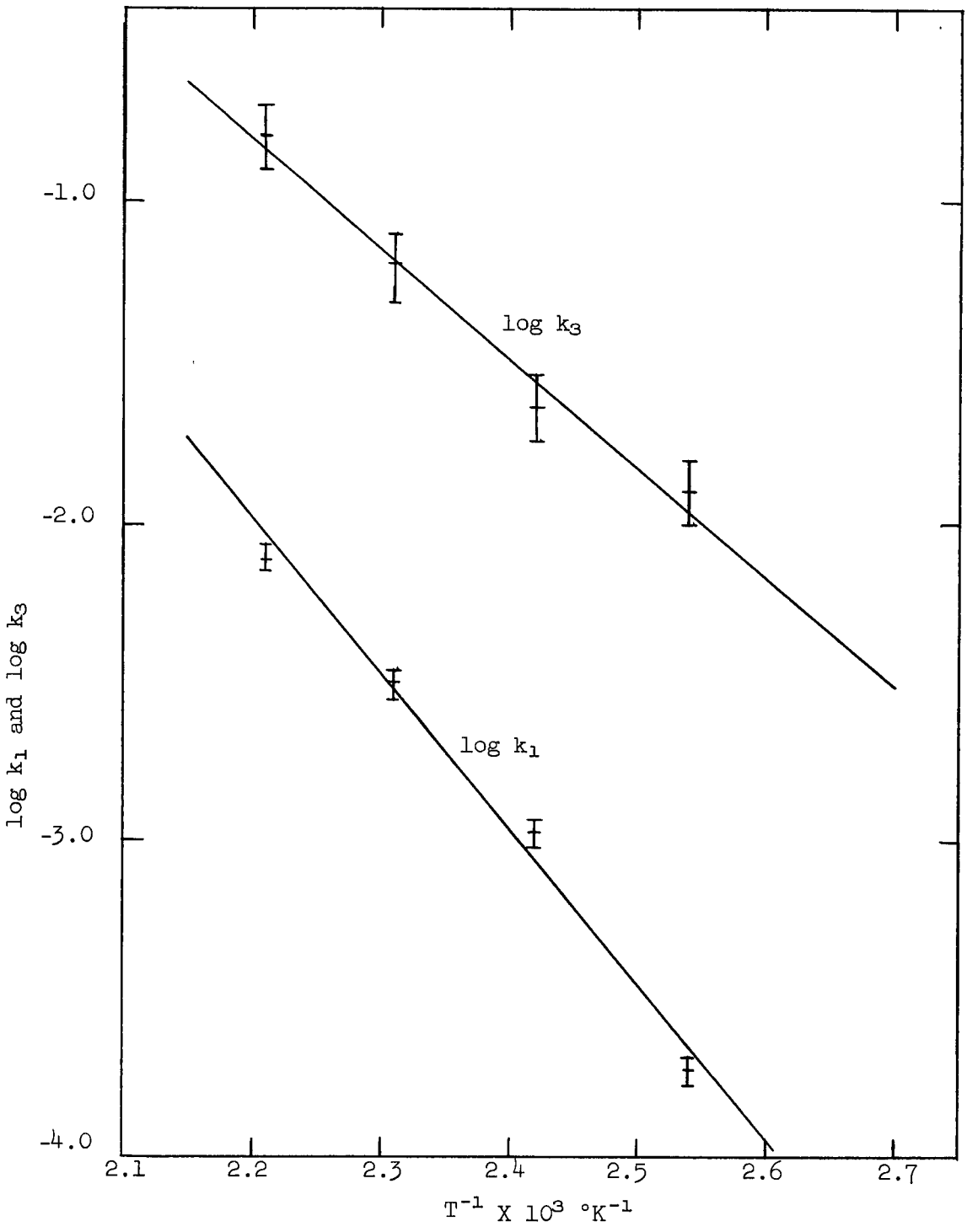

Figure 29. Plots of log k_1 and log k_3 vs T^{-1}

vs $T^{-1}°K^{-1}$. From the slopes of these Arrhenius plots the following experimental activation energies were obtained:

$$E_1 = 22.4 \pm 2.2 \text{ kcal/mole}$$

$$E_3 = 15.3 \pm 1.4 \text{ kcal/mole}$$

Values of $\Delta S^{\ddagger}$ for each rate constant were also calculated with the above figures of E and the relation

$$k_{exp} = \frac{ekT}{h}\left(\exp\frac{-E}{RT}\right)\left(\exp\frac{\Delta S^{\ddagger}}{R}\right) \quad \text{(reference 47)} \qquad \ldots\ldots(49)$$

and are

$$\Delta S_1^{\ddagger} = - 21 \pm 5 \text{ eu}$$

$$\Delta S_2^{\ddagger} = - 31 \pm 3 \text{ eu}$$

These data are summarized for comparison in Table VII together with those of other workers.

TABLE VII.

Summary of Activation Energies and Entropies

System	E_1 kcal/mole	$\Delta S_1^{\ddagger}$ eu	E_3 kcal/mole	$\Delta S_3^{\ddagger}$ eu	Source
Sulphate	22.4 ± 2.2	- 21 ± 5	15.3 ± 1.4	- 31 ± 3	This work
Sulphate	24	-	9.3	-	ref. 26
Sulphate	23.5	- 10.4	15.9	- 34.5	ref. 48
Perchlorate	25.8 ± 1.7	- 12.1 ± 4.5	-	-	ref. 35

Although possible variations in $\frac{k_{-1}}{k_2}$ with temperature were not taken into account in the estimation of errors in k_1 the values of E_1 and $\Delta S_1^{\ddagger}$ are in reasonable agreement with the other data. A similar good agreement is apparent for E_3 and $\Delta S_3^{\ddagger}$ where the same approximations as shown above were used in calculating k_3. The low value of 9.3 kcal for E_3 is from published work[26] relating to a thesis[48]

and could be an error in interpretation by the authors since the same experimental work is described in both references.

The Deuterium Exchange Experiments

The reaction steps for activation of molecular hydrogen shown in the mechanisms of copper reduction (equations 34 and 36) indicate that both the reactive intermediates CuH^+ and CuH should react with hydrogen ions in solution to regenerate molecular hydrogen. Hence, if deuterium is substituted for hydrogen in a copper reduction experiment it should be possible to determine the rate of the back reaction by measuring the appearance of HD in the gas phase.

This reaction takes place according to

$$Cu^{II} + D_2 \xrightarrow{k_1} CuD^+ + D^+ \qquad .....(34)$$

$$CuD^+ + H^+ \xrightarrow{k_{-1}} Cu^{II} + HD \qquad .....(-34)^{\star}$$

for the cupric activation path. For the cuprous catalyzed reaction path it is

$$Cu^{I} + D_2 \xrightarrow{k_3} CuD + D^+ \qquad .....(36)$$

$$CuD + H^+ \xrightarrow{k_{-3}} Cu^{I} + HD \qquad .....(-36)$$

Experiments involving the use of D_2O enriched ordinary water instead of substituting D_2 for H_2 had been suggested earlier by Macgregor[37] for the copper reduction work. Webster[49] had observed the appearance of HD in exchange experiments involving the Ag^+ catalyzed hydrogen reduction of dichromate, by using water with a 20 mol% D_2O content. The rate of appearance of HD was found to increase with acidity, and in the absence of Ag^+ no exchange took place. Qualitative experiments by Potter[48] using copper sulphate solutions and a mixture of H_2 and D_2 showed an enrichment of the gas in HD content which was interpreted as being due to catalysis by copper ions in solution.

$\star$ The - sign designates the back reaction of equation 34.

Evidence for copper catalyzed deuterium exchange in non-aqueous solvents has been reported in the literature[29,50]. A small number of exchange experiments were also done in the present work. These included using both copper sulphate and perchlorate solutions and deuterium was introduced from either the gas phase as D_2 or the solvent as D_2O.

Five exchange experiments were performed in all and the experimental conditions are shown in Table VIII. The rate of exchange was measured by taking gas samples periodically and analyzing them mass spectrometrically for D_2, HD and H_2.

TABLE VIII.

Experimental Conditions for Exchange Experiments

Experiment Number	$[Cu^{II}]_o$ ✱	$[H_2SO_4]_o$	$[HClO_4]_o$	Solvent	P_{D_2}	P_{H_2}	Temperature °C.	$[H^+]_o$
D_2-A ✱✱	0.15 M	0.50 M	-	H_2O	5 atm.	-	160	~0.1 ✱✱✱ M
D_2-B	0.15	0.85	-	H_2O	5	-	160	0.72
D_2-C	0.07	-	0.10 M	H_2O	15	-	160	0.10
H_2-D	0.15	0.85	-	D_2O	-	5 atm	160	0.72
D_2-E ‡	0.00	0.50	-	H_2O	5	-	160	~0.1

✱ $CuSO_4$ except for experiment D_2-C in which $Cu(ClO_4)_2$ was used.
✱✱ Solution 0.35 M in $[MgSO_4]$
✱✱✱ Assuming the bisulphate dissociation constant K_b is $\sim 10^{-2} M^{-1}$ at 160°C.
‡ Solution 0.50 M in $[MgSO_4]$

In addition several liquid samples were taken, usually directly after a gas sample, to measure the rate of appearance of cuprous ions.

The normalized results (Appendix I) for these experiments are shown in Figures 30 to 33.

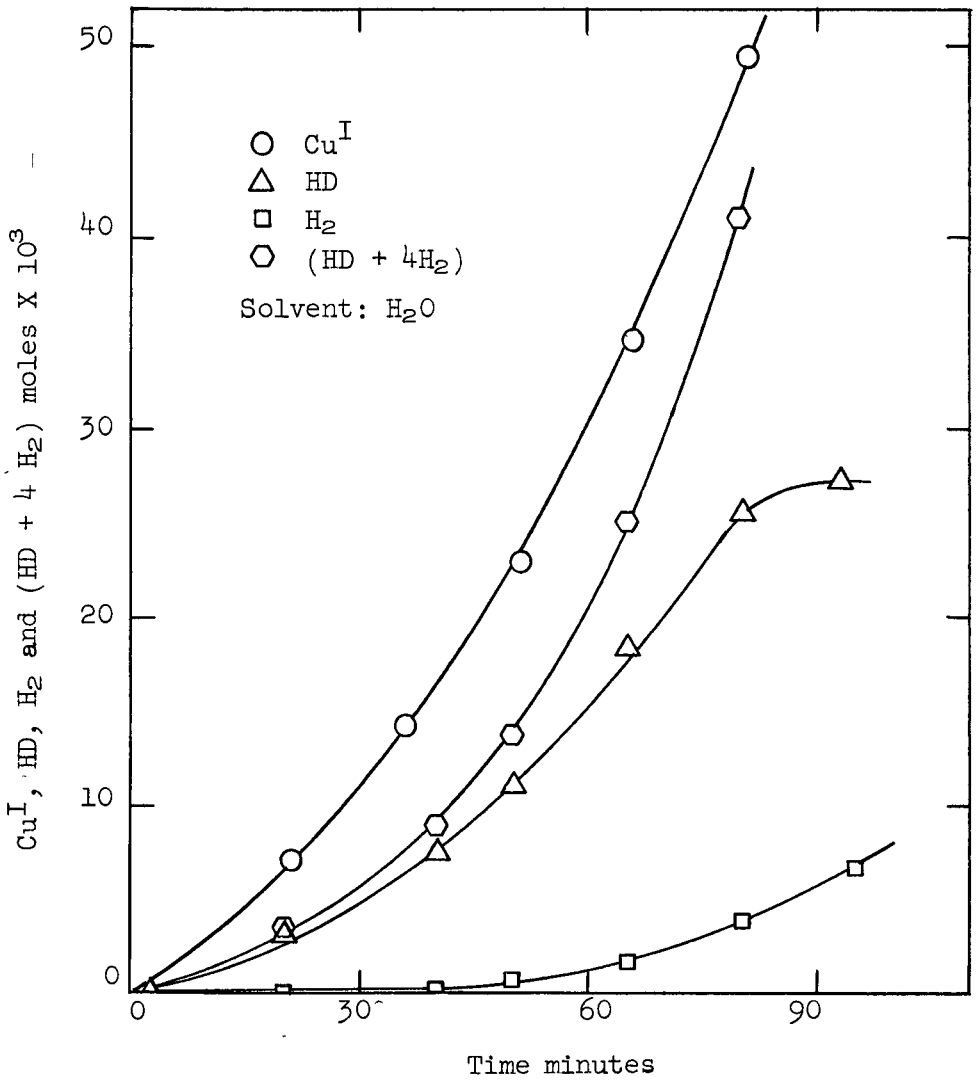

Figure 30. Rate Curves of Total Cu^I, HD, H_2 and (HD + $4H_2$) Experiment D_2-A; 0.15 M[$CuSO_4$]$_o$, 0.50 M[H_2SO_4]$_o$, 0.35 M[$MgSO_4$] , Initial D_2 5 atm, 160°C.

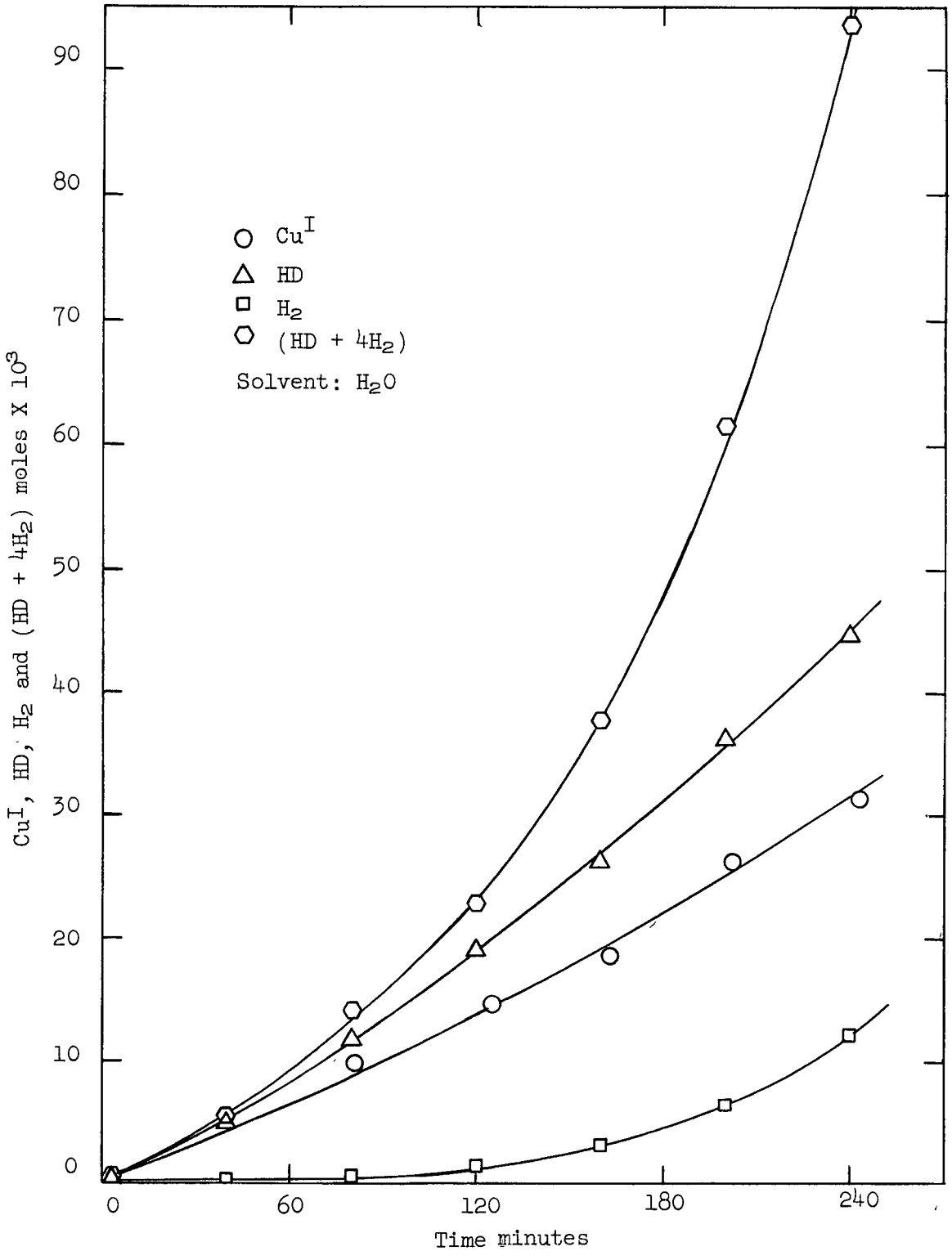

Figure 31. Rate Curves of Total Cu^I, HD, H_2 and (HD + $4H_2$), Experiment D_2-B; 0.15 M $[CuSO_4]_o$, 0.85 M$[H_2SO_4]_o$, Initial D_2 5 atm, 160°C.

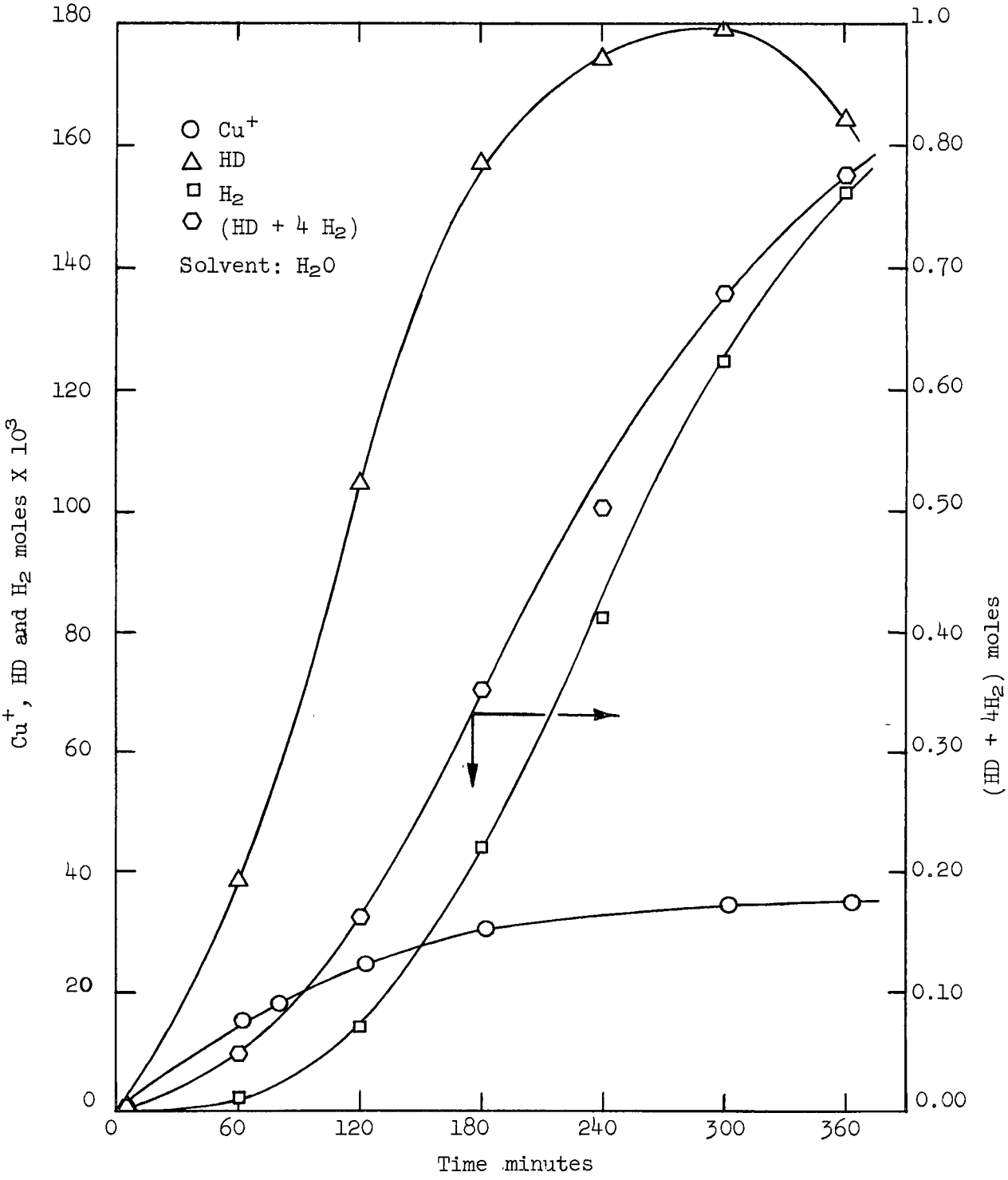

Figure 32. Rate Curves of Total Cu^{+}, HD, H_2 and (HD + $4H_2$), Experiment D_2-C; 0.07 M[$Cu(ClO_4)_2$], 0.10 M[$HClO_4$], Initial D_2 15 atm, 160°C.

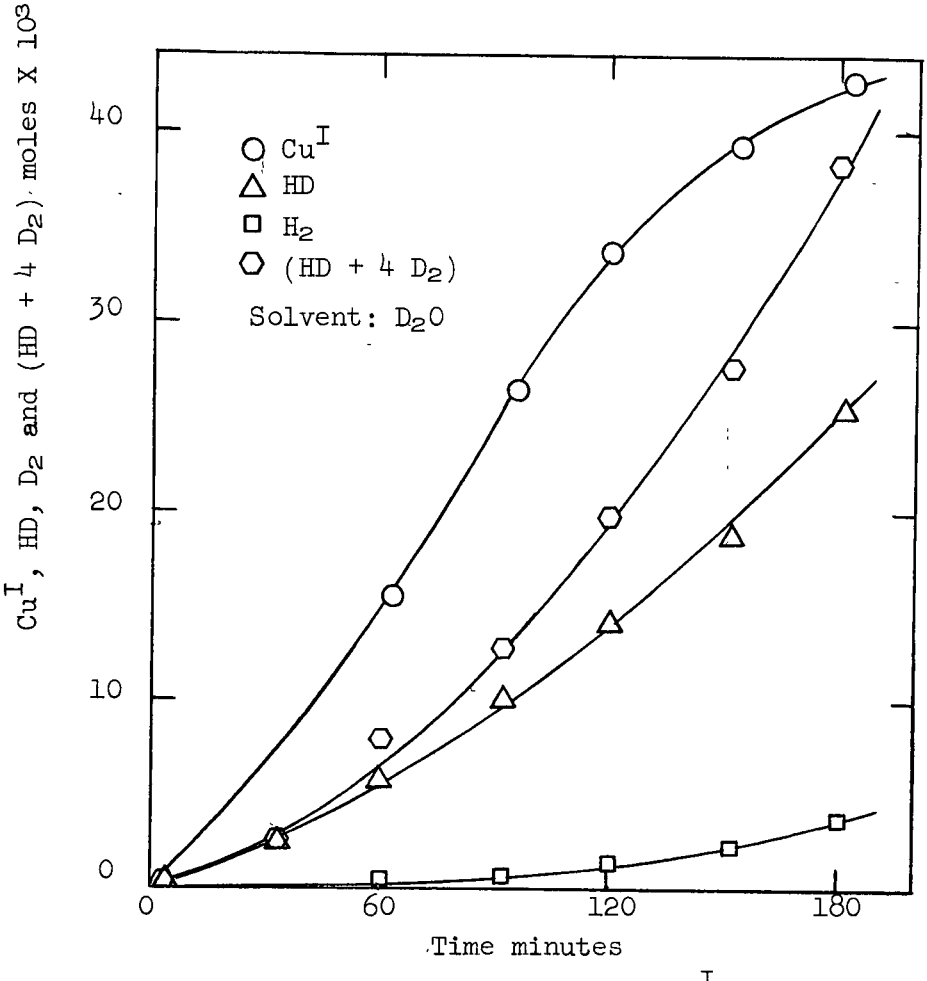

Figure 33. Rate Curves of Total Cu^I HD, D_2 and (HD + 4 D_2), Experiment H_2-D; 0.15 M $[CuSO_4]_o$, 0.85 M$[H_2SO_4]_o$, Initial H_2 5 atm, 160°C.

The appearance of H_2 in the gas phase results from exchange following the reaction of HD with copper ions and back reaction with H^+ to form hydrogen. The plot of $(HD + 4H_2)$* is the rate curve for the total exchange taking place during the experiment assuming that the only reactionswhereby exchange occurs are those given by equations -34 and -36.

No exchange was observed in the experiment D_2-E without copper in solution, indicating that the presence of either cupric or cuprous is required to support the exchange reaction. It is known that deuterium exchange may also be catalyzed by hydroxyl ions[32] but the exchange rate due to this is too small to be observable in the present acid solutions.

Rate measurements were made at several Cu^I levels of both the net forward rate $\frac{1}{2}\frac{dCu^I}{dt}$** and the exchange rate $\frac{d(HD + 4H_2)}{dt}$** and are shown plotted in moles/sec against Cu^I in Figure 34.

Kinetically the exchange rates can be related to the net forward rates by the following equation

$$\frac{d(HD + 4H_2)}{dt} = R_{exch} = \frac{k_{-1}}{k_2}\frac{[H^+]}{[Cu^{II}]} \cdot \frac{1}{2}\frac{dCu^I}{dt} + \frac{k_{-3}[H^+]}{k_4[Cu^{II}]} \cdot R_{Cu^I}\left(\frac{k_{-1}[H^+]}{k_2[Cu^{II}]} + 1\right) \quad .....(50)$$

where R_{Cu^I} is the cuprous catalyzed portion of the net forward rate.

---

* The factor 4 before H_2 results from the exchange following the reaction of HD with Cu^{II} (or Cu^I) which first of all gives rise to a factor of 2. An additional factor of 2 must be used because this exchange can take place by two equally probable paths if isotope effects are neglected, i.e.,

$$Cu^{II} + HD \xrightarrow{k_1} \begin{matrix} CuD^+ \\ CuH^+ \end{matrix} + \begin{matrix} H^+ \\ D^+ \end{matrix}$$

and

$$\begin{matrix} CuD^+ \\ CuH^+ \end{matrix} + H^+ \xrightarrow{k_{-1}} Cu^{II} + \begin{matrix} HD \\ H_2 \end{matrix}$$

** Rate measurements are listed in Appendix I.

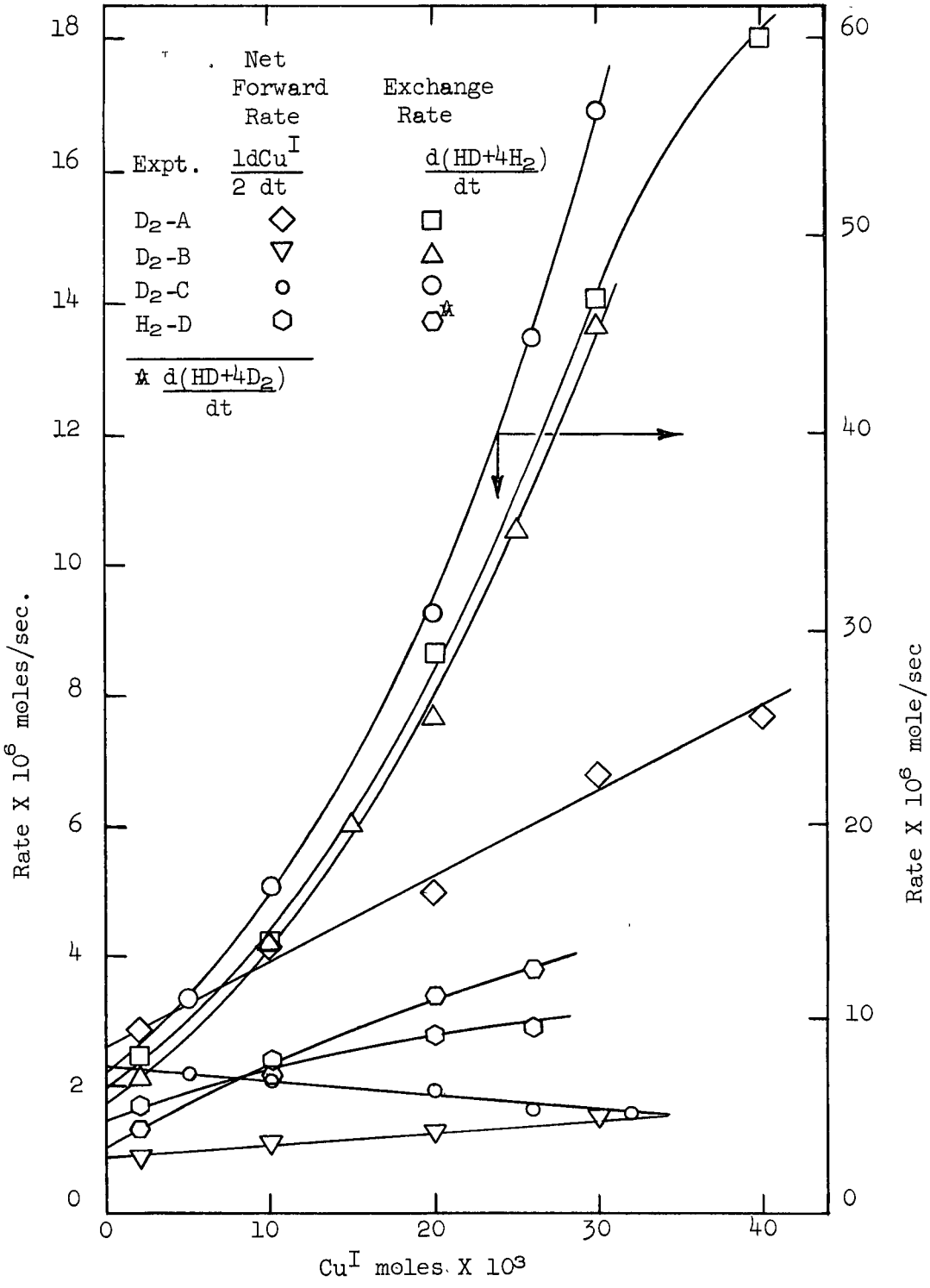

Figure 34. Plots of Net Forward Rate and Exchange Rate vs. Cu^I for Each Exchange Experiment

Equation 50 was derived from the copper reduction mechanism (equations 34 to 37) by using the steady state approximation in CuH^+ and CuH together with the expression for the net forward rate (equation 38). At $Cu^I = 0$, $R_{Cu}I$ is also zero and equation 50 reduces to

$$R_{exch} = \frac{k_{-1}}{k_2} \frac{[H^+]}{[Cu^{II}]} \cdot \frac{1}{2} \frac{dCu^I}{dt} \qquad \ldots\ldots(51)$$

Equation 51 maybe used to estimate $\frac{k_{-1}}{k_2}$ from the exchange and net forward rates and zero cuprous, i.e., the intercepts of the plots in Figure 34 provided isotope effects are disregarded.

Values of this ratio are listed in Table IX. for each experiment together with figures for $\frac{k_{-3}}{k_4}$ estimated with equation 50 from the rates measured at $Cu^I = 0.01$ moles (Figure 34) and the previously obtained values of $\frac{k_{-1}}{k_2}$.

TABLE IX.

Values of $\frac{k_{-1}}{k_2}$ and $\frac{k_{-3}}{k_4}$ from Exchange Experiments

Experiment	$\frac{k_{-1}}{k_2}$	$\frac{k_{-3}}{k_4}$ at $Cu^I = 0.01$ moles
D_2-A	1.15	0.33
D_2-B	0.41	0.41
D_2-C	2.24	-
H_2-D	0.15	0.03

Although these values exhibit some variation those obtained for the high acid experiment (D_2-B) are of the same order of magnitude as the ratios obtained previously in the acid series (Table V). This can be considered as evidence that the exchange reaction takes place, at least in part, according to the mechanism of reduction of cupric sulphate given in equations 34 to 37.

The ratios of exchange rate to net forward rate were determined for each experiment and are shown plotted in Figure 35. In sulphate solutions these ratios are greater for the high acid (D_2-B) than for the low acid (D_2-A) experiment, and this is as expected from the copper reduction mechanism.

The exchange rates of the low acid experiment are slightly higher than those of the high acid run (Figure 34) although the opposite should be tru according to equations -34 and -36. A possible explanation for this discrepancy might be that additional deuterium exchange occurs by other unobserved reactions, e.g.,

$$Cu(OH)^+ + D_2 \longrightarrow Cu(OD)^+ + HD \qquad .....(52)$$

The exchange rates measured in the cupric perchlorate experiment, D_2-C are much greater than those of the sulphate runs (Figure 34). Also the ratios of exchange to net forward* rate (Figure 35) are considerably greater and increase markedly with cuprous. The strong effect of the cuprous ion on the exchange rate suggests that this species catalyzes the exchange between D_2 and H^+. This is of interest in view of the earlier reported low catalytic activity of cuprous in the reduction of cupric perchlorate (Figure 7). If in perchlorate solutions a similar mechanism applies for hydrogen activation by cuprous as in the sulphate system the above results would suggest a much greater ratio of $\frac{k_{-3}}{k_4}$ in the perchlorate system.

The exchange rates measured in experiment H_2-D, where D_2O was the solvent, are considerably lower than those of D_2-B although the acidity and initial cupric concentrations were the same in both. This difference in rates might be a solvent effect and likely due to a lower thermodynamic activity of

---

* The net forward rates were corrected for the perchlorate decomposition effect.

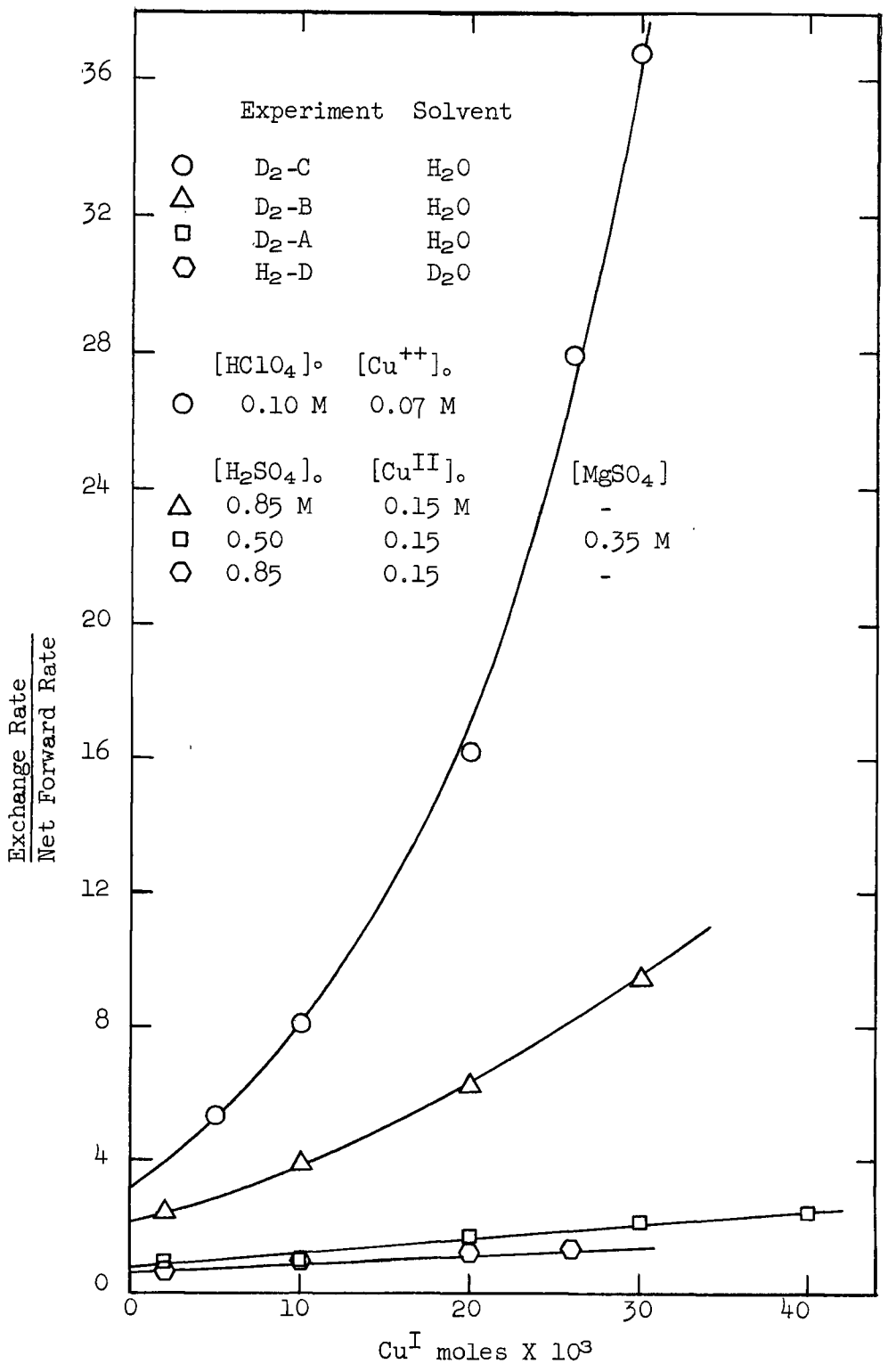

Figure 35. Plots of Exchange Rate over Net Forward Rate vs Cu^{I} for Each Exchange Experiment.

D^+ in D_2O relative to that of H^+ in H_2O, resulting from the ability of D_2O to hydrate ions more strongly than H_2O[51].

The net forward rates were also measured in terms of moles/liter/sec, i.e., $\frac{1}{2}\frac{d[Cu^I]}{dt}$, and compared with those obtained from experiments in which H_2 was used (Appendix I). They were about 20 to 50% slower than the latter, and this may be attributed to the isotope effect. This effect is similar in magnitude to that observed in the reduction of cupric acetate in quinoline solutions[52]. The net forward rates in experiment H_2-D, using D_2O and H_2 were however, virtually the same as those of the corresponding experiment with ordinary water and H_2, indicating that in sulphate solution D_2O as solvent has no effect on the activity of Cu^{II} and Cu^I toward hydrogen. This observation is in line with that of Harrod and Halpern[53] who found that the ratio of rate constants $\frac{k_{H_2O}}{k_{D_2O}}$ was close to unity (0.93) for hydrogenation reactions if cupric ions were complexed with acetate. For cupric aquo complexes this ratio was found to be larger (1.20) and the difference was ascribed to the ability of D_2O to hydrate metal ions more strongly[51] than H_2O (hence $k_{D_2O} \lesssim k_{H_2O}$). Therefore, one explanation for the zero solvent effect in the present experiment is that both Cu^{II} and Cu^I may be complexed with sulphate rather than with D_2O.

The Activation of Hydrogen by Cuprous Ions

The experimental evidence of this study indicates that in aqueous sulphate solutions both cupric and cuprous ions activate hydrogen. This probably takes place by heterolytic splitting of the H_2 molecule resulting in the formation of a copper hydride (CuH^+ or CuH) and the simultaneous release of a proton in the activation step. Atlhough the nature of these hydrides in aqueous solution has not been determined by direct observation, their existence appears fairly conclusive on kinetic evidence. CuH^+ appears to have been observed spectro-

scopically[54] and its formation in the activation of hydrogen by aqueous cupric ions was shown to be probable on energetic grounds[41]. CuH has been prepared in the solid state[55] and thermochemical data of the gaseous species have been published[56, 57]. It is analogous to AgH which has been proposed to account in part for the kinetics of hydrogen activation by aqueous Ag^{+}[18].

Using published thermochemical data[*] the endothermicity of the activation reaction can be represented as follows,

$$Cu^{I} + H_2 \longrightarrow CuH + H^{+}; \quad \Delta H = 53 \text{ kcal} + \Delta H_{s_{CuH}} \quad .....(53)$$

where $\Delta H_{s_{CuH}}$ is the solvation energy of gaseous CuH. With $\Delta H^{\ddagger}$ = 14.5 kcal this requires that $\Delta H_{s_{CuH}}$ is - 38.5 kcal/mole if CuH is effectively the activated complex and more negative than this if CuH is significantly more stable than the activated complex.

The mechanism for hydrogen activation by Cu^{II} and Cu^{I} (equations 34 to 37) is similar to that given by Chalk and Halpern[30] for the activation of H_2 by cupric and cuprous heptanoates in organic solvents such as diphenyl octadecane and heptanoic acid above 120°C. This mechanism also involves heterolytic splitting of the hydrogen molecule by both copper species. Calvin and Wilmarth[28], on the other hand observed a homolytic activation of hydrogen by cuprous ions in quinoline solutions at 100°C according to

$$2\ Cu^{I} + H_2 \longrightarrow 2Cu^{I}H \quad .....(54)$$

but this was not found in the heptanoate and aqueous sulphate systems.

---

[*] The following standard enthalpies of formation were used: $Cu^{+}_{(aq)}$ 17.1 kcal[58]; $H_{2(aq)}$ 0.9 kcal (calculated for 25°C from Figure 1, reference 59); $CuH_{(g)}$ 71 kcal[57]; $H^{+}_{(aq)}$ 0.

The cuprous mechanism may be compared with that of silver ions[18] in aqueous perchlorate solutions where activation of hydrogen by both homolytic and heterolytic splitting takes place. The latter path predominates at higher temperatures (100 to 120°C) and dilute silver solutions ($\sim$ 0.01 M) whereas the former is prevalent in the range of 30 to 50°C at higher concentrations of Ag^+ ($\sim$ 0.10 M). In view of this it is plausible that cuprous ions also activate H_2 by homolytic splitting in aqueous systems but this reaction never becomes important because at high temperatures it is masked by the heterolytic path and at low temperatures the cuprous ions disproportionate to such an extent in acid solutions that concentrations high enough to permit observation of any activity cannot be obtained.

An important observation from the present study is the considerable activity of cuprous ions in both sulphate and perchlorate solutions toward deuterium exchange. However in the reduction of cupric ions the enhancing effect of Cu^I is significant only in sulphate solutions, and appears relatively small in the perchlorate system. If it is assumed that the mechanism of hydrogen activation by cuprous ions is the same in both systems this would mean that the ratio $\frac{k_{-3}}{k_4}$ must be considerably larger in perchlorate solutions than the value of 0.45 obtained in the sulphate system. From the reactions associated with these rate constants, i.e.,

$$CuH + H^+ \xrightarrow{k_{-3}} Cu^I + H_2 \qquad .....(-36)$$

$$CuH + Cu^{II} \xrightarrow{k_4} CuH^+ + Cu^I \qquad .....(37)$$

it appears likely that the change in $\frac{k_{-3}}{k_4}$ is due primarily to a change in k_4. Reaction 37 is an electron transfer process which would proceed more rapidly if a bridging ligand such as sulphate were present to facilitate the transfer[60,61].

Thus k_4 would be expected to be larger in sulphate than in perchlorate solutions where Cu^{II} is complexed as the aquo ion only. Provided that k_{-3} is not much different in both systems, this will explain why Cu^{I} makes a very small contribution to copper reduction but a surprisingly large contribution to deuterium exchange in perchlorate solutions relative to sulphate solutions. Thus it seems that this analysis has permitted an effect to be observed that involves a very fast reaction, namely the electron transfer process of equation 37, because it competes with another similarly fast reaction which is the back reaction, equation -36.

This argument can also be applied to the Cu^{II} activated reduction path where $\frac{k_{-1}}{k_2}$ is about 0.13 in sulphate solutions and 0.4 to 0.5 in perchlorate solutions. Thus, the complexing of Cu^{II} in the sulphate system would enhance the value of k_2 over that in the perchlorate system in much the same way as for k_4.

CONCLUSION

The present work describes an investigation of the reduction of cupric ions by molecular hydrogen in aqueous perchlorate and sulphate solutions. The objective was to resolve the kinetics of this reaction and particularly to establish the role of cuprous ions in the reduction mechanism.

In the sulphate system considerable catalytic activity of cuprous ions was found and the mechanism describing the reduction kinetics has been postulated to be

$$Cu^{II} + H_2 \underset{k_{-1}}{\overset{k_1}{\rightleftharpoons}} CuH^+ + H^+$$

$$CuH^+ + Cu^{II} \xrightarrow{k_2} 2Cu^{I} + H^+$$

$$Cu^{I} + H_2 \underset{k_{-3}}{\overset{k_3}{\rightleftharpoons}} CuH + H^+$$

$$CuH + Cu^{II} \xrightarrow{k_4} CuH^+ + Cu^{I}$$

This mechanism gives rise to a two term rate law of which one depends on cupric only and the other exhibits a first order dependence on cuprous concentration. This rate law has the form

$$-\frac{d[H_2]}{dt} = \frac{k_1[Cu^{II}]^2[H_2]}{\frac{k_{-1}}{k_2}[H^+]+[Cu^{II}]} + \frac{k_3[Cu^{II}]^2[Cu^{I}][H_2]}{\left(\frac{k_{-1}}{k_2}[H^+]+[Cu^{II}]\right)\left(\frac{k_{-3}}{k_4}[H^+]+[Cu^{II}]\right)}$$

The studies in perchlorate solutions showed that the kinetics are adequately described by the first two reactions in the above mechanism represented by the first term of the rate law and that the enhancing effect of Cu^+ on rates was only slight. A correction of rate measurements due to perchlorate decomposition had to be taken into account in order that a meaningful analysis of the data could be obtained and only then was the small Cu^+ effect observable.

Exchange experiments with deuterium in place of hydrogen gave rates consistent with the proposed mechanism although in perchlorate solutions much higher exchange rates were observed than in sulphate solutions. This indicated that $\frac{k_{-3}}{k_4}$ is much greater in perchlorate than in sulphate solutions.

REFERENCES

1. F. A. Schaufelberger and T. K. Roy, Trans. Inst. Min. and Met. 64, 375 (1955).

2. F. A. Schaufelberger, Trans. A.I.M.E., 206, 695 (1956); J. Metals 8, 695 (1956).

3. D. J. I. Evans, S. Romanchuk and V. N. Mackiw, C.I.M.M. Bull. 54, 530, (1961).

4. V. H. Ryan and H. J. Tschirner, Proc. Metal Powder Assoc. 1, 25 (1957).

5. F. A. Forward, Trans. C.I.M M., 56, 363 (1956).

6. F. A. Forward, Bull. Inst. Metals, 2, 113 (1954).

7. V. N. Mackiw, W. C. Lin and W. Kunda, Trans. A.I.M.E., 209, 786 (1957).

8. R. F. Pearce, J. P. Warner and V. N Mackiw, J. Metals, 12, 28 (1960).

9. J. Halpern, Trans. A.I.M.E., 209, 280 (1957); J. Metals, 9, 280 (1957).

10. E. Peters and J. Halpern, Can. J. Chem, 33, 356 (1955).

11. E. Peters and J. Halpern, J. Phys. Chem, 59, 793 (1955).

12. H. F. McDuffie, E. L. Compere, H. H. Stone, L. F. Woo and C. H. Secoy, J. Phys. Chem. 62, 1030 (1958).

13. V. N. Ipatieff, and W. Werschowski, Chem. Ber., 42, 2078 (1909).

14. J. Halpern and R. G. Dakers, J. Chem. Phys. 22, 1272 (1954).

15. R. G. Dakers and J. Halpern, Can. J. Chem., 32, 969 (1954).

16. E. Peters and J. Halpern, Can. J. Chem., 34, 554 (1956).

17. A. H. Webster and J. Halpern, J. Phys. Chem. 60, 280 (1956).

18. A. H. Webster and J. Halpern, J. Phys. Chem. 61, 1239, 1245 (1957).

19. J. Halpern and J. B. Milne, Actes Congr. Intern. Catalyse, 2°, Paris, 1, 445 (1960).

20. J. Halpern, G. J. Korinek and E. Peters, Research, 7, 61 (1954).

21. a) G. J. Korinek and J. Halpern, J. Phys. Chem., 60, 285, (1956);
    b) G. J. Korinek and J. Halpern, Can. J. Chem., 34, 1372 (1956).

22. J. Halpern, J. F. Harrod and P. E. Potter, Can. J. Chem., 37, 1446 (1959).

23. J. F. Harrod and J. Halpern, Can. J. Chem. 37, 1933 (1959).

24. J. F. Harrod, Stefania Ciccone and J. Halpern, Can. J. Chem., 39, 1372 (1961).

25. J. Halpern, B. R. James and A. L. W. Kemp, J. Am. Chem. Soc., 83, 4097 (1961).

26. W. J. Dunning and P. E. Potter, Proc. Chem. Soc., 244 (July 1960).

27. M. Calvin, a) Trans. Farad. Soc., 34, 1181 (1938);
b) J. Am. Chem. Soc., 61, 2230 (1939).

28. M. Calvin and W. K. Wilmarth, J. Am. Chem. Soc., 78, 1301, (1956).

29. L. Wright, S. Weller and G. A. Mills, J. Phys. Chem., 59, 1060, (1955).

30. A. J. Chalk and J. Halpern, J. Am. Chem. Soc., 81, 5846, 5852 (1959).

31. J. Halpern, J. Phys. Chem., 63, 398 (1959).

32. J. Halpern, Advances in Catalysis, 11, 301 (1959).

33. J. Halpern, E. R. Macgregor and E. Peters, J. Phys. Chem., 60, 1455 (1956).

34. E. R. Macgregor and J. Halpern, Trans. Met. Soc. A.I.M.E., 212, 244 (1958).

35. E. A. Hahn and E. Peters, Can. J. Chem. 39, 162 (1961).

36. J. Y-P. Tong and E. L. King, J. Am. Chem. Soc. 75, 6180 (1953).

37. E. R. Macgregor, Master's Thesis, The University of British Columbia, 1956.

38. F. J. Welcher, "The Analytical Uses of Ethylenediaminetetraacetic Acid", D. Van Norstrand Co. Inc., Princeton, N.J. (1958)p. 241.

39. A. T. Vogel, "Quantitative Inorganic Analysis" 2nd ed., Longmans Green and Co., Toronto, 1951.

40. R. T. McAndrew, Ph.D. Thesis, The University of British Columbia, 1962.

41. E. Peters, Ph.D. Thesis, The University of British Columbia, 1956.

42. E. Heinerth, Z. Electrochem., 37, 61 (1931).

43. W. G. Courtney, J. Phys. Chem., 60, 1461 (1956).

44. C. M. Criss, "Thermodynamic Properties of High Temperature Aqueous Solutions", Purdue University, Ph.D. Thesis 1961, University Microfilms Inc., Ann Arbor, Michigan, Mic 61-2466.

45. A. Seidell, "Solubilities of Inorganic and Metal Organic Compounds", 3rd ed., Vol. 1, D. Van Norstrand Co. Inc., New York (1940), pp. 553-561.

46. R. T. McAndrew, E. Hirsch, J. J. Byerley and E. Peters, to be published.

47. S. Glasstone, K. J. Laidler, H. Eyring, "The Theory of Rate Processes", McGraw Hill Book Co., Inc., New York (1941), p. 199.

48. P. E. Potter, Ph.D. Thesis, The University of Bristol, 1958.

49. A. H. Webster, Ph.D. Thesis, The University of British Columbia, 1957.

50. S. Weller and G. A. Mills, J. Am. Chem. Soc. 75, 769 (1953), L. W. Wright and S. Weller, ibid. 76, 3345 (1954).

51. J. Halpern and A. C. Harkness, J. Phys. Chem. 31, 1147 (1959).

52. W. K. Wilmarth and M. K. Barsh, J. Am. Chem. Soc., 78, 1305 (1956).

53. J. F Harrod and J. Halpern, J. Phys. Chem., 65, 563 (1961).

54. P. C. Mahanti, Nature, 127, 557 (1931).

55. H. J. Emeléus and J. S. Anderson, "Modern Aspects of Inorganic Chemistry", 3rd ed., Routledge and Kegan Paul, Ltd., London (1960), p. 415.

56. W. M. Latimer, "Oxidation Potentials" 2nd ed., Prentice Hall, Inc., Englewood Cliffs, N J. (1952), p. 184.

57. F. D. Rossini, D. D. Wagman, W. H. Evans, S. Levine, and I. Jaffe, "Selected Values of Chemical Thermodynamic Properties", National Bureau of Standards Circular 500, U. S. Government Printing Office, Washington D.C., (1952), p. 208.

58. D. D. Wagman, J. Am. Chem. Soc 73, 5463 (1951).

59. D. M. Himmelblau, J. Chem. and Eng. Data, 5, 11 (1960).

60. D. R. Stranks in J. Lewis and R. G. Wilkins, "Modern Coordination Chemistry", Interscience Publishers, Inc., New York (1960), p. 78.

61. J. Halpern, Quarterly Reviews, 15, 207 (1961).

APPENDICES

APPENDIX A

Report on Research Work for the Period of May 1st to September 1st, 1960

Introduction:

The purpose of this investigation was to determine whether Ni^{II}, Fe^{+++}, Co^{++} and Cr^{+++} in aqueous solutions were active as catalysts in the hydrogen reduction of dichromate. These ions had been studied previously[1] for their catalytic activity in the hydrogen reduction of oxygen between 200 and 300°C, and a pressure drop method was used for following the rates. Although no activity had been observed in that work it was decided to reinvestigate these ions by measuring the rate of disappearance of dichromate, since this method is more sensitive for observing rates than that of determining pressure drops. Most experiments were performed at 258°C using both sulphate and perchlorate solutions.

Experimental:

The experiments were carried out in a one-gallon high pressure autoclave described earlier[2]. The silicon-carbide powder packing in the annular space between the titanium liner and the autoclave vessel was removed since corrosion attack on the titanium liner and the vessel was observed at 258°C. Although the liner was placed loosely into the vessel with only a steam-gas mixture in the annular space, good temperature control (± 0.5°C) was obtained up to 258°C. The stirrer shaft stuffing box was fitted with John Crane Chemlon (molded teflon) V-rings which provided an excellent pressure seal. However rapid wear of the rings at the extreme conditions of 258°C and 800 psig required addition of an extra V-ring after each run.

All chemicals were of reagent grade quality manufactured by Baker and Adamson Company Limited. Hydrogen and nitrogen were supplied by Canadian

Liquid Air Company and used without further purification.

The experimental procedure comprised heating of the solution to temperature under a nitrogen atmosphere, sampling once or twice within one hour to check if reduction of dichromate took place in the absence of hydrogen, flushing nitrogen, adding hydrogen, and periodic sampling to follow the course of dichromate reduction.

Analyses of dichromate were made either spectrophotometrically or by titrating with ferrous ammonium sulphate solution.

Results and Discussion:

Most experiments were made at 258°C and 10 atm hydrogen partial pressure with an initial dichromate concentration of 0.003 M, and the experimental results for each ion investigated are summarized below.

Ni^{II} - A number of experiments with 0.1 to 0.2 M[$NiSO_4$] and 0.2 to 0.72 M[H_2SO_4] solutions showed that Ni^{II} is not active as a catalyst for hydrogenation of dichromate.

Co^{++} - No reduction of dichromate was observed during 160 minutes for solutions 0.075 to 0.1 M in $Co(ClO_4)_2$ and 0.1 M in $HClO_4$.

Fe^{+++} - No reduction of dichromate took place during 100 to 170 minutes in solutions of 0.004 M[$Fe(ClO_4)_3$](prepared from 99.9% pure iron test wire) and 0.1 to 0.5 M[$HClO_4$]. Dichromate reduction did take place when reagent grade $FeCl_3$ was used, but this was probably due to small amounts of active impurities present in the salt (e.g. 0.003% Cu^{++}). In all experiments partial hydrolysis of Fe^{+++} occurred and its extent depended on the acidity of the solution.

$\underline{Cr^{+++}}$ - No reduction of dichromate occurred using 0.01 M $CrCl_3$, 0.1 M $HClO_4$, 10 atm. H_2 and 258, 220, and 210°C. The solutions were heated under 10 atm. H_2 to prevent oxidation of Cr^{+++} by ClO_4^- to dichromate. Cr^{+++} hydrolyzed slowly in each experiment at temperature.

The results of this investigation have shown conclusively that sulphate or perchlorate salts of Ni^{II}, Fe^{+++}, Co^{++} and Cr^{+++} possess no catalytic activity toward hydrogen in aqueous solutions.

---

1. H. F. McDuffie et al., J. Phys. Chem. 62, 1030 (1958).

2. E. A. Hahn, Master's Thesis, The University of British Columbia, 1960.

APPENDIX B.

Rate Measurements[*] for Experiments in Perchlorate System[**]

TABLE B-1

Acid Series: 0.030 M[$Cu(ClO_4)_2$]$_o$, 10 atm H_2, 160°C.
Experiment H^+ - 5, 0.015 M[$HClO_4$]$_o$

$[Cu^+]$M	$\frac{1}{2}\frac{d[Cu^+]}{dt}$ Msec^{-1}	$-\frac{d[H_2]}{dt}$ Msec^{-1}	$[H^+]$M
4 X 10^{-3}	1.93 X 10^{-6}	1.93 X 10^{-6}	19 X 10^{-3}
8	1.60	1.61	23
12	1.00	1.02	27
16	0.445	0.48	31
18	0.273	0.31	33
	Experiment H^+ - 10, 0.030 M[$HClO_4$]$_o$		
4 X 10^{-3}	1.38 X 10^{-6}	1.39 X 10^{-6}	34 X 10^{-3}
8	1.02	1.04	38
12	0.713	0.75	42
16	0.330	0.38	46
18	0.195	9.26	48
	Experiment H^+ - 8, 0.050 M[$HClO_4$]$_o$		
4 X 10^{-3}	0.800 X 10^{-6}	0.82 X 10^{-6}	54 X 10^{-3}
8	0.662	0.70	58
12	0.390	0.46	62
16	0.190	0.29	66
18	0.112	0.22	68
	Experiment H^+ - 11, 0.070 M[$HClO_4$]$_o$		
4 X 10^{-3}	0.647 X 10^{-6}	0.68 X 10^{-6}	74 X 10^{-3}
8	0.546	0.60	78
12	0.282	0.37	82
16	0.117	0.26	86
	Experiment H^+ - 9, 0.100 M[$HClO_4$]$_o$		
4 X 10^{-3}	0.416 X 10^{-6}	0.47 X 10^{-6}	104 X 10^{-3}
8	0.285	0.40	108
12	0.157	0.34	112

[*] Rate measurements were made with the mirror image method at several $[Cu^+]$ levels along the rate curves of each experiment.

[**] In the perchlorate system, measured rates were corrected for the perchlorate decomposition effect i.e., $-\frac{d[H_2]}{dt} = \frac{1}{2}\frac{d[Cu^+]}{dt} + 4k_{Cl}[Cu^+][H^+][ClO_4^-]$, $k_{Cl} = 2.07 \times 10^{-4} M^{-2} sec^{-1}$ (Appendix C).

TABLE B-2.

Cuprous Series: 10 atm H_2, 160°C.

Experiment Cu^+ - 20, 0.060 M[$Cu(ClO_4)_2$]$_o$, 0.070 M[$HClO_4$]$_o$

$[Cu^+]$ M	$\frac{1}{2}\frac{d[Cu^+]}{dt}$ Msec^{-1}	$-\frac{d[H_2]}{dt}$ Msec^{-1}	$[H^+]$ M	$[Cu^{++}]$ M
20×10^{-3}	1.50×10^{-6}	1.78×10^{-6}	90×10^{-3}	40×10^{-3}
25	1.10	1.47	95	35
30	0.66	1.13	100	30
Experiment Cu^+ - 21, 0.050 M[$Cu(ClO_4)_2$]$_o$, 0.080 M[$HClO_4$]$_o$				
10×10^{-3}	1.29×10^{-6}	1.43×10^{-6}	90×10^{-3}	40×10^{-3}
15	1.05	1.26	95	35
20	0.76	1.06	100	30
Experiment Cu^+ - 22, 0.040 M[$Cu(ClO_4)_2$]$_o$, 0.090 M[$HClO_4$]$_o$				
10×10^{-3}	0.68×10^{-6}	0.82×10^{-6}	100×10^{-3}	30×10^{-3}

TABLE B-3.

Cupric Series: 0.100 M[$HClO_4$]$_o$, 10 atm H_2, 160°C.

Experiment H^+ - 9, 0.030 M[$Cu(ClO_4)_2$]$_o$

$[Cu^+]$ M	$\frac{1}{2}\frac{d[Cu^+]}{dt}$ Msec^{-1}	$-\frac{d[H_2]}{dt}$ Msec^{-1}	$[Cu^{++}]$ M
4 X 10^{-3}	0.416 X 10^{-6}	0.47 X 10^{-6}	26 X 10^{-3}
8	0.285	0.40	22
12	0.157	0.34	18
14	0.082	0.30	16
Experiment $[Cu^{++}]$ - 1, 0.040 M[$Cu(ClO_4)_2$]$_o$			
4 X 10^{-3}	0.794 X 10^{-6}	0.86 X 10^{-6}	36 X 10^{-3}
8	0.678	0.81	32
12	0.554	0.75	28
14	0.430	0.67	26
16	0.290	0.57	24
18	0.185	0.50	22
Experiment $[Cu^{++}]$ - 2, 0.050 M[$Cu(ClO_4)_2$]$_o$			
4 X 10^{-3}	1.173 X 10^{-6}	1.24 X 10^{-6}	46 X 10^{-3}
8	1.058	1.20	42
12	0.981	1.20	38
14	0.880	1.14	36
16	0.777	1.08	34
18	0.607	0.97	32
Experiment $[Cu^{++}]$ - 3, 0.060 M[$Cu(ClO_4)_2$]$_o$			
4 X 10^{-3}	1.68 X 10^{-6}	1.76 X 10^{-6}	56 X 10^{-3}
8	1.68	1.84	52
12	1.49	1.73	48
14	1.38	1.67	46
16	1.27	1.61	44
18	1.12	1.51	42
Experiment $[Cu^{++}]$ - 4, 0.070 M[$Cu(ClO_4)_2$]$_o$			
4 X 10^{-3}	1.98 X 10^{-6}	2.06 X 10^{-6}	66 X 10^{-3}
8	2.10	2.27	62
12	2.04	2.31	58
14	1.94	2.26	56
16	1.83	2.20	54
18	1.78	2.20	52

APPENDIX C.

Determination of the Perchlorate Reduction Rate Constant k_{Cl}

Chloride ions resulting from attack of ClO_4^- by Cu^+ will appear during the hydrogen reduction of Cu^{++} according to the stoichiometry

$$8Cu^+ + 8H^+ + ClO_4^- \longrightarrow 8Cu^{++} + Cl^- + 4H_2O \qquad .....(C-1)$$

The rate of this reaction is assumed to be represented by

$$\frac{d[Cl^-]}{dt} = k_{Cl}\,[Cu^+][H^+][ClO_4^-] \qquad .....(C-2)$$

Solving for k_{Cl}, this equation in the integrated form becomes

$$k_{Cl} = \frac{[Cl^-]\,t}{[ClO_4^-]\int_0^t ([Cu^+]^2 + [H^+]_o[Cu^+])\,dt} \qquad .....(C-3)$$

since $[H^+]$ is $[H^+]_o + [Cu^+]$. $[ClO_4^-]$ is assumed to remain constant during the course of an experiment because the amount reduced is small. The subscript t is the time at which $[Cl^-]$ is measured, usually at the end of a run, and to which the integration is performed.

The integral in equation C-3 is evaluated graphically by estimating $[Cu^+]$ values from the rate curve of a Cu^{++} reduction experiment (e.g. Figure C-1)* for a number of equal time intervals up to time t. The value of the integral thus obtained from the rate curve in Figure C-1 is 0.654 M^2 min at t = 600 min, and with $[ClO_4^-]$ = 0.13 M and $[Cl^-]_t = 0.99 \times 10^{-3}$ M k_{Cl} is calculated to be 1.93×10^{-4} $M^{-2}sec^{-1}$.

Values of k_{Cl} were calculated for eight experiments and are listed in Table C-1 together with the initial experimental conditions for each run.

---

* Experiment H^+-11; see Table C-1 for experimental conditions.

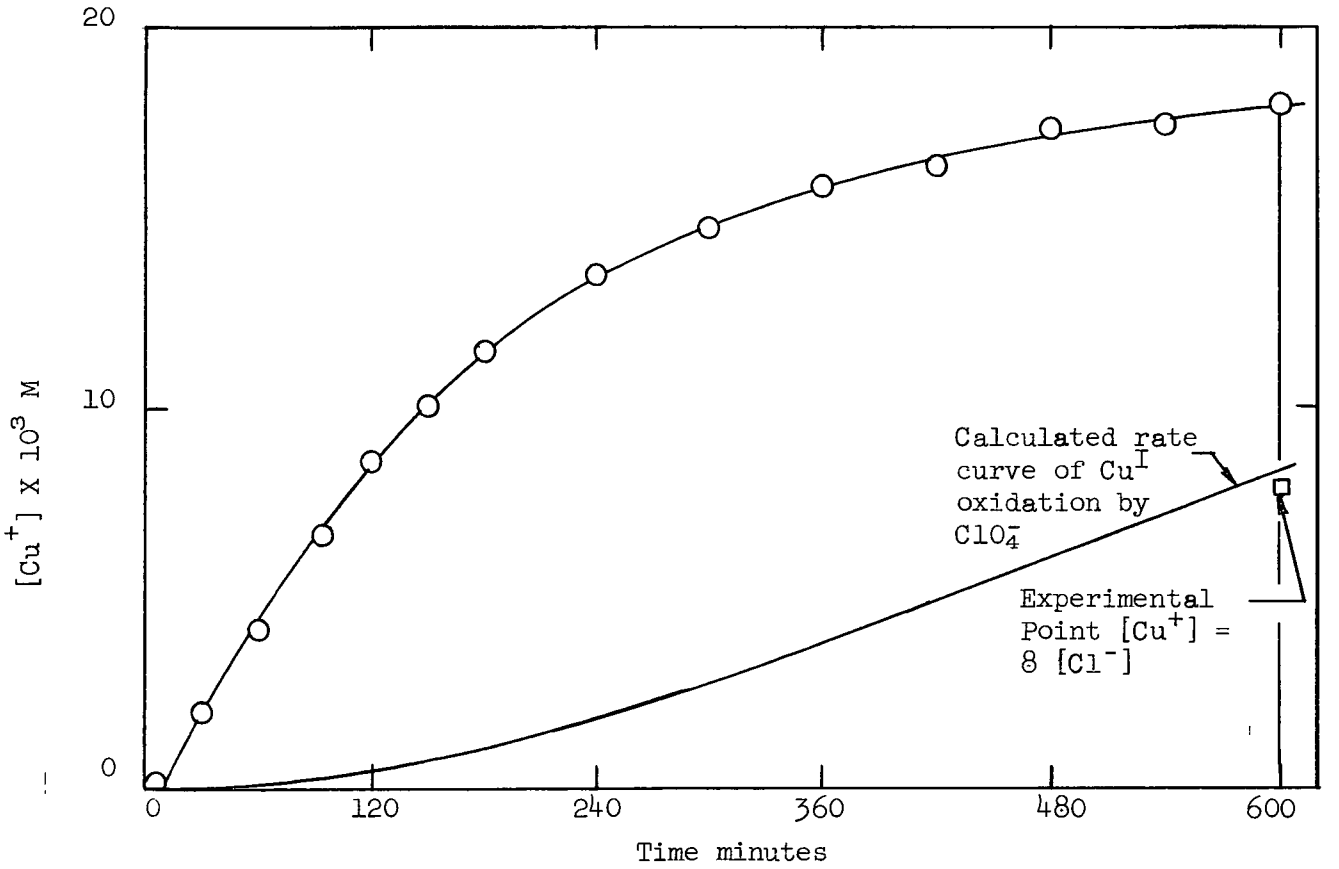

Figure C-1. Rate Curve of Experiment H^+-11 for Determination of k_{Cl} by Graphical Integration and Calculated Curve of Cu^+ Oxidation by ClO_4^-.

The average value obtained for this constant is 2.07 X 10^{-4} ± 7% $M^{-2}sec^{-1}$.

TABLE C-1.

Values of k_{Cl} from Eight Experiments and Data* of Initial Experimental Conditions

Experiment Number	$k_{Cl} M^{-2}sec^{-1}$	$[Cu^{++}]_o M$	$[H^+]_o$ M	$[ClO_4^-]$ M	$[Cl^-]$ M	Time min
Cu^{++}-1	2.14 X 10^{-4}	0.04	0.10	0.18	1.01 X 10^{-3}	330
Cu^{++}-2	2.27	0.05	0.10	0.20	1.46	300
Cu^{++}-3	1.94	0.06	0.10	0.22	1.90	300
Cu^{++}-4	1.94	0.07	0.10	0.24	2.65	300
H^+-8	2.15	0.03	0.05	0.11	0.56	480
H^+-9	1.85	0.03	0.10	0.16	1.18	600
H^+-10	2.27	0.03	0.03	0.09	0.43	480
H^+-11	1.94	0.03	0.07	0.13	0.99	600
Average	2.07 X 10^{-4} ± 7% $M^{-2}sec^{-1}$					

* 10 atm H_2 and 160°C for all experiments.

Using this value and the equation

$$[Cu^+]_{oxidized} = 8[Cl^-] = 8\, k_{Cl}[ClO_4^-] \int_o^t ([Cu^+]^2+[H^+]_o[Cu^+])\, dt \qquad .....(C-4)$$

a theoretical curve for the oxidation of cuprous ions was calculated for experiment H^+-11 and is shown in Figure C-1. As expected, the rate of cuprous oxidation at first increases with rising $[Cu^+]$ but then becomes constant as the $[Cu^+]$ rate curve levels off.

APPENDIX D.

TABLE D-1.

Thermodynamic Data* for Calculating ΔF°_T for the Disproportionation Reaction

	ΔF°_f kcal/mole	S°_t eu
$Cu^{++}(aq)$	15.5	-23.6
$Cu^{+}(aq)$	12.0	9.4
$Cu^\circ(s)$	0.0	8.0

* All data are from W. M. Latimer, "Oxidation Potentials" 2nd ed. Prentice Hall, Inc., Englewood Cliffs N.J., (1952), except those for $Cu^{+}(aq)$ which are taken from D. D. Wagman, J. Am. Chem. Soc., 73, 5463 (1951).

APPENDIX E

Integrated Rate Curves for the Perchlorate System

(a) Before disproportionation of Cu^+.

The rate curve was calculated i) with equation 26 and ii) by graphical integration of equation 17 that includes the perchlorate decomposition correction. The initial experimental conditions were: 0.03 M[$Cu(ClO_4)_2$], 0.07 M[$HClO_4$], 10 atm. H_2, 160°C.

i) Values of t as a function of [Cu^+] obtained with equation 26 are listed in Table E-1 and were obtained by using $k_1 = 6.0 \times 10^{-3} M^{-1} sec^{-1}$, $\frac{k_{-1}}{k_2} = 0.45$, $[H_2] = 11.8 \times 10^{-3}$ M.

TABLE E-1.

t as a Function of [Cu^+] Calculated with Equation 26

[Cu^+] M	t min
4×10^{-3}	36
8	85
12	151
16	252
20	425
24	809

ii) Equation 17 was rearranged to the form

$$t = \int_0^x \frac{[f(e + x) + (b - x)]\, dx}{a(b - x)^2 - gx\,(e + x)[f(e + x) + (b - x)]}$$

and t calculated as a function of x by graphical integration; the symbols being:

$x = [Cu^+]$ M

$\Delta x = 2 \times 10^{-3}$ M

$a = 2k_1[H_2] = 2 \times 6.6 \times 10^{-3} \times 11.8 \times 10^{-3}$ sec^{-1} ✱
$b = [Cu^{++}]_o = 30 \times 10^{-3}$ M
$e = [H^+]_o = 70 \times 10^{-3}$ M
$f = \frac{k_{-1}}{k_2} = 0.49$ ✱
$g = 8k_{Cl}[ClO_4^-] = 8 \times 2.07 \times 10^{-4} \times 0.13$ M^{-1}sec^{-1}

TABLE E-2.

t as a Function of $[Cu^+]$ from Graphical Integration of Equation 17.

$[Cu^+]$ M	t min
2×10^{-3}	16
4	36
6	58
8	85
10	119
12	162
14	225
16	321
18	562

(b) After disproportionation of Cu^+.

The initial experimental conditions were 0.137 M$[Cu(ClO_4)_2]$, 0.103 M$[HClO_4]$, 10 atm H_2, 160°C.

The rate curve was calculated by graphical integration of an expression that included the rate law after disproportionation, equation 31, and the perchlorate decomposition correction, i.e., $4\ k_{Cl}[Cu^+][H^+][ClO_4^-]$. This expression has the form

$$t = -\int_{x_o}^{x} \frac{\left(1 + \frac{1}{1 + 4K^{1/2}x^{1/2}}\right) dx}{\left(\frac{a\,x^2}{b[H^+] + x} - \frac{c\,x^{1/2}[H^+]}{K^{1/2}}\right)}$$

✱ Different values of k_1 and $\frac{k_{-1}}{k_2}$ were used here than in i) to check if these slight changes had any effect on the shape of the rate curves. The effect was however, found to be small.

where $x = [Cu^{++}]$ M

$\Delta x = 5 \times 10^{-3}$ M

$a = k_1[H_2] = 6.0 \times 10^{-3} \times 11.8 \times 10^{-3}$ sec^{-1}

$b = \frac{k_{-1}}{k_2} = 0.50$

$c = 4k_{Cl}[ClO_4^-] = 4 \times 2.07 \times 10^{-4} \times 0.356^{*}$ M^{-1} sec^{-1}

$K = 26_{Cl}$ M^{-1}

$[H^+] = \left([H^+]_o + 2x_o - 2x - (\frac{x}{K})^{1/2}\right)$ M

Values of t as a function of $[Cu^{++}]$ are listed in Table E-3.

TABLE E-3.

t as a Function of $[Cu^{++}]$ After Disproportionation of Cuprous Ions

$[Cu^{++}]$ M	t min
105 X 10^{-3}	17
100	46
95	96
90	162
85	270
80	495

* Average value of $[ClO_4^-]$ over course of entire run taking into account loss due to decomposition to Cl^-.

APPENDIX F.

Estimation of Hydrogen Ion Concentration in Sulphate System at 160°C.

No information was available for the bisulphate dissociation constant, K_b, at 160°C. Hence, for determining hydrogen ion concentrations in the sulphate system K_b was estimated to be within the range of 10^{-3} to 10^{-2} M at that temperature.

This estimate is based in part on the published change in K_b in the range of 5 to 55°C where it is found to decrease from 1.8×10^{-2} M at 5°C to 4.1×10^{-3} M at 55°C.[1] Extrapolation of a linear log K_b vs temperature plot of the published data gave a value of 2.2×10^{-4} M at 160°C. However, this decrease is offset to some extent by the high ionic strengths in the experimental solutions. For example, the average values of K_b in the range of 20 to 50°C was shown to increase from 2.5×10^{-2} M at 0.1 M H_2SO_4 to 1.0×10^{-1} M at about 1.4 M H_2SO_4[2]. This increase will be enhanced if H_2SO_4 is replaced in part by $CuSO_4$ and $MgSO_4$, and, assuming the ionic strength effect to be similar at 160°C, this is likely to bring the value of K_b into the range of 10^{-3} to 10^{-2} M at that temperature.

In calculating the hydrogen ion concentrations at 160°C the effect of complexing of sulphate by cupric ions was neglected. Although some information exists on the association constant for the reaction

$$Cu^{++} + SO_4^{=} \underset{}{\overset{K_a}{\rightleftharpoons}} CuSO_4$$

at room temperature[3] ($K_a = 4.5\ M^{-1}$) and at 110°C[4] ($K_a = 6.7\ M^{-1}$) no data are available for 160°C.

---

1. R. W. Gurney, "Ionic Processes in Solution", Dover Publications Inc., New York, 1962, p. 121.
2. M. E. Wadsworth and D. R. Wadja, J. Metals 7, 755 (1955).
3. R. Näsänen and B. Klaile, Suomen Khemistilehti, B 27, 50 (1954).
4. E. Peters and J. Halpern, Can. J. Chem., 34, 554, (1956).

APPENDIX G.

Rate Measurements* for Experiments in Sulphate System

TABLE G-1.

Acid Series: 0.15 M[$CuSO_4$]$_o$, 5 atm H_2, 160°C.

Experiment:	H_2SO_4 - 2	H_2SO_4 - 1	Cu^{II} - 1	H_2SO_4 - 3
[H_2SO_4]$_o$ M:	0.50	0.60	0.70	0.85
[$MgSO_4$] M:	0.35	0.25	0.15	0.00

$[Cu^I]$ M	$-\frac{d[H_2]}{dt}$ Msec^{-1}**			
5×10^{-3}	4.32×10^{-6}	3.66×10^{-6}	-	2.04×10^{-6}
6	-	-	2.98×10^{-6}	-
10	5.90	4.65	3.48	2.51
20	9.01	6.68	4.90	3.01
30	12.2	8.66	6.10	3.59
40	14.8	10.7	7.15	3.98

TABLE G-2.

Cupric Series: 0.70 M[H_2SO_4]$_o$, 5 atm H_2, 160°C.

Experiment:	Cu^{II} - 5	Cu^{II} - 2	Cu^{II} - 1	Cu^{II} - 3	Cu^{II} - 4
[$CuSO_4$]$_o$ M:	0.05	0.10	0.15	0.20	0.25
[$MgSO_4$] M:	0.25	0.20	0.15	0.10	0.05

$[Cu^I]$ M	$-\frac{d[H_2]}{dt}$ Msec^{-1}				
2×10^{-3}	0.58×10^{-6}	1.46×10^{-6}	-	-	-
4	-	-	-	2.92×10^{-6}	-
5	0.66	1.70	-	-	4.44×10^{-6}
6	-	-	2.98×10^{-6}	-	-
10	0.71	1.99	3.48	4.09	5.38
20	0.71	2.58	4.90	5.88	7.37
30	-	2.94	6.10	7.67	9.35
40	-	-	7.15	9.36	10.9
50	-	-	-	10.6	11.8
60	-	-	-	11.3	13.1

* By mirror image method.

** $-\frac{d[H_2]}{dt} = \frac{1}{2}\frac{d[Cu^I]}{dt}$

TABLE G-3.

Sulphate Series: 0.15 M[$CuSO_4$]$_o$, 5 atm H_2, 160°C.

Experiment:	H_2SO_4 - 2	$SO_4^=$ - 1	$SO_4^=$ - 2	$SO_4^=$ - 3	$SO_4^=$ - 4
[$MgSO_4$] M:	0.35	0.45	0.55	0.65	0.75
[H_2SO_4]$_o$ M:	0.50	0.40	0.30	0.20	0.10
[Cu^I] M	$-\frac{d[H_2]}{dt}$ $Msec^{-1}$				
5×10^{-3}	4.32×10^{-6}	5.04×10^{-6}	6.46×10^{-6}	6.46×10^{-6}	5.95×10^{-6}
10	5.90	7.32	8.66	9.99	8.50
20	9.01	11.3	14.1	14.8	15.1
30	12.2	15.2	20.2	21.1	-
40	14.8	18.7	24.5	24.2	-

TABLE G-4.

Temperature Series: 0.15 M[$CuSO_4$]$_o$, 0.70 M[H_2SO_4]$_o$
0.15 M[$MgSO_4$], 5 atm H_2

Experiment:	T - 3	T - 1	Cu^{II} - 1	T - 2
Temperature °C:	120	140	160	180
[Cu^I] M	$-\frac{d[H_2]}{dt}$ $Msec^{-1}$			
2×10^{-3}	0.148×10^{-6}	-	-	6.60×10^{-6}
5	0.175	0.825×10^{-6}	-	7.53
6	-	-	2.98×10^{-6}	-
8	0.251	-	-	-
10	-	1.06	3.48	9.76
12	0.336	-	-	-
20	-	1.46	4.90	13.2
30	-	1.81	6.10	15.6
40	-	-	7.15	-

APPENDIX H.

The Integrated Rate Curve for the Sulphate System

The integration was performed graphically for one experiment* using an expression obtained by rearranging the rate law, equation 38, e.g.,

$$t = \int_0^x \frac{(c + a - x)(e + a - x)\,dx}{b(a - x)^2(e + a - x) + fx(a - x)^2}$$

where $x = [Cu^I]$

$\Delta x = 0.01\ M[Cu^I]$

$a = [Cu^{II}]_o = 0.15\ M$

$b = 2k_1[H_2] = 2 \times 3.2 \times 10^{-3} \times 5.9 \times 10^{-3}\ sec^{-1}$

$c = \frac{k_{-1}}{k_2}[H^+]$** $= 0.13 \times 0.7\ M$

$e = \frac{k_{-3}}{k_4}[H^+] = 0.44 \times 0.7\ M$

$f = 2k_3[H_2] = 2 \times 6.2 \times 10^{-2} \times 5.9 \times 10^{-3}\ sec^{-1}$

The values of t obtained as a function of $[Cu^I]$ are shown in Table H-1.

TABLE H-1.

t as a Function of $[Cu^I]$

$[Cu^I]$ M	t min
5×10^{-3}	22
10	41
20	73
30	100
40	127
50	152

---

* Experimental conditions: 0.15 $M[CuSO_4]_o$, 0.85 $M[H_2SO_4]_o$, 5 atm H_2, 160°C.

** The increase in $[H^+]$ due to $[Cu^{II}]$ reduction was disregarded as a first approximation.

APPENDIX I.

Rate Curves and Rates of Exchange Experiments

(a) Data for Rate Curves

TABLE I-1

Experiment D_2-A: 0.15 M[$CuSO_4$]$_o$, 0.50 M[H_2SO_4]$_o$, 0.35 M[$MgSO_4$], 5 atm D_2, 160°C, solvent H_2O.

Time min.	HD %	H_2 %	V gas* at 160°C ml	P** atm	HD‡ moles X 10^{+3}	H_2‡ moles X 10^{+3}	[Cu^I] M X 10^{+3}	V solution* at 25°C.	Cu^I moles X 10^{+3}
2	0.59	-	915	5.1	0.77	-	-	950	-
20	2.44	0.05	956	4.9	3.10	0.07	-	950	-
21	-	-	995	-	-	-	7.45	912	7.08
36	-	-	995	-	-	-	15.2	876	14.15
40	6.11	0.25	995	4.5	7.60	0.32	-	876	-
50	8.93	0.48	995	4.5	11.14	0.61	-	876	-
51	-	-	1040	-	-	-	25.2	831	22.91
65	13.75	1.17	1040	5.2	18.49	1.66	-	831	-
66	-	-	1090	-	-	-	39.4	789	34.71
80	18.70	2.66	1090	4.7	25.62	3.81	-	789	-
81	-	-	1137	-	---	-	53.6	746	49.41
95	19.95	3.68	1137	4.1	27.22	6.45	-	746	-

* After sampling of solution

** Excluding steam pressure

‡ Moles present in gas phase; amount dissolved in solution and amounts removed with gas and liquid samples were disregarded.

TABLE I-2.

Experiment D_2-B: 0.15 M[$CuSO_4$]$_o$, 0.85 M[H_2SO_4]$_o$, 5 atm D_2, 160°C solvent H_2O.

Time min.	HD %	H_2 %	V gas at 160°C ml	P atm	HD moles X 10^{+3}	H_2 moles X 10^{+3}	[Cu^I] M X 10^{+3}	V solution at 25°C	Cu^I moles X 10^{+3}
3	0.6	-	915	5.0	0.78	-	-	950	-
40	3.99	0.08	915	4.80	4.96	0.10	-	950	-
80	9.63	0.45	915	4.67	11.73	0.54	-	950	-
81	-	-	954	-	-	-	10.3	915	9.78
120	16.03	1.23	954	4.27	19.05	1.42	-	915	-
125	-	-	996	-	-	-	15.5	877	14.5
160	22.6	2.55	996	4.00	26.21	2.90	-	877	-
163	-	-	1040	-	-	-	20.2	837	18.7
200	30.0	5.04	1040	4.67	36.33	6.30	-	837	-
202	-	-	1082	-	-	-	29.2	799	26.0
240	36.0	9.18	1082	4.67	44.84	12.18	-	-	-
243	-	-	1135	-	-	-	36.0	751	31.3

TABLE I-3.

Experiment D_2-C: 0.07 M[$Cu(ClO_4)_2$]$_o$, 0.10 M[$HClO_4$]$_o$,
15 atm D_2, 160°C, solvent H_2O

Time min.	HD %	H_2 %	V gas at 160°C	P atm.	HD moles X 10^{+3}	H_2 moles X 10^{+3}	[Cu^I] M X 10^{+3}	V solution at 25°C	Cu^I moles X 10^{+3}
2	0.53	-	915	14.8	2.02	-	-	950	-
60	10.4	0.54	915	15.2	40.6	2.07	-	950	-
62	-	-	880	-	-	-	~15.8[A]	880	15.0
80	-	-	851	-	-	-	19.1	851	17.8
120	26.7	3.50	851	14.1	107	14.1	-	851	-
122	-	-	813	-	-	-	27.0	813	24.6
180	38.9	10.4	813	14.3	159	43.6	-	813	-
182	-	-	769	-	-	-	33.8	769	30.2
240	42.9	19.4	769	13.7	176	82.2	-	769	-
300	44.2	29.4	769	13.5	182	125	-	769	-
302	-	-	730	-	-	-	39.0	730	34.2
360	40.5	36.3	730	12.5	166	153	-	730	-
362	-	-	691	-	-	-	39.8	691	34.7

[A] Estimated by interpolation from [Cu^+] vs time plot

TABLE I-4.

Experiment H_2-D: 0.15 M[$CuSO_4$]$_o$, 0.85 M[H_2SO_4]$_o$, 5 atm H_2, 160°C, solvent D_2O.

Time min.	HD %	D_2 %	V gas at 160°C ml	P atm	HD moles X 10^{+3}	D_2 moles X 10^{+3}	[Cu^I] M X 10^{+3}	V solution at 25°C	Cu^I moles X 10^{+3}
3	0.2	18.55*	860	5.0	0.24	-	-	1000	-
33	2.17	14.25	860	5.0	2.52	-	-	1000	-
60	5.04	14.73	860	4.7	5.78	0.55	-	1000	-
63	-	-	902	-	-	-	15.6	962	15.6
92	9.1	14.86	902	4.1	10.0	0.68	-	962	-
95	-	-	933	-	-	-	26.8	934	24.6
120	13.3	15.60	933	3.8	14.2	1.42	-	934	-
122	-	-	957	-	-	-	34.6	912	33.7
152	18.23	16.40	957	3.5	18.8	2.17	-	912	-
154	-	-	989	-	-	-	40.7	883	39.2
181	24.8	17.85	989	3.7	25.6	3.66	-	883	-
183	-	-	1024	-	-	-	44.5	851	42.6

* Helium used for flushing autoclave was measured as D_2; therefore assumed zero % D_2 up to 33 min.

TABLE I-5.

Experiment D_2-E: 0.00 M[$CuSO_4$], 0.5 M[H_2SO_4] 0.5 M[$MgSO_4$], 5 atm D_2, 160°C solvent H_2O

Time	% HD
4 min	0.58
45	0.55
80	0.57
120	0.51
Cylinder Sample	0.59

(b) Rate Measurements for Exchange Experiments

TABLE I-6.

Experiment D_2-A

Time min.	Cu^I moles	$\frac{1}{2}\frac{dCu^I}{dt}$ * moles/sec	$(HD + 4H_2)$ moles	$\frac{d(HD + 4H_2)}{dt}$ ** moles/sec
7	2×10^{-3}	2.82×10^{-6}	2.4×10^{-3}	2.42×10^{-6}
28	10	4.07	4.8	4.18
47	20	4.95	12.0	8.62
61	30	6.76	21.8	14.05
72	40	7.64	32.0	18.00

Experiment D_2-B

22	2×10^{-3}	0.83×10^{-6}	2.6×10^{-3}	2.10×10^{-6}
93	10	1.08	16.0	4.20
130	15	-	27.5	6.00
165	20	1.23	42.0	7.67
197	25	-	60.0	10.50
228	30	1.43	82.0	13.60

Experiment D_2-C

	Cu^+ moles	$\frac{1}{2}\frac{dCu^+}{dt}$ *** moles/sec		
19	5×10^{-3}	2.11×10^{-6}	10×10^{-3}	11.1×10^{-6}
40	10	2.10	27	16.9
90	20	1.90	97	30.8
133	26	1.61	200	44.8
180	30	1.53	350	56.3

Experiment H_2-D

	Cu^I moles	$\frac{1}{2}\frac{dCu^I}{dt}$ moles/sec	$(HD + 4\ D_2)$ moles	$\frac{d(HD + 4\ D_2)}{dt}$ moles/sec
10	2×10^{-3}	1.67×10^{-6}	0.6×10^{-3}	1.29×10^{-6}
43	10	2.36	4.0	2.16
76	20	2.74	9.0	3.36
94	26	2.88	12.8	3.78

* Net forward rate

** Exchange rate - The rate of oxidation of HD and H_2 by Cu^{II} was not added to the rate measurements as it only came to 5 to 6% at the highest $HD+4H_2$ levels toward the end of the experiments.

*** Corrected for perchlorate decomposition effect (Appendix C).

(c) Isotope Effects on Net Forward Rates at 160°C.

TABLE I-7.

i) Experimental conditions: 0.15 M[$CuSO_4$]$_o$, 0.5 M[H_2SO_4]$_o$, 0.35 M[$MgSO_4$], solvent H_2O, 5 atm D_2 or H_2

Experiment: D_2-A H_2SO_4-2

$[Cu^I]$ M	$\frac{1}{2}\frac{d[Cu^I]}{dt}$ ✱ M sec^{-1}	$-\frac{d[H_2]}{dt}$ M sec^{-1}	$\frac{R_{D_2}}{R_{H_2}}$
10×10^{-3}	4.4×10^{-6}	5.9×10^{-6}	0.69
20	6.78	9.0	0.76
30	9.77	12.2	0.80
40	11.60	14.8	0.78

ii) Experimental conditions: 0.15 M[$CuSO_4$]$_o$, 0.85 M[H_2SO_4]$_o$, solvent H_2O, 5 atm D_2 or H_2

Experiment: D_2-B H_2SO_4-3

10×10^{-3}	1.20×10^{-6}	2.51×10^{-6}	0.48
20	1.57	3.01	0.52
30	2.03	3.59	0.57

iii) Experimental conditions: 0.07 M[$Cu(ClO_4)_2$]$_o$, 0.10 M[$HClO_4$]$_o$, solvent H_2O, 10 atm D_2 or H_2

Experiment: D_2-C Cu^{++}-4

$[Cu^+]$ M	$\frac{1}{2}\frac{d[Cu^+]}{dt}$ ✱ M sec^{-1}		
10×10^{-3}	1.67×10^{-6} ‡	2.26×10^{-6} ‡	0.74
20	1.72	2.16	0.80

iv) Experimental conditions: 0.15 M[$CuSO_4$]$_o$, 0.85 M[H_2SO_4]$_o$, solvent D_2O or H_2O, 5 atm H_2

Experiment: H_2-D H_2SO_4-3

$[Cu^I]$ M	$\frac{1}{2}\frac{d[Cu^I]}{dt}$ M sec^{-1} in D_2O	$-\frac{d[H_2]}{dt}$ M sec^{-1} in H_2O	$\frac{R_{D_2O}}{R_{H_2O}}$
10×10^{-3}	2.47×10^{-6}	2.51×10^{-6}	0.99
20	3.12	3.01	1.03

✱ Net forward rate using D_2. Rate measurements corrected to 5 (10 for experiment D_2-C) atm D_2 pressure.

‡ Corrected for perchlorate decomposition effect (Appendix C).